

**T.R.
SAKARYA UNIVERSITY
GRADUATE SCHOOL OF NATURAL AND APPLIED SCIENCES**

**EXTRACELLULAR BIOSYNTHESIS AND CHARACTERIZATION
OF ZINC OXIDE AND NISIN-LOADED ZINC OXIDE
NANOPARTICLES USING *BACILLUS SUBTILIS* ZBP4**

PhD THESIS

Mohammed HAMK

Food Engineering Department

JANUARY 2023

**T.R.
SAKARYA UNIVERSITY
GRADUATE SCHOOL OF NATURAL AND APPLIED SCIENCES**

**EXTRACELLULAR BIOSYNTHESIS AND CHARACTERIZATION
OF ZINC OXIDE AND NISIN-LOADED ZINC OXIDE
NANOPARTICLES USING *BACILLUS SUBTILIS* ZBP4**

PhD THESIS

Mohammed HAMK

Food Engineering Department

Thesis Advisor: Assoc. Prof. Dr. Ayşe AVCI

JANUARY 2023

The thesis work titled “EXTRACELLULAR BIOSYNTHESIS AND CHARACTERIZATION OF ZINC OXIDE AND NISIN-LOADED ZINC OXIDE NANOPARTICLES USING *BACILLUS SUBTILIS* ZBP4” prepared by Mohammed HAMK was accepted by the following jury on 27/01/2023 by unanimously/majority of votes as a PhD THESIS in Sakarya University Graduate School of Natural and Applied Sciences, Food Engineering Department.

Thesis Jury

Head of Jury : Prof. Dr. Serap COŞANSU AKDEMİR

Sakarya University

Jury Member : Assoc. Prof. Dr. Ayşe AVCI (Advisor)

Sakarya University

Jury Member : Prof. Dr. Gülnur ARABACI

Sakarya University

Jury Member : Prof. Dr. Sevgi ERTUĞRUL KARATAY

Ankara University

Jury Member : Assoc. Prof. Dr. Evrim GÜNEŞ ALTUNTAŞ

Ankara University

STATEMENT OF COMPLIANCE WITH THE ETHICAL PRINCIPLES AND RULES

I declare that the thesis work titled "EXTRACELLULAR BIOSYNTHESIS AND CHARACTERIZATION OF ZINC OXIDE AND NISIN-LOADED ZINC OXIDE NANOPARTICLES USING *BACILLUS SUBTILIS* ZBP4", which I have prepared in accordance with Sakarya University Graduate School of Natural and Applied Sciences regulations and Higher Education Institutions Scientific Research and Publication Ethics Directive, belongs to me, is an original work, I have acted in accordance with the regulations and directives mentioned above at all stages of my study, I did not get the innovations and results contained in the thesis from anywhere else, I duly cited the references for the works I used in my thesis, I did not submit this thesis to another scientific committee for academic purposes and to obtain a title, in accordance with the articles 9/2 and 22/2 of the Sakarya University Graduate Education and Training Regulation published in the Official Gazette dated 20.04.2016, a report was received in accordance with the criteria determined by the graduate school using the plagiarism software program to which Sakarya University is a subscriber, I accept all kinds of legal responsibility that may arise in case of a situation contrary to this statement.

(27/01/2023)

Mohammed HAMK

I dedicate my thesis to my father (God mercy him)

ACKNOWLEDGMENTS

First and foremost, I would like to thank Almighty Allah for giving me health and patience to finish this effort. This work was produced under the admirable and professional guidance of my supervisor Assoc. Prof. Dr. Ayşe Avcı, who helped and supported me always, and without her, I would not have been able to complete my research. I would like to express my deepest thankfulness to her. Also, I must express my very profound gratitude to my family, specially my parents, for providing me with unlimited support and continuous encouragement throughout my study.

I would like to express sincere gratitude to Mr. Wassfee Thabit and my wife for patience and support. I want to take the opportunity to thank all staff of Halabja Technical College of Applied Sciences and I would like to express my gratitude and appreciation for all my friends who helped me directly and indirectly, especially Mr. Hawrez Nadir and Mr. peshrow abdulkerim.

My deepest thanks to each of the Presidency for Turks Abroad and Related Communities, Sakarya University and the Department of Food Engineering and Sincere thanks are due to Fikriye Alev Akcay for her kind assistance.

I cannot forget all members of the dissertation committee, especially Prof. Dr. Serap Coşansu Akdemir and Prof. Dr. Gülnur Arabacı. Also, I would like to thank my teachers, Dr. Karkaz Thalij, Dr. Ahmed AL-Ogailı, Mehmet Karakaya, Dr. Bayan Alabdulla and Dr. Thaer Hasan for their help in this work, Thanks to every teacher who contributed to my education in my life.

I would like to extend my thanks to Assist. Erdem Kılıçaslan, Dr. Şeyma Dombaycıoğlu, Fuat Kayış, Dr.Özlem Güldalı, Prof Dr. Ahmet Alp and Sezer Tany for their effort in experimental analysis.

I would like to thank the Sakarya University Scientific Research Projects Unit (Project No: 2022-7-25-46).

Mohammed HAMK

TABLE OF CONTENTS

| | <u>Page</u> |
|---|-------------|
| STATEMENT OF COMPLIANCE WITH THE ETHICAL PRINCIPLES AND RULES | v |
| ACKNOWLEDGMENTS | ix |
| TABLE OF CONTENTS | xi |
| ABBREVIATIONS | xiii |
| LIST OF TABLES | xvii |
| LIST OF FIGURES | xix |
| SUMMARY | xxiii |
| ÖZET | xxv |
| 1. INTRODUCTION | 1 |
| 2. LITERATURE REVIEW | 5 |
| 2.1. Nanotechnology | 5 |
| 2.2. History of Nano Science | 5 |
| 2.3. Application of Nanotechnology | 6 |
| 2.4. Methods of Nanoparticles Synthesis..... | 7 |
| 2.5. Biological Synthesis of Nanoparticles | 8 |
| 2.6. Zinc Oxide Nanoparticles | 10 |
| 2.7. Bacterial Synthesis of Zinc Oxide NPs..... | 11 |
| 2.8. General Characteristics of <i>Bacillus</i> spp | 12 |
| 2.9. Application of Zinc Oxide NPs..... | 15 |
| 2.10. Application of ZnO NPs as Antimicrobial Agent..... | 16 |
| 2.11. Mechanisms of Action of ZnO NPs | 16 |
| 2.12. Nanoparticle Conjugates | 17 |
| 2.13. Nisin Peptide and Nisin Loaded NPs | 19 |
| 2.14. Nanoparticles Characterization | 20 |
| 3. MATERIALS AND METHODS | 23 |
| 3.1. Materials | 23 |
| 3.1.1. Microorganisms | 23 |
| 3.1.2. The laboratory instruments | 25 |
| 3.1.3. Chemical and biological materials | 26 |
| 3.1.4. Culture media | 27 |
| 3.1.5. Solutions | 27 |
| 3.2. Methods | 28 |
| 3.2.1. Screening and biosynthesis of ZnO NPs | 28 |
| 3.2.2. Optimization of ZnO NPs biosynthesis by <i>Bacillus subtilis</i> ZBP4..... | 28 |
| 3.2.3. Biosynthesis of nisin loaded ZnO NPs | 29 |
| 3.2.4. Characterization of nanoparticles | 30 |
| 3.2.4.1. UV-VIS spectroscopy | 30 |
| 3.2.4.2. Harvest of nanoparticles..... | 30 |
| 3.2.4.3. Transmission electron microscopy analysis (TEM)..... | 30 |

| | |
|--|------------|
| 3.2.4.4. Field emission scanning electron microscope (FESEM) analysis | 30 |
| 3.2.4.5. Energy dispersive spectroscopy (EDS) analysis | 31 |
| 3.2.4.6. X-ray diffraction (XRD) analysis..... | 31 |
| 3.2.4.7. Fourier Transform Infrared spectroscopy analysis..... | 32 |
| 3.2.4.8. Zeta potential..... | 32 |
| 3.2.4.9. Energy bandgap of nanoparticles | 32 |
| 3.2.5. Antimicrobial activity of nanoparticles | 32 |
| 3.2.6. Growth inhibition curves in liquid medium..... | 33 |
| 3.2.7. Antioxidant activity of nanoparticles..... | 33 |
| 3.2.8. Storage stability of nanoparticles..... | 34 |
| 3.2.9. Cytotoxicity assay..... | 34 |
| 3.2.10. Statistical analysis..... | 35 |
| 4. RESULTS and DISCUSSION..... | 37 |
| 4.1. Screening and Selection of <i>Bacillus</i> Strains for ZnO NPs Biosynthesis..... | 37 |
| 4.2. Biosynthesis of ZnO NPs by <i>Bacillus subtilis</i> ZBP4 | 38 |
| 4.3. Effect of Zinc Sulfate Concentration on ZnO NPs Biosynthesis | 38 |
| 4.4. Effect of pH on the Biosynthesis of ZnO NPs | 41 |
| 4.5. Effect of Incubation Temperature on ZnO NPs Synthesis..... | 44 |
| 4.6. Biosynthesis of Nisin Loaded Zinc Oxide NPs..... | 45 |
| 4.7. Characterization of Nanoparticles..... | 47 |
| 4.7.1. Transmission electron microscopy | 47 |
| 4.7.2. Field emission scanning electron microscopy | 50 |
| 4.7.3. Energy dispersive x-ray spectrometer..... | 52 |
| 4.7.4. X-ray diffraction spectroscopy | 54 |
| 4.7.5. Fourier transform infrared spectroscopy | 55 |
| 4.7.6. Zeta potential | 57 |
| 4.7.7. Energy bandgap of nanoparticles..... | 58 |
| 4.8. Antimicrobial Activity of ZnO NPs | 60 |
| 4.8.1. Antimicrobial activity of ZnO NPs against Gram positive bacteria..... | 60 |
| 4.8.2. Antimicrobial activity of ZnO NPs against Gram negative bacteria..... | 62 |
| 4.8.3. Antifungal activity of ZnO NPs against <i>Candida albicans</i> | 63 |
| 4.9. Minimum Inhibitory Concentration (MIC) of ZnO NPs..... | 64 |
| 4.10. Antibacterial Activity of Nisin or Nisin-ZnO NPs..... | 67 |
| 4.11. Antibacterial Activity of Nisin and N-ZnO NPs..... | 67 |
| 4.11.1. Antibacterial activity of nisin or nisin-ZnO NPs against Gram positive bacteria | 67 |
| 4.11.2. Antibacterial activity of nisin or nisin-ZnO NPs against Gram negative bacteria | 69 |
| 4.12. Antimicrobial Activity of ZnO NPs in Liquid Medium..... | 72 |
| 4.13. Growth Inhibition Curves of ZnO NPs, Nisin and N-ZnO NPs in Liquid Medium..... | 73 |
| 4.14. Antioxidant Activity of ZnO NPs and N-ZnO NPs | 78 |
| 4.15. Effect Storage on Shelf Life of Nanoparticles | 79 |
| 4.16. Cytotoxicity assay | 82 |
| 5. CONCLUSIONS AND RECOMMENDATIONS | 85 |
| REFERENCES | 87 |
| APPENDICES | 111 |
| CURRICULUM VITAE | 115 |

ABBREVIATIONS

| | |
|------------------------|--|
| nm | : Nano meter |
| ZnO NPs | : Zinc Oxide nanoparticles |
| FDA | : Food and Drug Administration |
| eV | : Electron volts |
| NPs | : Nanoparticles |
| UV | : Ultraviolet light |
| kDa | : Kilo dalton |
| sp. | : Species |
| N-ZnO NPs | : Nisin conjugated Zinc Oxide nanoparticles |
| UV-VIS | : Ultraviolet–visible |
| TEM | : Transmission electron microscopy |
| FESEM | : Field Emission Scanning Electron Microscopy |
| XRD | : X-ray Diffraction |
| EDS | : Energy Dispersive X-ray analysis |
| FTIR | : Fourier Transform Infrared spectroscopy |
| ISO | : International Organization for Standardization |
| 1D | : One-dimensional |
| 2D | : Two-dimensional |
| 3D | : Three-dimensional |
| BC | : Before Christ |
| STM | : Scanning Tunneling Microscope |
| DNA | : Deoxyribonucleic acid |
| WHO | : World Health Organization |
| FDA | : Food and Drug Administration |
| ZnO | : Zinc Oxide |
| TiO₂ | : Titanium Oxide |
| AuNPs | : Gold nanoparticles |
| Fig. | : Figure |
| NADH | : Nicotinamide adenine dinucleotide |

| | |
|---|---|
| meV | : Megaelectron volt |
| Zn | : Zinc |
| µg | : Microgram |
| mg | : Milligram |
| g | : gram |
| cm | : Centimeter |
| °C | : Centigrade degree |
| M | : Molar |
| mM | : Milimolar |
| µL | : Microlitre |
| mL | : Mililitre |
| L | : Liter |
| h | : Hour |
| ZnSO₄.7H₂O | : Zinc sulfate heptahydrate |
| PBA | : Phenylboronic acid |
| PBA-ZnO | : Phenylboronic acid conjugated Zinc Oxide |
| MCF-7 | : Breast cancer cells |
| ROS | : Oxidative stress |
| N | : Free nisin |
| Eg | : Energy bandgap |
| TSB | : Tryptic soy broth |
| min | : Minute |
| rpm | : Revolutions per minute |
| DPPH | : 2,2-diphenyl-1-picrylhydrazyl |
| <i>B. cereus</i> | : <i>Bacillus cereus</i> |
| <i>E. coli</i> O157:H7 | : <i>Escherichia coli</i> O157:H7 |
| <i>L. monocytogenes</i> | : <i>Listeria monocytogenes</i> |
| <i>P. aeruginosa</i> | : <i>Pseudomonas aeruginosa</i> |
| <i>S. Typhimurium</i> | : <i>Salmonella</i> Typhimurium |
| <i>S. aureus</i> | : <i>Staphylococcus aureus</i> |
| <i>E. coli</i> Type 1 | : <i>Escherichia coli</i> Type 1 |
| <i>S. Enteritidis</i> | : <i>Salmonella</i> Enteritidis |
| <i>C. albicans</i> | : <i>Candida albicans</i> |
| CFS | : Cell-free supernatant |
| SPSS | : Statistical Package for the Social Sciences |

| | |
|---|---|
| SPR | : surface plasmon resonance |
| (NH₂)₂SO₄ | : Ammonia sulfate |
| keV | : Kilo electron volt |
| 2θ | : 2theta |
| % | : percent |
| JCPDS | : Joint Committee on Powder Diffraction Standards |
| ICDD | : International Center for Diffraction Data |
| a.u | : arbitrary units |
| mV | : millivolts |
| IZD | : inhibition zone diameters |
| MIC | : minimum inhibitory concentration |
| mg/mL | : Milligrams per Milliliter |
| µg/mL | : Microgram per Milliliter |
| mm | : millimeter |
| OD | : Optical density |
| MFU | : McFarland unit |
| IC₅₀ | : Half-maximal inhibitory concentration |

LIST OF TABLES

| | <u>Page</u> |
|---|-------------|
| Table 2.1. Some physical properties of ZnO..... | 11 |
| Table 2.2. The bacterial used in biosynthesis of ZnO NPs. | 14 |
| Table 3.1. Isolates were obtained from different sources used in the study..... | 24 |
| Table 3.2. Laboratory instruments, company and origin used in the study. | 25 |
| Table 3.3. Materials and tools used in the study. | 26 |
| Table 4.1. Weight and atomic percentage composition of prepared ZnO NPs. | 53 |
| Table 4.2. Weight and atomic percentage composition of 10 mg nisin loaded-ZnO NPs. | 53 |
| Table 4.3. Assignment of different peaks in the FTIR spectra of ZnO NPs, nisin loaded ZnO NPs..... | 57 |
| Table 4.4. Antimicrobial activity of varying amounts of ZnO NPs synthesized at pH 7.5, 33 °C using 8 mM ZnSO ₄ .H ₂ O. | 66 |
| Table 4.5. The inhibition percentage of ZnO NPs, free nisin and nisin- ZnO NPs against <i>L. monocytogenes</i> and <i>S. aureus</i> at 6 hours. | 77 |
| Table 4.6. Free radical scavenging activity of ZnO NPs and N-ZnO NPs determined by DPPH assay..... | 79 |

LIST OF FIGURES

| | <u>Page</u> |
|---|-------------|
| | <u>Page</u> |
| Figure 2.1. Top-down and bottom-up approaches for synthesis inorganic nanoparticles, this figure deduced by Azharuddin et al. (2019)..... | 8 |
| Figure 2.2. Mechanism of nanoparticle synthesis by microorganisms (Salunke et al, 2016)..... | 9 |
| Figure 2.3. The description of ZnO structures: (a) hexagonal wurtzite, (b) zinc blende and (c) rock salt (Yıldırım, 2014)..... | 10 |
| Figure 2.4. The strategies that NPs impact on bacteria cells..... | 17 |
| Figure 4.1. The UV–VIS spectra of screening of ZnO NPs synthesized by some <i>Bacillus</i> sp..... | 38 |
| Figure 4.2. UV-VIS spectra of ZnO NPs biosynthesized at various concentrations of zinc sulfate concentration. a) 24 h, b) 48 h, c) 72 h..... | 39 |
| Figure 4.2. (Continued) UV-VIS spectra of ZnO NPs biosynthesized at various concentrations of zinc sulfate concentration. a) 24 h, b) 48 h, c) 72 h..... | 40 |
| Figure 4.3. Effect of Zinc sulfate concentration on ZnO NP synthesis..... | 41 |
| Figure 4.4. UV-VIS spectra of ZnO NPs biosynthesized at various pH values. a) 24 h, b) 48 h, c) 72 h..... | 42 |
| Figure 4.4. (Continued) UV-VIS spectra of ZnO NPs biosynthesized at various pH values. a) 24 h, b) 48 h, c) 72 h..... | 43 |
| Figure 4.5. Effect of pH on ZnO NPs synthesis..... | 44 |
| Figure 4.6. Effect of temperature on ZnO NPs synthesis..... | 45 |
| Figure 4.7. Nisin conjugation ZnO NPs synthesis with different concentrations of nisin after 24 h and 48 h..... | 46 |
| Figure 4.8. TEM micrograph ZnO NPs (a) and average distribution of ZnO NPs (b)..... | 48 |
| Figure 4.9. TEM micrograph N-ZnO NPs (a) and average distribution of N-ZnO NPs (b)..... | 49 |
| Figure 4.10. FESEM image of biosynthesized ZnO NPs (a) and particle size distribution (b) of ZnO NPs synthesized by <i>Bacillus subtilis</i> ZBP4..... | 51 |
| Figure 4.11. FESEM image of N-ZnO NPs..... | 52 |
| Figure 4.12. Energy dispersive X-ray spectrum of the ZnO NPs..... | 53 |
| Figure 4.13. Energy dispersive X-ray spectrum of the N-ZnO NPs..... | 54 |
| Figure 4.14. X-ray diffraction pattern of ZnO and N-ZnO NPs..... | 55 |
| Figure 4.15. The Fourier transforms infrared (FTIR) spectroscopy measurement of ZnO NPs, nisin and N-ZnO NPs..... | 56 |

| | |
|--|----|
| Figure 4.16. Zeta potential distribution of ZnO NPs (a) and N-ZnO NPs at 10 mg/mL (b)..... | 58 |
| Figure 4.17. UV–VIS absorption spectrum of ZnO NPs and Tauc's plot of ZnO NPs (a) and N-ZnO NPs (b) deduced from the spectrum..... | 59 |
| Figure 4.17. (Continued) UV–VIS absorption spectrum of ZnO NPs and Tauc's plot of ZnO NPs (a) and N-ZnO NPs (b) deduced from the spectrum..... | 60 |
| Figure 4.18. Antimicrobial activity of ZnO NPs. 0.01 mg/mL, 0.05 mg/mL, 0.1 mg/mL, 0.5 mg/mL, 1 mg/mL, 2 mg/mL, 5 mg/mL, 10 mg/mL used disc diffusion test (A) <i>B. cereus</i> , (B) <i>L. monocytogenes</i> ATCC 7644, (C) <i>S. aureus</i> ATCC 25923..... | 61 |
| Figure 4.19. Antibacterial activity of ZnO NPs. 0.01 mg/mL, 0.05 mg/mL, 0.1 mg/mL, 0.5 mg/mL, 1 mg/mL, 2 mg/mL, 5 mg/mL, 10 mg/mL used disc diffusion test (a) <i>E. coli</i> O157:H7 NCTC 12900, (b) <i>P. aeruginosa</i> , (c) <i>S. Typhimurium</i> , (d) <i>E. coli</i> Type 1..... | 62 |
| Figure 4.19. (Continued) Antibacterial activity of ZnO NPs. 0.01 mg/mL, 0.05 mg/mL, 0.1 mg/mL, 0.5 mg/mL, 1 mg/mL, 2 mg/mL, 5 mg/mL, 10 mg/mL used disc diffusion test (a) <i>E. coli</i> O157:H7 NCTC 12900, (b) <i>P. aeruginosa</i> , (c) <i>S. Typhimurium</i> , (d) <i>E. coli</i> Type 1..... | 63 |
| Figure 4.20. Antifungal activity of ZnO NPs against <i>C. albicans</i> . 0.01 mg/mL, 0.05 mg/mL, 0.1 mg/mL, 0.5 mg/mL, 1 mg/mL, 2 mg/mL, 5 mg/mL, 10 mg/mL used disc diffusion test..... | 64 |
| Figure 4.21. Antibacterial activity of ZnO NPs, nisin and nisin loaded ZnO NPs. 1 mg/mL, 2 mg/mL, 5 mg/mL, 10 mg/mL used disc diffusion test (a) <i>B. cereus</i> , (b) <i>L. monocytogenes</i> ATCC 7644, (c) <i>S. aureus</i> ATCC 25923..... | 68 |
| Figure 4.21. (Continued) Antibacterial activity of ZnO NPs, nisin and nisin loaded ZnO NPs. 1 mg/mL, 2 mg/mL, 5 mg/mL, 10 mg/mL used disc diffusion test (a) <i>B. cereus</i> , (b) <i>L. monocytogenes</i> ATCC 7644, (c) <i>S. aureus</i> ATCC 25923..... | 69 |
| Figure 4.22. Antibacterial activity of ZnO NPs, nisin and nisin loaded ZnO NPs. 1 mg/mL, 2 mg/mL, 5 mg/mL, 10 mg/mL used disc diffusion test (a) <i>E. coli</i> O157:H7 NCTC 12900, (b) <i>P. aeruginosa</i> , (c) <i>S. Typhimurium</i> , (d) <i>E. coli</i> Type 1, (e) <i>S. Enteritidis</i> ATCC 13076... | 70 |
| Figure 4.22. (Continued) Antibacterial activity of ZnO NPs, nisin and nisin loaded ZnO NPs. 1 mg/mL, 2 mg/mL, 5 mg/mL, 10 mg/mL used disc diffusion test (a) <i>E. coli</i> O157:H7 NCTC 12900, (b) <i>P. aeruginosa</i> , (c) <i>S. Typhimurium</i> , (d) <i>E. coli</i> Type 1, (e) <i>S. Enteritidis</i> ATCC 13076..... | 71 |
| Figure 4.22. (Continued) Antibacterial activity of ZnO NPs, nisin and nisin loaded ZnO NPs. 1 mg/mL, 2 mg/mL, 5 mg/mL, 10 mg/mL used disc diffusion test (a) <i>E. coli</i> O157:H7 NCTC 12900, (b) <i>P. aeruginosa</i> , (c) <i>S. Typhimurium</i> , (d) <i>E. coli</i> Type 1, (e) <i>S. Enteritidis</i> ATCC 13076..... | 72 |
| Figure 4.23. Growth curve of <i>P. aeruginosa</i> (a) and <i>L. monocytogenes</i> ATCC 7644 (b) in tryptic soy broth in the presence of various concentrations of ZnO NPs..... | 73 |
| Figure 4.24. Bacterial growth curve of <i>L. monocytogenes</i> ATCC 7644 in TSB... | 75 |
| Figure 4.24. (Continued) Bacterial growth curve of <i>L. monocytogenes</i> ATCC 7644 in TSB..... | 76 |

| | |
|---|----|
| Figure 4.25. Bacterial growth curve of <i>S. aureus</i> ATCC 25923 in TSB..... | 76 |
| Figure 4.25. (Continued) Bacterial growth curve of <i>S. aureus</i> ATCC 25923 in TSB..... | 77 |
| Figure 4.26. DPPH Scavenging activity of ZnO NPs and N-ZnO NPs synthesized using <i>Bacillus subtilis</i> ZBP4..... | 79 |
| Figure 4.27. UV–Visible Spectra of ZnO NPs, nisin loaded ZnO NPs after storage for 120 days a) ZnO NPs; b) nisin loaded ZnO NPs at 5 mg /mL; c) nisin loaded ZnO NPs at 10 mg /mL; d) nisin loaded ZnO NPs at 15 mg /mL..... | 80 |
| Figure 4.27. (Continued) UV–Visible Spectra of ZnO NPs, nisin loaded ZnO NPs after storage for 120 days a) ZnO NPs; b) nisin loaded ZnO NPs at 5 mg /mL; c) nisin loaded ZnO NPs at 10 mg /mL; d) nisin loaded ZnO NPs at 15 mg /mL..... | 81 |
| Figure 4.28. Cytotoxicity of various concentrations of N-ZnO NPs on epithelial cells using the MTT assay..... | 84 |
| Figure 4.29. Calculation of IC50 values in Graph Pad Software..... | 84 |

EXTRACELLULAR BIOSYNTHESIS AND CHARACTERIZATION OF ZINC OXIDE AND NISIN-LOADED ZINC OXIDE NANOPARTICLES USING *BACILLUS SUBTILIS* ZBP4

SUMMARY

In recent years, the biosynthesis of zinc oxide nanoparticles (ZnO NPs) is gaining considerable interest as an alternative to chemical and physical routes, due to its cheap, environmentally friendly, and large-scale manufacturing potential. This study was conducted in the laboratories of the Food Engineering Department at Sakarya University from 1 January 2021 to 1 June 2022. Firstly, the biosynthesis of ZnO NPs was screened using 45 different *Bacillus* strains previously isolated from soil and food samples. The biosynthesis reactions were performed extracellularly after centrifugation of bacterial culture grown in nutrient broth for 24 h. The best isolate (*Bacillus subtilis* ZBP4) was selected and the reaction conditions affecting the biosynthesis of ZnO NPs were optimized, including reaction pH (5-9), temperature (30-40°C), ZnSO₄.7H₂O concentration (2- 10 mM) and incubation time (0-72 hours) and the optimum conditions were determined at 8 mM ZnSO₄.7H₂O concentration, pH 7.5, 33 °C and 24 h. The color change from white to yellow was used to preliminary examine the production of ZnO NPs, and the sharpe peak was identified to be at 341 nm. The crystalline nature of synthesized ZnO NPs are characterized with UV–VIS spectroscopy. Also, the size and shape of the synthesized NPs were determined by Field Emission Scanning Electron Microscopy (FESEM) and Transmission electron microscopy (TEM), and the NPs displayed a quasi-spherical form with nanoscale of 26 nm. Fourier Transform Infrared Spectroscopy (FTIR) and Energy-dispersive X-ray spectroscopy (EDS) were used to confirm nanoparticle synthesis. The formation of nisin loaded Zinc Oxide nanoparticles (N-ZnO NPs) were verified by using UV-VIS spectroscopy, the sharp peak and high absorbance of the reaction mixture was observed at 341 nm created by the surface plasmon resonance (SPR) of nanoparticles.

TEM was used to analyze the size and shape of the N-ZnO NPs and NPs shapes were quasi-spherical with diameters ranging from 14-40 nm. The nanoparticles synthesis were validated by Energy-dispersive X-ray spectroscopy analysis. X-ray diffraction used to identify the natural of NPs, which showed amorphous and alone broad peaks at 2θ angles (2θ = 26.99°). The active groups attributed to presence of protein were detected by FTIR that acted as reducing and stabilizing agents. The zeta potential measurements of NPs exhibited negative surface charges were -19.0 and -17.7 mV for ZnO and N-ZnO NPs respectively, indicating that the particles are moderately stable. Results showed that N-ZnO NPs synthesized by *Bacillus* remained stable for 120 days without color change.

Kirby-Bauer Disk Diffusion Susceptibility Test was used to assess the antimicrobial activity of ZnO and N-ZnO NPs against Gram-positive (*Bacillus cereus*, *Staphylococcus aureus* ATCC 25923, and *Listeria monocytogenes* ATCC 7644) and Gram-negative (*Escherichia coli* Type 1, *Escherichia coli* O157:H7 NCTC 12900, *Pseudomonas aeruginosa*, *Salmonella* Enteritidis ATCC 13076 and *Salmonella*

Typhimurium). The ZnO NPs perform well against a variety of food pathogens, including Gram-positive and Gram-negative. Additionally, N-ZnO NPs showed high efficacy against pathogenic bacteria compared to the action of ZnO NPs and free nisin alone; the inhibition zones formed by N-ZnO NPs at 10 mg/mL against Gram-negative bacteria were 16 mm and 15.8 mm for *S. Enteritidis* ATCC 13076 and *P. aeruginosa* respectively. In addition, results revealed that the N-ZnO NP has strong bactericidal activity in liquid media against pathogenic bacteria compared with ZnO NPs and free nisin, which killed 94.98 and 96.79 % of the *L. monocytogenes* ATCC 7644 and *S. aureus* ATCC 25923 respectively at 150 µg/ mL within 6 hours of treatment.

As a result of this study, it was determined that *Bacillus subtilis* ZBP4, a local isolate, is a microorganism that can be used for biosynthesis ZnO NPs, and synthesized ZnO NPs can be a good antimicrobial agent. In addition, it has been demonstrated that when nisin is loaded to the biosynthesis medium, both the antibacterial and antioxidant properties of the synthesized nanoparticles can be significantly improved.

ÇİNKO OKSİT VE NİSİN-YÜKLÜ ÇİNKO OKSİT NANOPARTİKÜLLERİNİN *BACILLUS SUBTILIS* ZBP4 İLE HÜCRE DIŞI BİYOSENTEZİ VE KARAKTERİZASYONU

ÖZET

Son yıllarda mikroorganizmalar aracılığıyla çinko oksit nanopartiküllerinin (ZnO NP) sentezine olan ilgi, daha güvenli bir yöntem olması nedeniyle artmıştır. Kimyasal ve fiziksel sentez yöntemlerine alternatif olarak ZnO NP'lerin biyosentezi, uygun maliyetli, çevre dostu ve geniş ölçekli üretim olanakları nedeniyle daha avantajlıdır. Bu çalışma, 1 Ocak 2021 - 1 Haziran 2022 tarihleri arasında Sakarya Üniversitesi Gıda Mühendisliği Bölümü laboratuvarlarında gerçekleştirilmiştir. Bu çalışmada, ZnO NP sentezleme yeteneğinde olan *Bacillus* suşlarının belirlenmesi ve nanopartikül biyosentezinin optimizasyonu ile nanopartiküllerin özellikle potansiyel uygulama alanlarının belirlenmesi amaçlanmıştır. Bunun için, daha önce izole edilmiş olan ve Sakarya Üniversitesi, Gıda Mühendisliği Bölümü, Gıda Biyoteknoloji kültür koleksiyonunda bulunan 45 farklı *Bacillus* suşunun ZnO NP biyosentez yetenekleri araştırılmıştır. Bakteriler nutrient broth besiyerinde 33 °C'de 24 saat geliştirilmiş ardından hücreler santrifüj yardımıyla uzaklaştırılmış ve elde edilen hücresiz süpernatantta ZnO NP oluşumu UV-VIS spektrofotometre ile absorbans taraması yapılarak belirlenmiştir. Yapılan tarama çalışması sonucuna göre bir toprak örneğinden izole edilmiş olan *Bacillus subtilis* ZBP4 spektrofotometrede 341 nm dalga boyunda yüzey plasmon rezonansından kaynaklanan nanopartiküllere özgü bir absorbans piki vermiştir. Ayrıca, beyazdan sarıya renk değişimi de nanopartikül oluşumunun bir göstergesi olmuştur. Buna dayanarak *Bacillus subtilis* ZBP4 ZnO NP sentezleme yeteneğinde olduğu anlaşılmış ve sonraki çalışmalara bu bakteri ile devam edilmiştir.

Bacillus subtilis ZBP4 ile hücre dışı ZnO NP biyosentezinin optimizasyonu için farklı reaksiyon pH'ları (5-9), sıcaklık (30-40°C), ZnSO₄.7H₂O konsantrasyonu (2-10 mM) ve reaksiyon sürelerinde (0-72 saat) biyosentezler gerçekleştirilmiştir. Biyosentez oranı reaksiyon ortamından alınan örneklerin absorbanslarının UV-VIS spektrofotometrede 341 nm dalga boyunda ölçülmesi ile belirlenmiştir. Yapılan çalışma sonucunda, *Bacillus subtilis* ZBP4'ün ZnO NP biyosentezi için optimum koşulların 8 mM ZnSO₄.7H₂O, pH 7.5 pH, 33°C ve 24 saat olduğu belirlenmiştir. Bir diğer çalışmada da ZnO NP'lerinin etkinliğini artırmak için optimum koşullarda hazırlanan biyosentez ortamına farklı konsantrasyonlarda (5, 10, 15 mg/mL) nisin eklenerek nisin yüklü ZnO NP (N-ZnO NP) üretimi gerçekleştirilmiştir. Ortama 10 mg/mL nisin eklendiğinde biyosentezin en iyi düzeyde olduğu saptanmıştır.

Çalışmanın bir diğer aşamasında optimum koşullarda elde edilen ZnO NP ve nisin-yüklü ZnO NP'lerinin karakterizasyonu yapılmıştır. Bunun için üretilen nanopartiküller santrifüj yardımıyla sıvı ortamda çöktürülüp yıkanmış ve ardından kurutulmuştur. Kurutulmuş nanopartiküllerin morfolojik özellikleri Alan Emisyon Taramalı Elektron Mikroskobu (FESEM) ve Geçirgen elektron mikroskobu (TEM) ile, elemental kompozisyonu Enerji dağılımlı X-ışını spektroskopisi (EDS), kristal yapısı

X-ışını kırınımı (XRD) spektrometresi ile belirlenmiştir. Ayrıca, zeta potansiyeli ölçümü ile nanopartiküllerin dispersiyon stabilitesi, ve Fourier Dönüşümü Kızılötesi Spektroskopisi (FTIR) ile de nanopartikül yüzeylerinde kaplama ajanı olarak görev yapan ve stabilizasyonu sağlayan organik maddelerin varlığı incelenmiştir.

TEM ile elde edilen görüntülere göre, nanopartiküllerin düzensiz küresel şekilde oldukları ve çaplarının da 50 nm'nin altında olduğu saptanmıştır. TEM analiziyle ZnO NP ve N-ZnO NP'lerin ortalama çapları sırasıyla 26 ve 23 nm olarak belirlenmiştir. N-ZnO NP'lerinin FESEM görüntülerinde nisin nanopartikül yüzeylerini ağ şeklinde kapladığı gözlenmiştir. Bu nedenle, ZnO NP'lerinin morfolojik yapısı FESEM ile net olarak görüntülenebilmesine karşın N-ZnO NP'lerinin morfolojisi incelenememiştir. ZnO NP'lerinin FESEM görüntülerinde, TEM görüntülerine benzer şekilde düzensiz küresel şekillerde nanopartiküller gözlenebilmiştir. Bu analiz ile nanopartikül boyutlarının 21-59 nm arasında olduğu ve ortalama partikül çapının da 35 nm olduğu belirlenmiştir. Enerji dağılımlı X-ışını spektroskopisi (EDS) ile elde edilen nanopartikül örneklerinin elemental dağılımı incelenmiş ve ortamda elemental Zn ile birlikte C, O, N, P gibi elementlere de rastlanmıştır. Bu çalışma ile hem nanopartiküllerin varlığı doğrulanmış hem de ortamda nanopartiküller için kaplama ajanı görevi gören ve stabilitenin artmasını sağlayan organik moleküllerin olduğu tespit edilmiştir. Yapılan ölçümlere göre, ZnO NP ve N-ZnO NP'lerinin zeta potansiyeli -19 ve -17,7 mV olarak belirlenmiş olup nanopartiküllerin dispersiyon stabilitelerinin orta seviyede olduğu anlaşılmıştır. FTIR sonuçları organik maddelerin varlığı göstermiştir. Nanopartiküllerin enerji band aralığı UV-VIS spektrumlarından yararlanılarak Tauc eşitliğinden hesaplanmış ve 3.36 eV olarak belirlenmiş olup elde edilen sonuç nanopartiküllerin yarı-iletken özellikte olduğunu göstermiştir.

Elde edilen nanopartiküllerin Gram-pozitif (*Bacillus cereus*, *Staphylococcus aureus* ATCC 25923 ve *Listeria monocytogenes* ATCC 7644) ve Gram-negatif (*Escherichia coli* Tip 1, *Escherichia coli* O157:H7 NCTC 12900, *Pseudomonas aeruginosa*)'a gıda patojenlerine karşı antimikrobiyal etkileri disk difüzyon yöntemiyle belirlenmiştir. Yapılan çalışma sonucunda hem ZnO NP hem de N-ZnO NP'lerinin tüm bakterilere karşı antimikrobiyal etkisinin olduğu, minimum inhibisyon konsantrasyonlarının da 1-2 mg/mL arasında olduğu belirlenmiştir. Ayrıca, N-ZnO NP'ler, tek başına ZnO NP'lerin ve serbest nisin etkisine kıyasla patojen bakterilere karşı yüksek etkinlik gösterdiği gözlenmiştir. Bir diğer çalışmada da nanopartiküllerin sıvı besiyerinde antimikrobiyal etkileri belirlenmiştir. Bunun için, belli konsantrasyonlarda (0, 30, 75, 150 µg/mL) nisin, ZnO NP ve N-ZnONP'leri içeren Tryptic Soy Broth'ta *Listeria monocytogenes* ATCC 7644 ve *Staphylococcus aureus* ATCC 25923 geliştirilmiş ve belli aralıklarla bakteri gelişimi Mcfarland densitometresi ile ölçülmüştür. Serbest nisin ve ZnO NP içeren ortamlara kıyasla, N-ZnO NP içeren ortamlarda bakteri gelişmesinin önemli oranlarda inhibe edildiği, 150 µg/mL ZnO NP içeren ortamın bakterisidal etki gösterdiği belirlenmiştir. Bu çalışma ile ZnO NP'lerinin nisin yüklemesiyle yüksek oranda antimikrobiyal özellik kazandığı anlaşılmıştır.

Ayrıca, ZnO NP ve N-ZnO NP'lerinin antioksidan aktiviteleri de 2,2-diphenyl-1-picrylhydrazyl (DPPH) radikalini süpürme aktivitesi analizi ile belirlenmiştir. ZnO NP'lerinin antioksidan aktivitesi düşük olmakla beraber N-ZnO NP'leri ile antioksidan aktivite iki katına çıkmıştır.

Bu çalışma sonucunda, yerel bir izolat olan *Bacillus subtilis* ZBP4'ün ZnO NP biyosentezi için kullanılabilecek özellikte bir mikroorganizma olduğu ve bununla üretilen ZnO NP'lerin iyi bir antimikrobiyal ajan olabileceği belirlenmiştir. Ayrıca

biyosentez ortamına nispeten eklendiğinde üretilen nanopartiküllerin hem antibakterial hem de antioksidan özelliklerinin önemli oranda iyileştirilebileceği ortaya konmuştur.

1. INTRODUCTION

The nanotechnology is a modern technology that provides a well-developed application of exceptionally miniature things and became important in our life. It is immensely applied in many areas such as biotechnology, the science of materials, chemistry and the food industry (Huang et al, 2007). Nanotechnology is based on materials ranging from 1 to 100 nm at least in one of the three possible dimensions, called as nanoparticles (NPs) (Sahoo et al, 2007). Currently, nanoparticles acquire attraction because of their high surface area compared with volume, lead up to give new chemical and physical properties comparing with macro-sized particles. Some of these properties are optical absorption, biological activity, melting point etc. (Di Guglielmo et al, 2010).

Zinc oxide nanoparticles (ZnO NPs) have significant importance for natural sciences because they are regarded as safe according to Food and Drug Administration (FDA). They are attractive for potential use in biomedicine and pro-ecological systems because of their known non-toxic, biocompatibility, and biodegradability. Furthermore, they have a high capability to resist environmental conditions and stability in the long term (Getie et al, 2017; Kadhim et al, 2019). They are also used in optical, semiconducting, chemical sensing, electric conductivity owing to their wide bandgap (3.37 eV), high bond energy (60 meV) and thermal and mechanical stability (Bacaksiz et al, 2008; Kulkarni et al, 2015; Kumar et al, 2013). ZnO NPs have also been proposed to be used as antimicrobial agents, in food packaging, drug delivery, and UV filtering devices (Akbarian et al, 2020; Kumar et al, 2019; Moghaddam et al, 2017; Mydeen et al, 2020; Singh et al, 2014).

Biological (which is regarded as green) synthesis of ZnO NPs is more acceptable than chemical or physical methods. It is characterized by being simple, low cost, and eco-friendly without using hazardous materials. The green methods have widely spread and as a viable method using extracts of plant, fungi and bacteria or their enzymes (Gurunathan et al, 2009; Iqtedar et al, 2020; Velsankar et al, 2020).

Unfortunately, food safety is still a big problem facing consumer's in many countries. Mead et al. (1999) reported that food-borne diseases in the United States of America (USA) cause ~76 million infections and 325,000 hospital cases. In addition to thousands of deaths every year, about >90% of deaths were food-related, known pathogens cause about 14 million illnesses, and 1.800 people die every year (Talaro and Talaro, 1992). Foodborne pathogens induced to increase in mortality rate, which included *S. aureus*, *L. monocytogenes* and *B. cereus* etc. (Van Cauteren et al, 2017). Also, antibiotic resistance of bacteria is a high prevalence, and it is considered a global problem. The overuse of antibiotics leads to the emergence of bacterial resistance among a broad range of human pathogens, which causes increased deaths. This is the reason that scientists encouraged to develop new antimicrobial substances such as nanoparticles (Hernández-Sierra et al, 2008; Kim et al, 2011). The high microbial resistance to antibiotics has made it necessary to use alternative agents to achieve control of microbial contamination and reduce the incidence of food spoilage and the resulting diseases (Singh, 2018). Consequently, nanoparticles were recently used as a new approach of eliminating harmful bacteria by depending on the fact that NPs have extremely small dimensions that make them possess alternative antimicrobial agents to overcome common resistant mechanisms (Baptista et al, 2018). The behavior of NPs is not well understood against pathogenic bacteria because it is affected by shape and size distribution.

The lactic acid bacterium *Lactococcus lactis*, a Gram-positive species, produces the antimicrobial peptide known as nisin. Nisin belongs to the family of bacteriocins and has strong antibacterial effects on a variety of Gram-positive and even Gram-negative bacteria. The two most prevalent forms of residues of nisins A and Z in 27 amino acid are histidine and asparagine, respectively. Additionally, it has a molecular weight of only about 3.3 kDa (Webber et al, 2021; Zhang et al, 2021). The previous reports showed that nisin can easily interact with the cell wall of bacteria and incorporate into peptidoglycan precursor lipid II or lipid bilayers (Crandall and Montville, 1998; Scherer et al, 2013; Wiedemann et al, 2001). In addition to excellent bacteriostatic action, nisin has exceptional safety. It has been extensively employed in the food industry and was given approval by the U.S. FDA in 1980 after being regarded as a safe safe preserver by the World Health Organization (WHO) in 1969 (Qian et al, 2021).

Therefore, the main goal of this study was developing an alternative green strategy to overcome the pathogenic bacteria using ZnO NPs alone or when conjugation with nisin. In order to achieve this goal, biosynthesis of ZnO NPs by bacteria was carried out using the supernatant of *Bacillus subtilis* ZBP4 and biosynthesis conditions were optimized to increase the synthesis rate. Then, nisin-ZnO NPs (N-ZnO NPs) conjugates were synthesized using the same bacterial supernatant for increasing the antimicrobial effect of the nanoparticles. Both ZnO NPs and N-ZnO NPs were characterized using different methods including UV-VIS spectrophotometer, FESEM, XRD, EDX and FTIR. In vitro inhibitory effect of the biosynthesized nanoparticles on common foodborne pathogen microorganisms have been determined, comparatively. Antioxidant properties have also been determined.

2. LITERATURE REVIEW

2.1. Nanotechnology

The nanotechnology deals with the production, characterization, exploration, and application of nanosized materials to develop science (Theron et al, 2008). The nano means small in size (is a Greek word) and it was posted almost half a century ago (Bhattacharya et al, 2019; Rajamani et al, 2013). The International Organization for Standardization (ISO) defined the nanomaterials in 2015 (ISO/TS 80004) as nanoparticles and nanofibers and confirmed the nanoscale level at least for one dimension between 1 to 100 nm (Bhattacharya et al, 2019). Nanoscience is the study of phenomena and manipulating materials in sizes not exceeding nanoscale limits (Buzea et al, 2007).

Nanostructures can be classified according to the source (natural, incidental and engineered), according to the phase of material (nanocomposite, nanofoam, nanoporous) and according to the number of dimensions at the nanoscale which is 1D (nanosheet), 2D (nanotube) and 3D (nanoparticles) (Bratovčić et al, 2015).

2.2. History of Nano Science

Nanotechnology has a long history, about 400 BC (Mohammadi and Ghasemi, 2018). Since ancient times, the Romans have used some metal nanoparticles to make Lycurgus cups. Due to the use of these nanoparticles in the glass, the light dispersion and absorption give different colors to the depiction of the death of one of their Kings (Freestone et al, 2007). Up to the Middle Ages, gold in soluble form was thought to have good curative properties for various ailments, including dysentery, epilepsy, and heart disease. It was also helpful in detecting diseases such as syphilis. The history of nanoparticles has been recounted by Daniel and Astruc Ages from ancient times through the Middle Ages (Daniel and Astruc, 2004).

The term "nanometer" was first proposed by 1925 Chemistry Nobel Laureate Richard Zsigmondy. He invented the term "nanometer" to define particle size and was the first to use a microscope to quantify the size of particles like gold colloids. (Hulla et al, 2015). Norio Taniguchi mentioned the word "nanotechnology" for the first time in

1974 when he presented research that included separating, binding and changing matter by atom and molecule and forming nanomaterials with high accuracy (Bhattacharjee, 2019).

The Chinese and Indians also used nanotechnology in different arts. Photography was developed in the 18th and 19th centuries by using silver at the nanoscale level. The scanning tunneling microscope (STM) was invented at IBM, which opened up a wide space for the advancement of nanosciences and technologies (Pfeiffer et al, 1997). After that, developments continued and led the scanning tunnel microscope to develop another microscope called the atomic force microscope, These instruments were used for the imaging surface and movement of individual atoms (Drexler, 1986).

The dawn of the 21st century saw nanotechnology flourish; the actual birth of nanotechnology began from famous words by the physicist Richard, Nobel Prize Winner of the American Physical Society in 1959, he said, "Nature has been working at the level of atoms and molecules for millions of years, so why do we not?" He also mentioned the possibility of dealing with individual atoms and molecules and finding ways to move them independently to obtain the required size (Mansoori and Soelaiman, 2005). An American physicist Eric Drexler, the de facto founder of nanotechnology, published a book entitled Engines of Creation in 1986 (Drexler, 1991). One of the most significant uses of nanotechnology in molecular biology is to increase the scale and complexity of self-assembled DNA a "one-pot" process, Paul Rothmund invented "scaffolded DNA origami" in 2006 (Bayda et al, 2019).

2.3. Application of Nanotechnology

Nanotechnology has many applications in our daily lives and is responsible for changing and developing the life of the people and society (He et al, 2019). Nanotechnology was applied in various aspects such as biotechnology, agriculture, food preservation, textile, and the environment (AL-Tamimi, 2021).

Many studies have been carried out on the application of nanotechnology in medicine such as treatment, diagnosis, and control of diseases caused by resistant microorganisms, which is one of the challenges that face humanity. For that, nanotechnology is one of the proposed solutions to eliminate resistant microorganisms (Singh et al, 2008a). Nanobiotechnology has been used as drug delivery to overcome

drug deficiencies to treat respiratory diseases (Luo et al, 2021), wound healing (Pachau, 2015), and anticancer (Suri et al, 2007).

Nanotechnology has brought a new industrial revolution in developed countries particularly in the food chain, including food processing, food packaging, storage, and quality monitoring (Neethirajan and Jayas, 2011). Nanotechnology applications in the food field and agriculture range from seed germination to the creation of on-demand interactive food agriculture includes everything from seed germination to the production of interactive, allowing the consumer considerably nutritional needs (Iqbal et al, 2021; Rawat, 2021; Sahani and Sharma, 2021). Several current studies have reported the detection of mycotoxins and pathogenic bacteria in food; these nano biosensors have wide application in microbial quality and safety monitoring in foods, including antibiotics, pesticides, heavy metals, aflatoxin, and adulterants (Gothandam et al, 2020).

The World Health Organization (WHO) and Food and Drug Administration (FDA) has issued guidelines regarding nanoparticles in cosmetics. Different types of NPs have been used in healthcare or cosmetics including ZnO, TiO₂, and AuNPs (Yadwade et al, 2021).

Nanotechnology has also been used in electronics, photonics, renewable energy, construction, textiles etc. (Asif and Hasan, 2018; Korkin et al, 2015; Zhu et al, 2004).

2.4. Methods of Nanoparticles Synthesis

The two practical methods in the nanotechnology field are known as top-down and bottom-up, which are the basic to crucial qualitative advancements in the field of nanoparticle synthesis as described in Figure (2.1). The bulk material is broken down into smaller molecules, which are subsequently transformed into nanoparticles. Top-down synthesis methods include grinding or milling, physical vapor deposition, and other damaging methods (Iravani, 2011). Naveed Ul Haq et al. (2017) have shown various chemical and physical synthesis routes have been used in the production of ZnO NPs including liquid phase synthesis, gas-phase synthesis, laser ablation etc.

Bottom- up process is dealing with particles created by the chemical assemblage of atoms or molecules, the bottom-up approach adheres to the same rules of molecular recognition as nucleotide synthesis from scratch. Biological and chemical methods are

examples of bottom-up approaches (Aldaimy, 2022). In "Bottom Up" synthesis, which focuses on reduction/oxidation as the primary reaction, NPs are created from small entities like atoms and molecules (Hussain et al, 2016). For example, sedimentation, reduction techniques (Khan et al, 2019), sol-gel processing (Parashar et al, 2020), and chemical vapor deposition (Singh et al, 2008b).

Physical and chemical routes are not desirable compared with the biological routes because these methods need to use of harmful materials to obtain the nanoparticles in addition to the high pressure and energy, employing biological agents for producing nanoparticles such as extract of plants, bacteria and fungi (Singh, 2018). The disadvantages of physical and chemical processes are high cost, need a long time, and generate waste from the chemical materials (Kharissova et al, 2013).

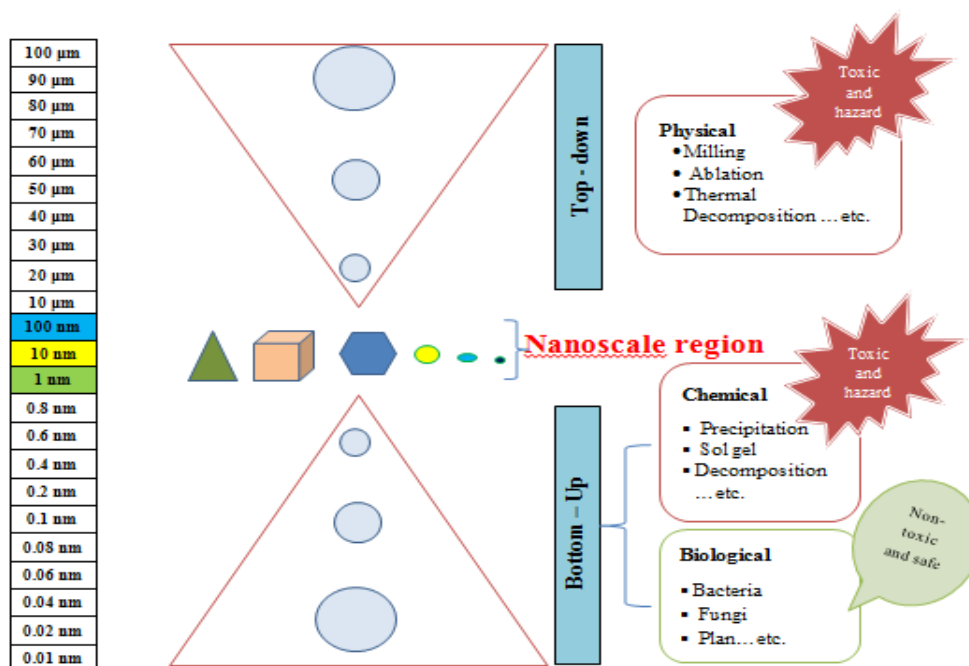


Figure 2.1. Top-down and bottom-up approaches for synthesis inorganic nanoparticles, this figure deduced by Azharuddin et al. (2019).

2.5. Biological Synthesis of Nanoparticles

Green technology is a promising method in the nanotechnology industry. It has been considered as safe, cheap, environmentally friendly, and less energy consuming, as it does not require high pressure and hazardous chemicals (Hussein et al, 2019; Nadaroğlu et al, 2017). The biosynthesis of nanoparticles by using microbes can be achieved either intracellularly or extracellularly (Figure 2.2) (Wong and Mann, 1996).

The intracellular synthesis is carried out after the ions are introduced into the cell, where the ions are converted into nanoparticles with the existence of enzymes (especially nitrate reductase), and coenzymes (NADH) (Prakash et al, 2010). The extracellular synthesis occurs after cell surface detention of the ions. The reaction of zinc with secreted organic components (like enzymes and sugars) provides the conversion of ions into nanoparticles (Salunke et al, 2015). Practically, extracellular synthesis is easy, economical, and does not require additional steps to obtain purified nanoparticles. For this reason, the extracellular approach has increased interest more than the other approaches (Deljou and Goudarzi, 2016; Markus et al, 2016).

Even more attention has been focused on the green synthesis of zinc oxide nanoparticles using biological material as the reducing and stabilizing agents (Bandeira et al, 2020), The authors described a biological method for producing zinc oxide nanoparticles by utilizing *Lactobacillus* spp (Suba et al, 2021), *S. aureus* (Rauf et al, 2017), *Sargassum muticum* (Sanaeimehr et al, 2018) and leaf extracts of *Cassia fistula* (Naseer et al, 2020).

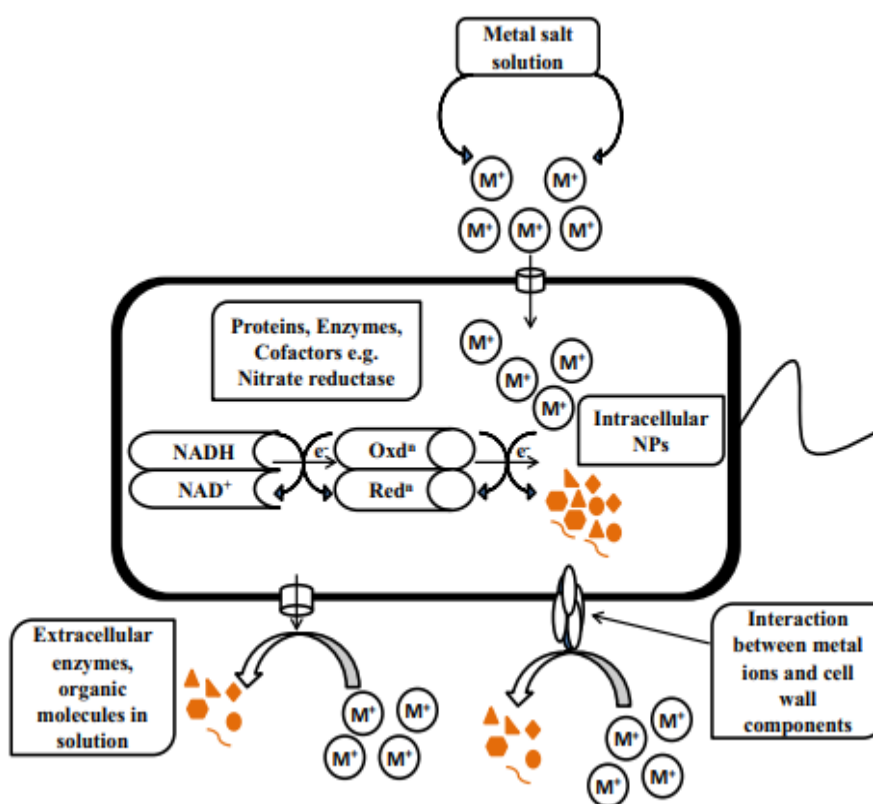


Figure 2.2. Mechanism of nanoparticle synthesis by microorganisms (Salunke et al, 2016).

2.6. Zinc Oxide Nanoparticles

Zinc Oxide is a material with many uses that is both strategic and multipurpose. A few examples of the materials and goods that contain ZnO powder include ceramics, glass, cement, rubber (such as car tires), lubricants, paints, ointments, adhesives, plastics, sealants, pigments, foods (a source of Zn nutrition), batteries, ferrites, and fire retardants (Sabir et al, 2014). In materials science, it is known as an II-VI semiconductor since zinc and oxygen are in the 2nd and 6th groups of the periodic table (Gong et al, 2007). It has attractive properties including a wide direct band gap (E_g) of 3.37 eV at room temperature (Kumar et al, 2013), high bond energy (60 meV) (Kulkarni et al, 2015), high optical gain, high thermal and mechanical stability at room temperature (Gümüő et al, 2006) and luminescence as well as piezoelectric properties (Lima et al, 2001). Thus those properties make it attractive for potential use in related applications (Bacaksiz et al, 2008).

Zinc Oxide is a piezoelectric and pyroelectric material that can be used as a photocatalyst, sensor, converter, energy producer, and energy storage device. Because of its hardness, stiffness, and piezoelectric constant, it is utilized in the ceramics industry (Chaari and Matoussi, 2012; Wang, 2008). The Zn atoms are tetrahedrally coordinated to four O atoms, where the Zn d-electrons combine with the O p - electrons to form a hybrid. Zinc atom-occupied layers alternate with oxygen atom occupied layers as shown in Figure 2.3 (Pearton et al, 2003). ZnO structures are wurtzite (hexagonal) and zinc blende (hexagonal) or cubic.

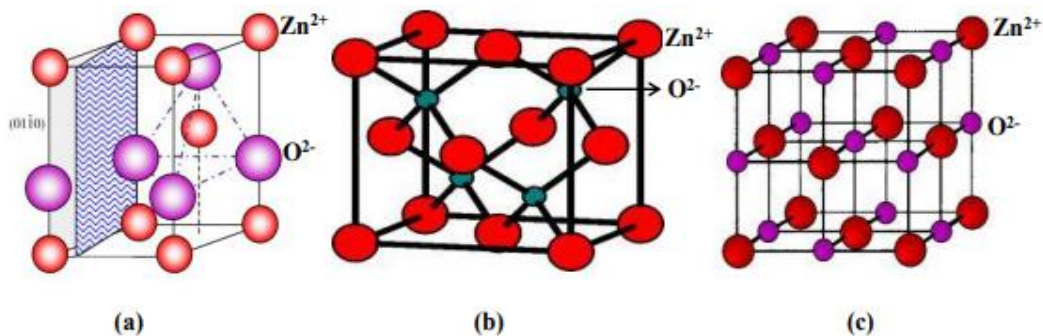


Figure 2.3. The description of ZnO structures: (a) hexagonal wurtzite, (b) zinc blende and (c) rock salt (Yıldırım, 2014).

In addition to splendid optical and electrical properties, ZnO is regarded as safe (according to FDA), thus it is an attractive substance for natural sciences (Kadhim et

al, 2019). The daily requirement of zinc for human is 10-15 mg (Siddiqi et al, 2018). Table 2.1 shows some physical properties of ZnO.

Table 2.1. Some physical properties of ZnO.

| Property | Value |
|-------------------------|--------------------------|
| Density | 5.606 g cm ⁻³ |
| Melting point | 1975 °C |
| Thermal conductivity | 0.6, 1–1.2 |
| Refractive index | 2.008, 2.029 |
| Electron effective mass | 0.24 |
| Type of semiconductor | n-type |

2.7. Bacterial Synthesis of Zinc Oxide NPs

Several reports introduced the synthesis of ZnO NPs from bacteria including Lactic acid bacteria, *Bacillus* spp., *Bacillus subtilis*, *Streptomyces* sp., *Lactococcus lactis* etc. Kadhim et al. (2018) showed that *Lactococcus lactis* spp. was capable to synthesize ZnO NPs at 31-36 nm diameter which inhibited the skin infecting bacteria and had anti-virulence factors activity. Selvarajan and Mohanasrinivasan (2013) successfully fabricated quasi-spherical ZnO NPs with a size range between 7-19 nm by using nonpathogenic bacteria *Lactobacillus plantarum* VITES07. The biosynthesis of ZnO NPs was reported using *B. cereus* MN181367 after optimizing reaction conditions, at 37 °C temperature, reaction time 48h , pH 9, and 0.01 M substrate concentration (Iqtedar et al, 2020). Zinc oxide nanoparticles of 50 nm size were reported to be synthesized by *Bacillus haynesii* isolated from the leaf of a date palm plant and the synthesis was done by combining 100 mL of zinc sulfate solution (1 mM) with 100 mL of CDL3's cell-free supernatant, and the combination was properly mixed by magnetic stirrer for 24 hours (Rehman et al, 2019). Using novel halo-alkaliphilic *Alkalibacillus*, biosynthesis of 17.5 nm-sized ZnO NPs was done and the nanoparticles were synthesized using an aqueous metal solution of 1 mM ZnSO₄·7H₂O under incubation temperature 35 °C (Al-Kordy et al, 2021). The extracellular biosynthesis of ZnO NPs using the supernatant of *B. cereus* and 0.1 M ZnSO₄·7H₂O, the nano size of NPs ranging between 21-35 nm, spherical and crystalline in appearance, as shown by TEM, SEM, Also XRD, and EDX results validated the presence of pure ZnO (Ahmed et al, 2021). Pomastowski et al, (2020) synthesized ZnO NPs using the

supernatant of *Lactobacillus paracasei* under shaking at 37 °C for 1 day. Ebadi et al. (2022) used cell filtrates of *Desertifilum* sp. EAZ03 to achieve ZnO NPs production. *Leuconostoc mesenteroides* supernatant is a unique natural source for the production of ZnO NPs and the creation of nanoparticles was established by detecting the white color precipitation (Kadhim et al, 2019). Sabir et al. (2020) reported the bacterial mediated synthesis of ZnO NPs using *Bacillus subtilis*, and significance of nutrition in supporting plant growth was established. Another example is the work of Busi et al. (2016), who carried out the synthesis of ZnO NPs by using cell-free filtrate after *Acinetobacter schindleri* culturing and zinc nitrate $Zn(NO_3)_2$ solution as a precursor.

To generate of ZnO-functionalized textile substrates has been reported by Jayaseelan et al. (2012). In the research, ZnO NPs were synthesized biologically using *Aeromonas hydrophila* at 30 °C for 1 day until white precipitation started. Similarly, Kundu et al. (2014) also investigated the production of biogenic ZnO NPs in the presence of 0.1 M $ZnSO_4 \cdot H_2O$ using *Rhodococcus pyridinivorans* bacteria at 30 °C. It was found that bacterial mediated NPs were moderately stable, hexagonal phase, and roughly spherical. However, different species of bacteria are utilized in microbiological processes to create ZnO NPs at a temperature of 37 °C. (Fatholahi et al, 2021; Jayabalan et al, 2019; Mahdi et al, 2021; Suba et al, 2021). A brief description of the biosynthesis of ZnO NPs using bacteria is shown in Table (2.2).

2.8. General Characteristics of *Bacillus* spp

The species of this genus are characterized by their rod-shape, and Gram-positive properties. Some of them are aerobic, and the other facultative anaerobic, including *B. cereus*. Endospore inside the cell at the cell center or end can be found. They usually form chains. Although they are mesophilic in character, psychrophilic and thermophilic types are also available. They utilize proteins by producing acid without the gas formation and convert the proteins to ammonia, which causes odor (Akçay, 2017; Baruzzi et al, 2011). The bacteria can not tolerate low acidity, however, they are resistant to high temperatures and other harsh conditions owing to their spores. Some types have transformed into vegetative cells after 150 thousand years (Maza et al, 2020). Most species of *Bacillus* are non-pathogenic, as well as their products, are considered safe for intended use in the medicine.

Bacillus subtilis can be isolated from soil and it is widely used in numerous industries such as enzyme (lysozyme, cellulase etc.) production (Ghadiri et al, 2021; Mahmoud et al, 2021; Naveed et al, 2022), and vitamin (vitamin K2, biotin, folic acid and riboflavin etc.) production (Baruzzi et al, 2011; Zhao et al, 2021). It has been known for more than 50 years that *B. subtilis* has the ability to produce antimicrobials. *B. subtilis* produces a large number of peptide-based antimicrobials, including subtilin, subtilosin A, ericin, and sublancin (Avcı et al, 2017). Due to their role in the creation of antimicrobials, many *Bacillus* species are considered one of the biological control methods, which are widely used in medicine and the pharmaceutical materials (Amin et al, 2015).

Table 2.2. The bacterial used in biosynthesis of ZnO NPs.

| Bacteria sp. | localization | Shape | Size (nm) | Application | References |
|--------------------------------|---------------|-----------------|-----------|---------------------------------------|----------------------------|
| <i>Lactobacillus paracasei</i> | Intracellular | spherical | 7–19 | antibacterial activity | (Król et al, 2018) |
| <i>Proteus mirabilis</i> | intracellular | quasi-spherical | 19.1 | antimicrobial activity | (Eltarahony et al, 2018) |
| <i>Bacillus subtilis</i> | Extracellular | quasi-spherical | 20 -30 | - | (Shamsuzzaman et al, 2014) |
| <i>Streptomyces</i> sp. | Extracellular | spherical | 20–50 | anticancer and antibacterial activity | (Balraj et al, 2017) |
| <i>Halomonas elongata</i> | Extracellular | spherical | 18.11 | Antibacterial activity | (Taran et al, 2018) |
| <i>Lactococcus lactis</i> | Extracellular | nano-spheres | 55- 60.5 | Electrochemical sensors | (Mahdi et al, 2021) |
| <i>Bacillus</i> sp. | Extracellular | nano-rods | 99 | Electrochemical sensors | |
| <i>Bacillus</i> sp. | Extracellular | spherical | 57.72 | anticancer and antimicrobial activity | (Hanumith et al, 2018) |
| <i>Bacillus subtilis</i> ZBP4 | | | | | Present study |

2.9. Application of Zinc Oxide NPs

Nowadays, industries are booming and developing at the expense of pollution at an alarming rate. Therefore, the materials used must be selected very carefully and meticulously. In this regard, ZnO NPs have shown potential for a variety of applications because ZnO is non-toxic and environmentally eco-friendly, and also it has attractive properties such as photocatalytic, electrical, electronic, optical, dermatological, and antibacterial properties (Becheri et al, 2008). ZnO NPs are used in dermatology including drug delivery to skin, cosmetic and personal health care providing strong UV absorbers, thus ZnO NPs gain the consumer's desired characteristics (Jiang et al, 2018; Papakostas et al, 2011).

They were also used in the textiles area, with a focus on the uniqueness and processes of ZnO action that impart distinctive characteristics to textile fibers. It can be applied in the rubber industry to increase or improve the performance of polymer and protect rubber composite from wear Moghaddas et al. (2020).

The researchers prepared an electrochemical sensor based on ZnO NPs and used it to detectable each ascorbic acid, dopamine, and uric acid at low concentrations (Pan et al, 2020). ZnO NPs have been utilized as sensors to detect biomolecules. According to Muthuchamy et al. (2020), the presence of ZnO NPs sensors has been used to detect cysteine and NADH. In addition, ZnO nanowire-reduced graphene oxide nanocomposites helped detect ammonia (NH₃) at room temperature (Wang et al, 2017).

A variety of metal nanoparticles were created and produced by researchers, especially ZnO NPs which are used for the delivery of chemotherapeutic agents to treat cancers. Sadhukhan et al. (2019) demonstrated that phenylboronic acid (PBA) conjugated ZnO NPs (PBA-ZnO), loaded with quercetin can act as cytotoxic potential on breast cancer cells (MCF-7). ZnO NPs have also been used for wound healing (Batool et al, 2021), diabetes treatment (San Tang, 2019), and anti-inflammatory (Nagajyothi et al, 2015).

The major benefit credited to ZnO NPs is that they can be used in food preservation. Biogenic fabrication of ZnO NPs showed that number of *L. monocytogenes* and *Salmonella* Typhimurium decreased with increasing of NPs concentration in film, so these film containing ZnO NPs is considered a suitable packaging material the preservation of smoked salmon with minimum defects (Baek and Song, 2018). ZnO

NPs can serve as effective bactericidal materials against *S. aureus*, *E. coli*, and *P. Aeruginosa*. Amjadi et al. (2019) performed the synthesis of nanocomposite film; using the gelatin-based nanocomposite containing chitosan nanofiber and the film was proposed to improve shelf life and quality of cheese and poultry meat.

2.10. Application of ZnO NPs as Antimicrobial Agent

Today, scientists connected technology with other sciences, especially biology, to develop antimicrobial agents. There are many available documents about some metal NPs like zinc (Pasquet et al, 2014), silver (Rajamani et al, 2013) and gold (Bindhu and Umadevi, 2014), which exhibit interesting antibacterial activity. ZnO NPs are considered as antibacterial agent against *K. aerogenes*, *P. aeruginosa*, *E. coli*, and *S. aureus* (Agarwal et al, 2018; Kim et al, 2017; Xie et al, 2011). For instance, it also showed slightly higher efficacy against multiple resistant bacteria such as *E. coli* (Melencion et al, 2020; Rai et al, 2012). Moreover, it can reduce the number of microorganisms on biomedical surfaces (Spirescu et al, 2021). *Acinetobacter schindleri* SIZ7 has been screened and successfully used to fabricate ZnO NPs and the results showed that 100 $\mu\text{g mL}^{-1}$ of these nanoparticles was able to eliminate *E. coli* and *S. enterica* bacteria (Busi et al, 2016). The previous studies revealed the bactericidal effect of ZnO NPs in combination with antibiotic against different microorganisms including *E. coli*, *Klebsiella* spp., *B. subtilis* and *Streptococcus* spp. (Tyagi et al, 2020). A study by Bhande et al. (2013) demonstrated a synergistic effect of cefotaxime, ampicillin, ceftriaxone, cefepime antibiotics with zinc oxide nanoparticles on inhibition of *E. coli*, *K. pneumoniae*, *S. paucimobilis*, and *P. aeruginosa*.

2.11. Mechanisms of Action of ZnO NPs

The antibacterial activity of NPs is mediated by three different mechanisms: damage of cell wall and cell membrane, intracellular damage, and cause oxidative stress (ROS) (Wang et al, 2017). Previous studies confirm with evidence that NPs can affect directly on cell wall or cell membrane and damage its structure, but indirectly effects on protein synthesis and DNA damage, beginning with the producing of reactive oxygen species, and then inhibition many metabolism of bacteria like enzymes synthesis and electron transport chain (Chamundeeswari et al, 2010; Dizaj et al, 2014; Johnston et al, 2010).

The antibacterial effect of nisin-loaded chitosan nanoparticles is that the nanoparticles penetrate the cell membrane, this causes the membrane to lose its permeability, and at the same time it develops pores and eventually leads to its disruption (Lee et al, 2018). Figure 2.4 show mechanisms of NPs action in bacteria cells.

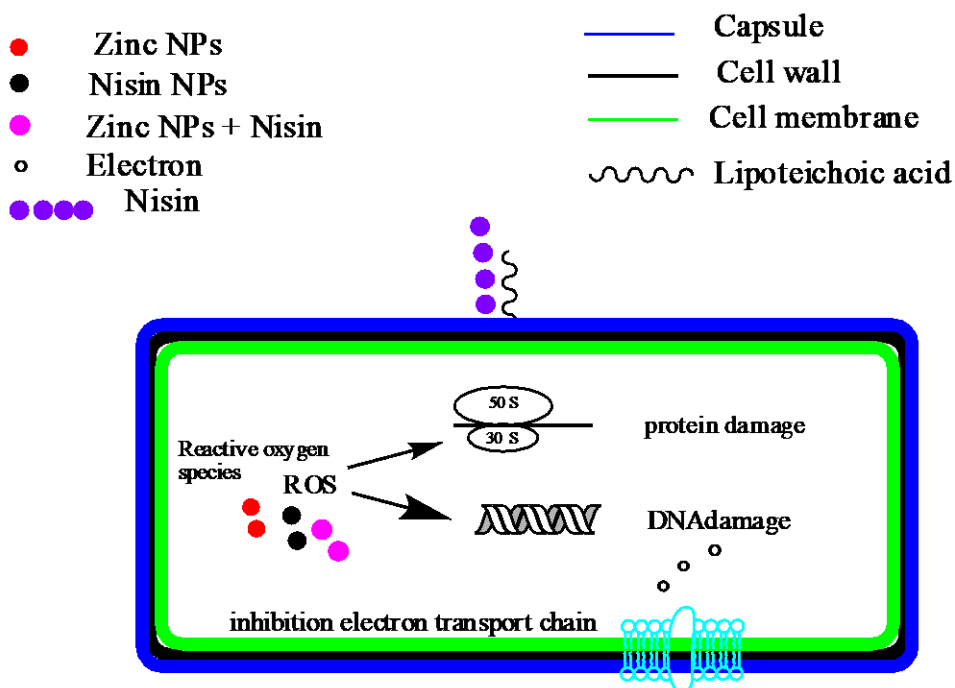


Figure 2.4. The strategies that NPs impact on bacteria cells.

2.12. Nanoparticle Conjugates

The nanoparticles must be able to reach the required location of action to be effective in biological applications; simply being able to achieve their intended goal is not enough. Penetrating microorganism cell walls by NPs is one of our most significant challenges; breaking down these barriers is one of biomedicine's largest difficulties. Polyethylenimine (PEI)-capped AuNPs have high transfection efficiency and antibacterial activity. Their positive charge leads to an extensive bacterial contact area, which causes a loss of permeability and cell death. In addition, peptide conjugated NPs can further improve cellular uptake; also, concentrate and preserve plasmid DNAs with reduced cytotoxicity (Peng et al, 2016). The researchers used CM-SH as a capping agent for preparing CM-SH-Au NPs. the thiol in the C terminal of AMP plays a significant role in the synthesis CM-SH-Au at the nanoscale with one step, and the condensing peptides around the nanoparticles increase their stability and antimicrobial activity (Rai et al, 2016). Poly (lactide-co-glycolide) (PLGA) nanoparticle-colistin

conjugate-assisted delivery of antimicrobial peptide effectively eliminates multi-drug resistant *P. aeruginosa*. The peptide-loaded NPs are considered promising drug candidates because they effectively penetrate into a bacterial biofilm and the decrease resistance developed by the target cell. Recently, a group of researchers have prepared stable antimicrobial peptide capped silver nanoparticles (Darwish and Salama, 2022; Gakiya-Teruya et al, 2020), gold nanoparticles (Amarasekara et al, 2022), gold/silver nanohybrids (Bajaj et al, 2017).

Other studies showed that peptide conjugated NPs with different size protect of influenza virus infection by conjunction with nanoparticle engineering, peptide ligands can be loaded and further changed to bind to diverse receptors (Alghair et al, 2019; Dykman et al, 2018; Lauster et al, 2017).

Usually, electrostatic interactions or covalent coupling techniques are used to bind cell-penetrating peptides (CPPs) to NP surfaces. The unspecific binding that results from the covalent attachment of CPPs by many amino and carboxylic acid groups can change the functioning of the molecular structure. Although the interactions between CPPs and NPs at the molecular level are not fully understood, their self-assembly on the surface of negatively charged NPs is greatly facilitated by the typically high positive net-charge of CPPs (Gessner and Neundorf, 2020).

Tumor tissue structural and functional abnormalities present numerous chances for NP penetration. Lanreotide peptide-gold nanoparticle conjugates can function to enhance the uptake of cancer cells (MCF-7 and AR42J). Conjugation of a peptide to AuNP helped uptake 2–3 times via the clathrine-mediated endocytosis route. Since AuNP and peptides exhibit significant electrostatic interactions due to different charges, it has been found that the pH of the solution is crucial for both their binding and colloidal stability (Shelar et al, 2020). The intestinal epithelial cells and the drug-loaded CSK-TMC conjugates interacted electrostatically. Also, the cellular uptake mechanisms depend on adsorptive-mediated peptide NP conjugates; depending on the time, the cell transport of the drug is relatively more than normal drug solution (Chen et al, 2018). The high cytotoxicity of hydrophobic peptides ZnO NP complex against cancer cells (HT29 cell) is attributed to hydrophobic amino acids; when the hydrophobic amino acids are introduced into the cell membrane, they form a stable structure that causes pores to form, which causes cell death by either necrosis or apoptosis (Bai Aswathanarayan et al, 2018).

NPs can easily be functionalized with peptides to create targeted agents that bind to surfaces with high affinity, making them useful in biomedical applications, particularly as drug delivery systems (Bourgat et al, 2021), immunogenicity assessment (Cheng et al, 2019; Farfán-Castro et al, 2021), treatment of Alzheimer's disease (Fan et al, 2018; Zhang et al, 2014).

2.13. Nisin Peptide and Nisin Loaded NPs

Nisin is a ribosomally synthesized peptide that is composed of 34 amino acid residues, and is one of the important natural antimicrobial agents. Nisin is a bacteriocin synthesized commercially using *Lactococcus lactis* and in many countries. It is allowed in some applications as a food preservative (Jones et al, 2005; Luo et al, 2019). It is known to exhibit antimicrobial activity against various Gram-positive bacteria, including *S. aureus*, *B. cereus* and the foodborne pathogens *L. monocytogenes* and *Clostridium botulinum* (Khusainov et al, 2013). The Food and Agriculture Organization of the United Nations (FAO) and The World Health Organization (WHO) documented that nisin is safe for human consumption and easily degraded by protease. Additionally, it is heat-stable, flavorless, and tolerant to low pH (Roshanak et al, 2020).

Recently, antimicrobial peptides have been incorporated into metal nanoparticles, to improve the antimicrobial efficacy. Mirhosseini (2016) has reported that nisin and heat enhanced the antibacterial action of MgO NPs due to increased distortion and cell wall damage. Cationic peptide-conjugated silver NPs exhibited significant antimicrobial inhibition against *E. coli* and *C. albicans* compared with peptide-conjugated gold NPs and unconjugated gold/silver nanoparticles (Bajaj et al, 2018). Jin and Gurtler (2011) inactivated *Salmonella* spp. in liquid egg white by storing in the jars coated with nisin, allyl isothiocyanate, and ZnO NPs. The use of a combination of chitosan-zinc oxide nanocomposite and nisin allowed inducing a synergistic effect, therefore completely inactivating *L. monocytogenes* in white cheese under storage at low temperature (4 °C) for 14 days (Divsalar et al, 2018). Zhao and Kuipers (2021) reported bactericidal activity of silver-nisin nanoparticles against clinically isolated multidrug resistance strains from wound infections including *A. baumannii*, *P. aeruginosa*, *E. coli*, *K. pneumoniae* and *S. aureus*.

2.14. Nanoparticles Characterization

The detection of the properties of nanoparticles prepared by different methods in shape, size, scattering, and other properties are done using many techniques such as ultraviolet-visible spectroscopy (UV-VIS), FESEM, EDS spectroscopy, X-ray diffraction technique, and Fourier Transform Infrared spectroscopy (FTIR) etc. UV-VIS spectroscopy is the simple and efficient method used to determine surface plasmonic resonance (SPR) peak in the range flanking ultraviolet-visible spectral region, the work of UV-VIS spectroscopy-based on Beer-Lambert Law which refers that the ratio of radiation absorbed to the number of the absorbing molecules in its path (Perkampus, 2013). Wood was the first to explain the phenomena of anomalous diffraction on diffraction gratings caused by the activation of surface plasma waves at the turn of the 20th century (Wood, 1902). Gustav Mie discovered in 1908 that when light interacts with metal nanoparticles, the metal-free electrons collectively oscillate about the nanoparticle lattice in resonance with the light field. The surface plasmon resonance is the name of this phenomenon (Jain et al, 2007).

X-Ray Diffraction (XRD) is an analytical technique used to analyze both molecular, crystal structures, and grain size of the sample through irradiation of X-rays and observing the spectra. X-ray diffraction is applied to identify the structure of NPs and compared with card no, published by International Center for Diffraction Data (ICDD) or Joint Committees on Powder Diffraction Standards (JCPDS) (Janaki et al, 2015; Wojcieszak et al, 2017). Thakur et al used X-ray line broadening to calculate the average crystallite size of ZnO NPs, and found to be between 27 and 54 nm (Thakur et al, 2021). Moreover, the measuring of XRD, the crystal nature was cubic and the crystalline levels formed were (101) and the highest peak was 36.20° (Pillai et al, 2020). Iqbal et al. (2022) measured full-width half maximum (FWHM) of peak to calculate the average crystallite size of powder ZnO NPs using X-ray line broadening, and it was measured at 36 nm.

Transmission Electron Microscope (TEM) is a powerful imaging technique for characterizing nano-materials. A heated filament (such as one made of tungsten or laB6) used in TEM produces an electron stream. With the use of an electron beam source, the electron beam is focussed second condenser lens after the first condenser lens sample condenser aperture objective lens first intermediate lens objective aperture additional intermediate lens a projector's lens, only the electrons that pass through the

sample unimpeded at the end hit the phosphor screen after the electrons interact with the sample (Fultz and Howe, 2012; Wang et al, 2018).

Field emission scanning electron microscope technique is widely used to characterize of NPs. It provides topographic information by scanning over the surface with the highest resolution (0.01nm). The scanning electron microscope directs high energy of electrons from source to specimen under a vacuum system, scattering electrons detected by the detector and converting this signal into an image (Hernández-Sánchez and Gutiérrez-López, 2015).

Another technique used in nanomaterials characterization is FTIR, FTIR that helps in the determination of the composition of functional groups in the sample by measuring to interpret the data gathered from all the wavelengths passing through the sample into the actual spectrum, the absorption of radiation ranges between (4000–400 cm^{-1}) (Mourdikoudis et al, 2018).

There are some other techniques used to study the properties of nanomaterials like zeta potential, which represents the particle surface charge, is a crucial and popular technique for characterizing nanometer-sized particles in liquids. Because the zeta potential varies on a number of variables, including the ion concentration, ion valence, pH level, surface roughness, and solution temperature (Liu, 2021). Two electrodes are located in a cell that has been introduced with a dispersion. When the samples are exposed to an electrical field, particles having a net charge will move toward the electrode that is negatively charged at a velocity known as the mobility that is linked with their zeta potential (Marsalek, 2014; Skoglund et al, 2017).

3. MATERIALS AND METHODS

3.1. Materials

3.1.1. Microorganisms

In the preliminary screening tests for the biosynthesis of ZnO NPs, a total 45 *Bacillus* strains were used that had previously been identified and saved in the Biotechnology Culture Collection at Department of Food Engineering, Sakarya University. The sources and the codes of the *Bacillus* strains are given in Table (3.1). Pathogen microorganisms (*E. coli* O157:H7 NCTC 12900, *S. Typhimurium*, *S. aureus* ATCC 25923 and *L. monocytogenes* ATCC 7644) that were used in the antimicrobial activity studies were provided by Dr. Serap Cosansu (Sakarya University, Department of Food Engineering), and *P. aeruginosa* by Dr. A. Kadir Halkman (Ankara University, Department of Food Engineering). All the microorganisms were kept in nutrient broth and 25 % glycerol with 1:1 (v/v) at – 45 °C

Isolates were obtained from soil and food sources used in the study

Table 3.1. Isolates were obtained from different sources used in the study.

| Isolates | Sources | City |
|--|--------------------------|------------------|
| EBTA 1, 2, 3, 4, 5, 6 and 7 | Fermented food (Tarhana) | Istanbul |
| SBT 7, 8, 9, 10 and 12 | Soil | Sakarya |
| ZBP 1, 2, 3, 4, 5, 6, 7, 8, 9, 10, 11, 12, 13, 14 and 15 | Soil | Geyve/ Sakarya |
| ZGT 5 and 9 | Soil | Geyve/ Sakarya |
| GIT 2 | Soil | Istanbul |
| EKT1 | Soil | Industrial area |
| BAT3 | Soil | Akyazı/ Sakarya |
| MDD1 | Soil- metals river | Sakarya |
| MDF1 | Soil- metals river | Sakarya |
| MDG 2 and 3 | Soil- metals river | Sakarya |
| MDH1 | Soil- metals river | Sakarya |
| MDI 5 | Soil- metals river | Sakarya |
| MDB1 | Soil- metals river | Sakarya |
| MDC1 | Soil- metals river | Sakarya |
| BMZE4 | Olive | Sakarya |
| AKS2 | Soil | Seydişehir/Konya |
| BAST2 | pickles | Sakarya |
| HTA 1 and 2 | Fermented food (Tarhana) | Düzce |

3.1.2. The laboratory instruments

The instruments used in the study are listed in Table 3.2.

Table 3.2. Laboratory instruments, company and origin used in the study.

| Instrument | Manufacturer company |
|--------------------------|---|
| Autoclave | WiseClave WAC-80 (Korea) |
| Burner | Shandon (England) |
| Centrifuge | Hettich Universal 320 R (Germany) |
| Distillator | Nüve ND8 (Turkey) |
| Incubator | Microtest (Turkey) |
| Hood | - |
| Loop | HiMedia (India) |
| Micropipette | Hamilton (USA) |
| Oven | Microtest min (Turkey) |
| Refrigerator | Profile (Turkey) |
| Deep freeze Refrigerator | DF 590 (Turkey) |
| Sensitive balance | Radwag AS 220.R2 (Poland) |
| Spectrophotometer | Shimadzu UVmini-1240 (Japan) |
| Water bath | WiseBath WSB-30 (Korea) |
| Shaking Incubator | Benchmark Incu-Shaker Mini (Korea) |
| pH meter | Mettler-Toledo SevenCompact S210 (China) |
| Magnetic stirrer | IKA CMAG HS 7 (Italy) |
| vortex | VELP Scientifica ZX3 (Italy) |
| TEM | FEI Tecnai G2 Spirit BioTwin (USA) |
| FESEM | FEI. Quanta, FEG 450, Eindhoven (Netherlands) |
| XRD | Rigaku, SA-HF3 D/max-2200/PC, Rigaku (Japan) |
| EDS spectroscopy | Octane Plus, Ametek (United States) |
| FTIR spectroscopy | Shimadzu IR, Prestige 21, Nakagyo-ku (Japan) |
| McFarland Densitometer | Biosan (Germany) |
| Muffle Furnace | Nüve (Turkey) |
| Zetasizer nano series | Malvern Panalytical, Atomika Teknik (Turkey) |
| Ultrasonic device | Bandelin Sonopuls (Germany) |

3.1.3. Chemical and biological materials

The materials used in the study are given in Table (3.3).

Table 3.3. Chemicals and tools used in the study.

| Material | Company |
|--------------------------------------|-------------------------|
| Alcohol (Ethanol) | Merck-Germany |
| ZnSO ₄ .7H ₂ O | Merck-Germany |
| NaOH | Merck-Germany |
| HCl | Sigma Aldrich- Germany |
| DPPH | Sigma Aldrich - Germany |
| Methanol | Honeywell-Poland |
| Distilled water | - |
| Glass beads | - |
| Eppendorf tubes | Merck-Germany |
| Quartz cuvette | |
| Agar-Agar | Himedia-India |
| Nutrient broth | Merck-Germany |
| Muller-Hinton agar | Oxoid-England |
| Tryptic soy broth | Merck-Germany |
| Drigalski spatula | - |
| Sterile petri dishes | - |
| Centrifuge tubes 10, 15 and 50 mL | - |
| Erlenmeyer flask 50 mL | - |
| Flask 100, 250, 500 and 1000 mL | - |
| Volumetric Cylinders 50, 100, 250 mL | - |
| Funnel | - |
| Beaker 50, 100, 250 mL | - |
| volumetric flask 50, 100, 250 mL | - |
| Filter paper-Whatman | Merck-Germany |
| Rack | Merck-Germany |
| Tips | LP (Italy) |

3.1.4. Culture media

Nutrient agar: Nutrient agar was used for the activation of the *Bacillus* strains. Eight g of nutrient and 15 g of agar-agar was mixed in one liter of distilled water and heated to dissolve agar-agar, then sterilized at 121 °C for 15 min. After cooling to 50 °C, it was distributed in sterile Petri dishes as 15 mL portions.

Nutrient broth: It was used for the cultivation of *Bacillus* strains for nanoparticles biosynthesis. The medium was prepared by dissolving 8 g of nutrient broth in one liter of distilled water and distributed in 100 mL Erlenmeyer flasks as 30 mL portions, then sterilized in the autoclave.

Muller-Hinton agar: It was used for antimicrobial activity tests. 21 g of Mueller-Hinton agar weighted and mixed with one liter of distilled water, then sterilized in the autoclave. After cooling the medium to 50 °C, it was poured in the Petri dishes.

Tryptic soy broth (TSB): It was used for the activation of pathogen microorganisms for antimicrobial activity tests. This medium was prepared by adding 30 g of TSB to one liter of distilled water. Then distributed in the test tubes as 10 mL portions and sterilized.

Yeast pepton glucose agar (YPGA): the media was prepared by dissolving yeast extract (10 g/L), glucose (20 g/L), agar agar (10 g/L) and pepton from meat (20 g/L) in one liter of distilled water, after sterilization at 120 °C for 15 min, the media cooled and poured in the Petri dishes.

3.1.5. Solutions

ZnSO₄.7H₂O Stock solution: 100 mL of stock solution (100 mM) was prepared by dissolving 2.88 g of ZnSO₄.7H₂O in 100 mL distilled water

Sodium hydroxide: Sodium hydroxide (NaOH) was prepared at certain molarity (0.1M) with an appropriate amount (0.4 g) of distilled water in 100 mL volumetric flasks. These solutions were used to adjust the pH of solutions.

Hydrochloride acid (HCl) solution: Hydrochloric acid (1N) was prepared by transferring 8.6 mL into 100 mL volumetric flasks and then completing the volume with distilled water. These solutions were used to adjust the pH of media

DPPH solution: 100 mL of DPPH solution was prepared by dissolving 2 mg of 2,2-diphenyl-1-picrylhydrazyl (DPPH) in methanol solution (70%).

3.2. Methods

3.2.1. Screening and biosynthesis of ZnO NPs

Zinc oxide nanoparticles were synthesized by *Bacillus* isolates via the bioreduction route according to protocol of Iqtedar et al. (2020) with slight modifications. The strains was revived by growing the bacteria on a nutrient agar plate and then left in orbital incubator at 33°C for 24 h. One loopful of activated bacteria was used to inoculate 30 mL of nutrient broth and kept in the incubator with shaking (120 rpm) for 24 hours at 33°C. After that, the supernatant was obtained by centrifugation at 9320 xg for 20 minutes, and kept for biosynthesis ZnO NPs. Dropwise additions of HCl (1N) or NaOH (4 M) solution were added to the supernatant to adjust its pH to the desired level of 7.5. To synthesize ZnO NPs, 2.4 mL of a 100 mM ZnSO₄·7H₂O solution were added drop-wise to 30 mL of the supernatant, and incubated at 33°C for 3 days. Daily samples were scanned using a UV-VIS spectrophotometer and the range of wavelengths between 300 and 600 nm. Among the 45 *Bacillus* strains tested, *Bacillus subtilis* ZBP4 showed the presence of highest absorption peaks at 341 nm. For that reason, it was selected for further experiments in biosynthesis studies. The bacterium was previously isolated from a soil sample obtained from Geyve at Sakarya district and was identified as *Bacillus subtilis* according to 16S rDNA sequence analysis (GenBank Accession no. KX811594). Moreover, the bacterium was Gram-positive, rod shaped and endospore-forming (Avcı et al, 2017). For that reason, it was selected for further experiments in biosynthesis studies. A supernatant without the added ZnSO₄·7H₂O was used as the control for each bacterial strain.

3.2.2. Optimization of ZnO NPs biosynthesis by *Bacillus subtilis* ZBP4

The biosynthesis of ZnO NP by *Bacillus subtilis* ZBP4 has been studied under a variety of reaction conditions, including temperature, pH, and precursor concentration. In all studies, 30 mL Cell free supernatant (CFS) was utilized in Erlenmeyer flasks (100 mL), and inoculum preparation and the biosynthetic process by *Bacillus subtilis* ZBP4 was done as described previously (Section 3.2.1). In order to determine the impact of media pH on the biosynthesis rate, the pH of the supernatants was adjusted to various pH values (5, 6, 7, 7.5, 8, and 9) using either 0.1M NaOH or 1N HCl; after that 6 mM of ZnSO₄·7H₂O was added to the supernatants and then all Erlenmeyer flasks were incubated at 33 °C for 72 h.

For the effect of reaction temperature studies, the supernatant as obtained after 24 h incubation in nutrient broth containing 6 mM ZnSO₄.7H₂O was incubated at different temperatures (30, 33, 37, and 40°C) without adjusting the pH. The samples were taken at 24 and 48 h during the incubation and the UV-VIS spectra between 300 and 600 nm were determined and absorbance values at 341 nm were recorded.

To determine the best concentration for maximal biosynthesis, different concentrations of ZnSO₄.7H₂O ranged between 2 and 10 mM were used and all specimens were incubated at 33°C for 72 hours with shaking (120 rpm). The samples taken after the 24 and 48 h of the incubation were analysed with UV-VIS spectrophotometer to detect the absorbances. Each experiment was repeated at least three times, and the average and standard error of the data were given.

3.2.3. Biosynthesis of nisin loaded ZnO NPs

For the biosynthesis of nisin loaded zinc oxide NPs, *Bacillus subtilis* ZBP4 strain was activated by culturing on nutrient agar plates and incubated at 33°C for 24 h. Ten mL of free nisin stock solution was prepared by combination 10 mg of free nisin in 10 mL of distilled water. In order to provide a true dispersion, the suspension was vortexed for 5 min. According to Pandit et al. (2017) procedure with some modifications, the culture was centrifuged in a 50 mL falcon tubes at 9000 rpm, at 4 °C for 20 min in a centrifuge. The pH of reaction mixture was set to pH 7.5 by using diluted HCl solution (1N). Then, 2.4 mL (8 mM concentration) of ZnSO₄.7H₂O solution was added to 30 mL supernatant, and then three different concentrations of nisin (5, 10, 15 mg/mL) were added. While gently stirred the Erlenmeyer flask and incubated again in an orbital shaker operating at 120 rpm and 33 °C for 48 h. The synthesis of N-ZnO NPs was confirmed by visual observation of the color change (which changed color from light yellow to dark yellow). The absorbance values were recorded daily by using a UV-VIS spectrophotometer.

Finally, the solution with N-ZnO NPs were centrifugated at 9000 rpm for 10 min. The precipitate of synthesized N-ZnO NPs was successive washed for twice with distilled water. The dried samples were stored in refrigerator for characterization and antibacterial studies.

3.2.4. Characterization of nanoparticles

3.2.4.1. UV-VIS spectroscopy

The initial characterization of biosynthesized NPs was carried out by a single beam UV–VIS spectrophotometer. The nanoparticles solutions were scanned in the range of wavelength between 300 and 600 nm. Software called "UVprobe ver 2.51" was installed on computer to connect with spectrophotometer instrument after that prepared base line correction and each sample was scanned and the data documented.

Base line correction of the spectrophotometer was carried out by using a blank reference. Samples from the reaction medium and appropriate dilutions (1:2, v/v) were prepared, and their absorbance spectra were analyzed using a UV-VIS spectrophotometer to identify the maximum absorbance peak created by the nanoparticles. The samples were diluted with distilled water (1:2, v/v) and their absorbance spectra drawn by the "excel 2010 and Origin 2019b".

3.2.4.2. Harvest of nanoparticles

The biosynthesis of ZnO NPs or N-ZnO NPs was carried out under optimal conditions (pH 7.5, 33 °C, 8 mM ZnSO₄.7H₂O, and 24 h). The final sample solution was centrifuged for 10 minutes at 9320 x g and then the precipitate underwent two washes with sterile distilled water. All samples were allowed to dry at ambient temperature, then NPs were weighed and stored for later processing in the refrigerator at 4 – 10 °C (Yurtluk et al, 2018).

3.2.4.3. Transmission electron microscopy analysis (TEM)

Transmission electron microscopy analysis was done at Middle East Technical University Central Laboratory (Ankara, Turkey). At least three images of each sample were taken to represent its size and dimensional morphology of NPs at the nanoscale. The TEM measurement was carried out on (TEM, FEI Tecnai G2 Spirit BioTwin) after operating the accelerating voltage at 100 Kv. The particle size distribution was determined with the help of ImageJ software (Schneider et al, 2012).

3.2.4.4. Field emission scanning electron microscope (FESEM) analysis

The surface morphology of the NPs were examined with field emission scanning electron microscopy. A thin film of each powder NPs was placed on motorized stages

and then FESEM was operated at a working distance 10.2 mm, 15-20 keV accelerating voltage low vacuum mode, a spot size 3, with different magnification. The FESEM analysis was done at Research Development and Application Center at Sakarya University. The particle size distribution was determined with the help of ImageJ software (Schneider et al, 2012).

3.2.4.5. Energy dispersive spectroscopy (EDS) analysis

Energy dispersive spectroscopy analyses were carried out to analyze the elemental analysis of the NPs. Compositional studies of points and maps were examined at a 15 KeV accelerating voltage, low-vacuum mode with 3 of spot size, and 10.2 of mm operating distances.

3.2.4.6. X-ray diffraction (XRD) analysis

The phase of molecular and crystal structures was identified by XRD analytical technique. The dried ZnO NPs samples were calcination at 600 °C for two hours using a Muffle Furnace device, while N-ZnO NPs were analyzed without the calcination process. The samples were analyzed by setting the copper anode on 40 mA, with Rikagu Diffractometer (CuK α 1 radiations = k 1.5405 Å) at 40 kV. The nanoparticles were exposed to X-rays at an angle between 30–80°. The X-ray diffraction scans were carried out in the laboratories of the Metallurgical and Materials Engineering Department at the University of Sakarya.

Crystalline nature were detected with database library in Joint Committee on Powder Diffraction Standards (JCPDS), that were saved in a MDI Jade 6 software. The Debye-Scherrer equation was used to calculate the particle size of ZnO NPs (3.1)

$$D = \frac{k\lambda}{\beta \cos\theta} \quad (3.1)$$

where D is crystal size perpendicular to the reflecting planes, K is constant (0.9), λ X-ray wavelength (1.5406 Å), β is the angular full width at half maximum in radians and θ is the Bragg's angle.

3.2.4.7. Fourier Transform Infrared spectroscopy analysis

Fourier Transform Infrared spectroscopy analysis were asses possible involvement of active groups for biosynthesis NPs. The IR spectra of NPs samples were recorded between 400 to 4000 cm^{-1} with FTIR spectroscopy (Naik et al, 2021). In order to evaluate and confirm the functional groups of the cationic peptide, free nisin FTIR spectra were prepared. FTIR analyses were done at Chemistry Department at Sakarya University.

3.2.4.8. Zeta potential

In this research work, Zetasizer Nano Series (Malvern, Great Britain) machine were used to determine mean stability of nanoparticles. The ZnO powder and N- ZnO NPs samples were dispersed with distilled water, 30 mg of each nanoparticles were added to distilled water (20 mL) and then mixed with the help of glass beads for 15 minutes prior to testing. For each sample, all measurements were taken automatically in triplicate (Marín et al, 2017).

3.2.4.9. Energy bandgap of nanoparticles

By using an UV-VIS absorption one beam spectrophotometer with a wavelength range of 300-600 nm, the optical characteristics of the nanoparticles were examined. (as described in 3.2.4.1.). According to absorption spectrum data, the graph of energy bandgap was plotted (Makuła et al, 2018).

The bandgap of the NPs was calculated with the help of Tauc's equation according to Tauc's equation (3.2).

$$\alpha hv = C(hv - E_g)^n \quad (3.2)$$

Where E_g is the bandgap energy in eV, α is the coefficient of absorbance, h is Plank's constant, v is the frequency of the photon, C is a constant, n is a factor related with nature electron transition and it is $\frac{1}{2}$ for semiconductors.

3.2.5. Antimicrobial activity of nanoparticles

The efficacy of the NPs against nine pathogens including *B. cereus*, *E. coli* O157:H7 NCTC 12900, *L. monocytogenes* ATCC 7644, *P. aeruginosa*, *S. Typhimurium*, *S. aureus* ATCC 25923, *E. coli* Type 1, *S. Enteritidis* ATCC 13076 and *C. albicans*. The

stock solution (10 mg/mL) was prepared by combination 80 mg of synthesized NPs in 8 mL of distilled water. The solution was vortexed for 15 minutes using glass beads (4 mm-diameter) to get a proper dispersion, and then ultrasonication has been employed (with the T104 probe, AMP 50%, for 4 minutes). Fresh microorganism cultures were prepared by inoculating stock cultures into 5 mL of tryptic soy broth (TSB) and incubating them at 37°C for 24 hours, with the exception of *L. monocytogenes* ATCC 7644, which was incubated at 30°C. Antibacterial activity experiments were conducted using the agar disk-diffusion test with a modifications (Bauer, 1966). Fifty μ L of each culture was spread on the surface of the Muller Hinton agar (MHA) by Drigalski then left for 30 min. After the paper discs with a standard diameter (6 mm) were placed on the Mueller Hinton agar, the discs were covered with 20 μ L of NPs at various concentrations (1, 2, 5, 10 mg/mL). All plates were incubated at suitable temperature and the inhibition zone diameter in millimeters was measured. The experiments were repeated at least three times, and the average and standard error of the data were given.

3.2.6. Growth inhibition curves in liquid medium

Two model bacteria (*L. monocytogenes* ATCC 7644 and *S. aureus* ATCC 25923) were selected to identify the antibacterial activity of ZnO NPs, free nisin, and N-ZnO NPs as a function of time. Growth inhibition curves were carried out in a liquid medium (tryptic soy broth) using a McFarland Densitometer. Different concentrations of samples were transferred into tubes, which contained 3 mL of sterile TSB broth and 50 μ L of bacterial inoculum, Also, nanoparticles control were prepared for each concentration (containing 3 mL of TSB with NPs). In addition, three tubes (control bacteria) were prepared containing 3 mL of TSB with bacterial inoculum, while three other tubes (blank) were prepared containing 3 mL of TSB (negative inhibition control). Immediately after the inoculation, all tubes were vortexed well, then, the tubes were incubated at 37 °C, and the optical density of samples at different times (0, 1, 2, 3, 4, 5, 6, 7, 8, 9, 10 and 24 h) were measured.

3.2.7. Antioxidant activity of nanoparticles

The antioxidant potential of NPs were measured with DPPH radical scavenging assay as mentioned by Forootanfar et al. (2014). This experiment aimed to bleach the samples with 2,2-diphenyl-1-picrylhydrazyl (purple-coloured) in order to assess the hydrogen atom or electron donation activities.

The NPs stock solution (10000 µg/mL) was carried out by mixing 30 mg of synthesized NPs in distilled water (3 mL). The suspension was vortexed for 30 minutes using glass beads (4 mm-diameter) to ensure the proper dispersion. At least, triplicate tubes were prepared on each group. Briefly, 200 µL of NPs with different concentration (1500–3500 µg/mL) and negative control were prepared in methanol (200 µL) with sample. At same time, sample control were prepared by transferring 200 µL of samples to 3 mL solution of methanol (%70) without DPPH.

The following formula (3.3) was used for the calculation of percent radical scavenging activities.

$$\text{DPPH scavenging activity (\%)} = [1 - (Aa - Ab) / Ac] \times 100 \quad (3.3)$$

Where Aa is the absorbance of the sample mixed with DPPH solution, Ab is the absorbance of the sample without DPPH solution, and Ac is the absorbance of the control solution.

3.2.8. Storage stability of nanoparticles

To investigate the effect of storage on the stability of ZnO and N-ZnO NPs, 1 mL of the liquid form NPs was stored in Eppendorf tubes and then appropriately closed to prevent solvent evaporation. The specimens were maintained in the refrigerator at 0-10 °C for 120 days. UV-VIS spectra of the samples were measured before and after the storage and the stability was determined by comparing absorbances (Rezazadeh et al, 2020).

3.2.9. Cytotoxicity assay

Cell proliferation was evaluated by the colorimetric method using water-soluble MTT (3-(4,5-dimethylthiazol-2-yl)-2,5-diphenyltetrazolium bromide). The stock nanoparticles were sterilized in a UV cabinet for 3 days. The nanoparticles were completely dissolved in Dimethyl Sulfoxide (DMSO) to prepare sequential dilutions (1, 10, 50, 250, 500, 750 and 1000 µg/mL). The MTT assay was done according to the international standard method mentioned by ISO 10993-5 (Kaviyarasu et al, 2017). Cytotoxicity analysis was done at SIA Analysis Laboratories Center in Izmir city (Turkey). The Vero epithelial cells (normal cells) were seeded in fresh Dulbecco's Modified Eagle Medium (DMEM) supplemented with 1% of glutamine, 1% sodium pyruvate and 10 % Fetal Bovine Serum (FBS). After being cultured in a humidified incubator at 37°C under enough amount of air containing 95 % moisture and 5% CO₂,

cultured cells were treated with different concentrations of nanoparticles and kept without light for 48 and 72 h. Control group was retained under same conditions without addition of N-ZnO NPs. Finally, the absorbance values were obtained using UV-VIS spectrophotometer at 570 nm. Also, the half-maximal inhibitory concentrations (IC_{50}) were determined by the global logistic regression model. For the determination the cytotoxicity of 23 nm of N-ZnO NPs, percentage cell viability was calculated by following formula as shown in (3.4).

$$\text{Cell viability (\%)} = (A_1/A_0) \times 100 \quad (3.4)$$

A_0 = optical density (OD) value of control

A_1 = optical density (OD) value of sample 1

3.2.10. Statistical analysis

The experiments were performed under the complete Randomized Design, and the variance analysis was carried out using the General Linear Model within the SPSS version 22 (Statistical Analysis System). Duncan (1955) was used in the case of significant differences between the different averages at level 0.05.

4. RESULTS AND DISCUSSION

4.1. Screening and Selection of *Bacillus* Strains for ZnO NPs Biosynthesis

In the study, firstly 45 *Bacillus* isolates were tested for the biosynthesis of ZnO NPs. The biosynthesis was observed either visually based on the color change from white to yellow or by monitoring the UV-VIS spectra. A sharp peak at UV-VIS absorption spectrum was the identification of the formation of nanoparticles which was created by the surface plasmon resonance (SPR) of the nanoparticles. Surface plasmon resonance is an excellent property of metal nanoparticles that is exerted when an electromagnetic light is applied to the nanoparticles. The electrons inside the nanoparticles oscillate and larger electric field than the incident light is generated around the nanoparticles. The nanoparticles absorb the incident light that cause oscillation (García, 2011). Among the 45 isolates, SPR peaks were observed at 341 nm with only 9 isolates that showed the formation of ZnO NPs (Figure 4.1). Absorption intensities were very low with 5 isolates which indicated the less amount of nanoparticles. The highest absorption intensity was obtained with *Bacillus subtilis* ZBP4, thus it was selected for further studies. Several studies showed that ZnO NPs give maximum absorbance at 310 to 380 nm which were dependent on the type of the microbial strain and the biosynthesis conditions. El-Ghwas (2022) studied the biosynthesis of ZnO NPs by using the cell free supernatant of *Bacillus foraminis* and reported the SPR peak as 380 nm.

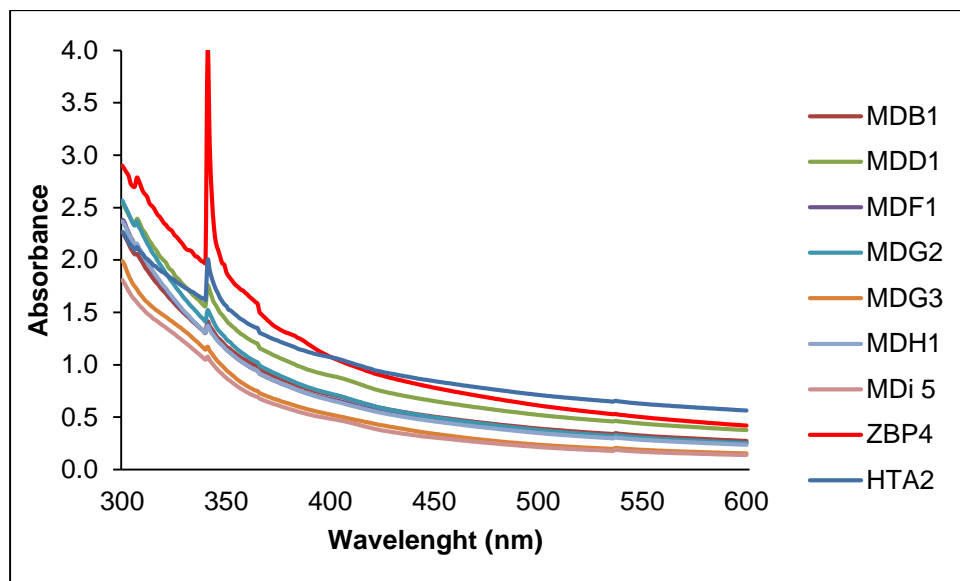


Figure 4.1. The UV–VIS spectra of screening of ZnO NPs synthesized by some *Bacillus* sp.

4.2. Biosynthesis of ZnO NPs by *Bacillus subtilis* ZBP4

As *Bacillus subtilis* ZBP4 was the most efficient isolate for the biosynthesis of ZnO NPs, biosynthesis conditions were optimized for this isolate. For this purpose, the effects of $\text{ZnSO}_4 \cdot 7\text{H}_2\text{O}$ concentration, time, and reaction pH on the biosynthesis rate were determined.

4.3. Effect of Zinc Sulfate Concentration on ZnO NPs Biosynthesis

One of the most important factors directly affecting the biosynthesis of NPs is the precursor concentration. Biosynthesis reactions were carried out using 2, 4, 6, 8 and 10 mM $\text{ZnSO}_4 \cdot 7\text{H}_2\text{O}$ concentrations. UV-VIS spectra of nanoparticles were monitored for three days period (Figure 4.2). Absorption peaks were observed at all the concentrations tested after 24 h (Figure 4.2). There was an increase at the peak intensities with the increasing concentrations and the highest peak intensities were obtained at 8 and 10 mM concentrations. Except 10 mM concentration, there was a decrease at the absorption intensities at 48 and 72 h incubations (Figure 4.2 b and c). The sharp peak at 341 nm was almost disappeared at the lowest concentration at prolonged incubations which indicated that the biosynthesis was completed in a shorter time at lower concentrations and further increase in time decreased the stability of nanoparticles. On the other hand, the formation of nanoparticles increased by time up to 72 h due to the higher amount of precursor in the reaction medium and maximum

absorption peak was observed in 72 h, at this concentration. Average absorbance values of the three replicates from each sample at 341 nm were depicted in Figure 4.3. Significant differences in the absorbances at various concentrations by time can be clearly seen from the Figure ($P>0.05$). Despite the higher absorption values obtained at 10 mM after 48 and 72 h, it was not statistically significant ($P<0.05$). Moreover, performing biosynthesis for longer times is not economically beneficial. Thus 8 mM $ZnSO_4 \cdot 7H_2O$ concentration was accepted as optimum at 24 h incubation time.

Similar to this study, Al-Kordy et al. (2021) have obtained maximum nanoparticle biosynthesis from the halophilic *Alkalibacillus* sp. W7 at 8 mM of $ZnSO_4 \cdot 7H_2O$. Another study conducted by Iqtedar et al. (2020) found that maximum biosynthesis of ZnO NPs occurred at 8 mM of $ZnSO_4 \cdot 7H_2O$ using filtrate of the *B. cereus* MN181367. Jayaseelan et al. (2012) also achieved reduction with 1g ZnO in the culture medium with the highest ZnO formation occurred after 24 h and the peak of growth at 374 nm.

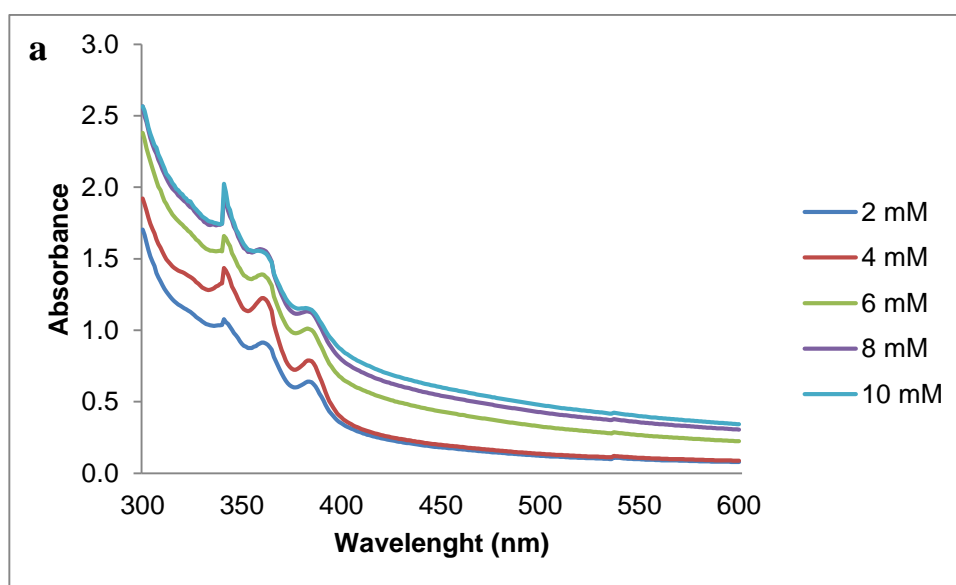


Figure 4.2. UV-VIS spectra of ZnO NPs biosynthesized at various concentrations of zinc sulfate concentration. a) 24 h, b) 48 h, c) 72 h.

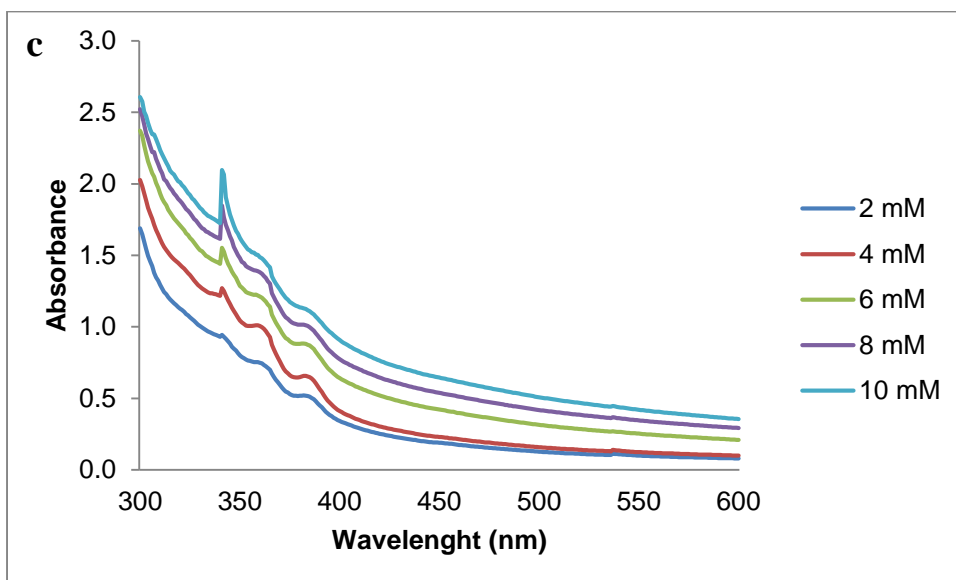
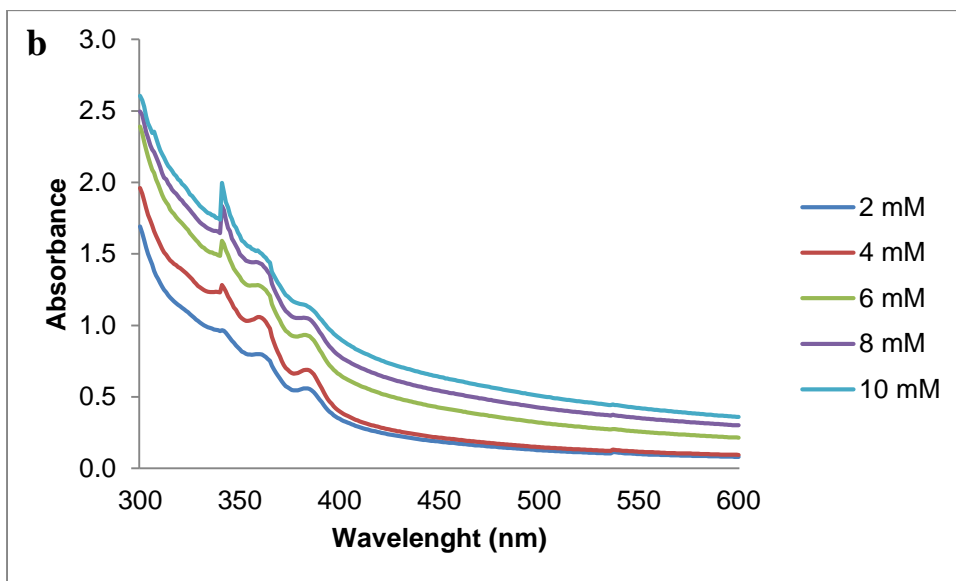


Figure 4.2. (Continued) UV-VIS spectra of ZnO NPs biosynthesized at various concentrations of zinc sulfate concentration. a) 24 h, b) 48 h, c) 72 h.

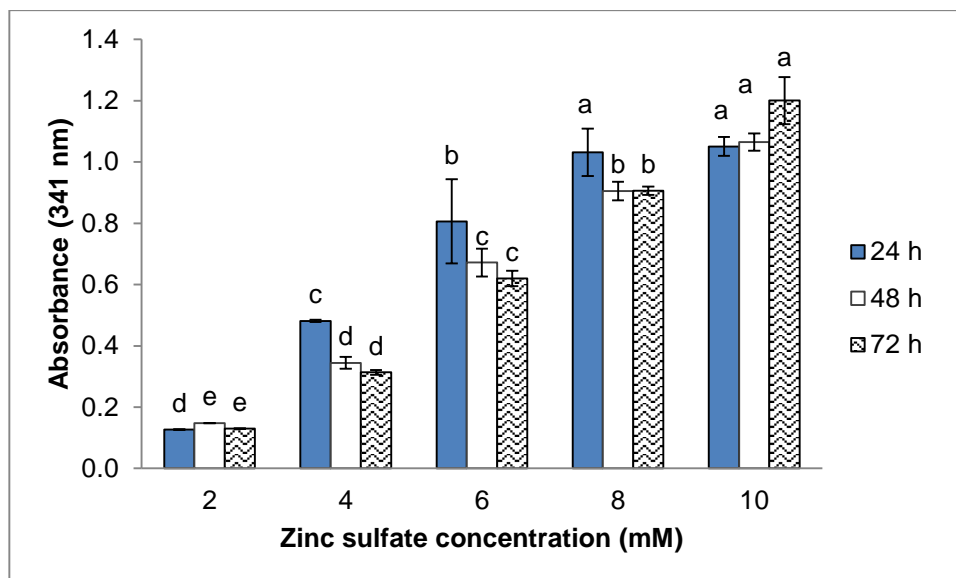


Figure 4.3. Effect of Zinc sulfate concentration on ZnO NP synthesis.

- The different letters refer to significant differences at $P < 0.05$ and statistical analysis was performed for each day individually.
- Sample diluted (1:2 v/v)

4.4. Effect of pH on the Biosynthesis of ZnO NPs

The pH of the reaction was optimized using 6 values (pH 5, 6, 7, 7.5, 8 and 9) and daily measurements were done during 72 h. Absorption spectra and the absorbance values of the samples are given in Figure 4.4 and 4.5, respectively. As can be seen from the figures, pH of the reaction medium is crucial for the biosynthesis of ZnO NPs by *Bacillus subtilis* ZBP4. The absorbance intensity increased significantly at pH 7.5, which demonstrated ZnO NPs' abundance in comparison to other groupings. Interestingly, biosynthesis rate diminished dramatically at the other pH values ($P < 0.05$). No prominent peak was observed at pH 9 during 72 h which indicated absence of the nanoparticles. Very small peaks were obtained at low pH (5 and 6) values. The intensities of absorption at pH 7 and 8 was approximately the same at 24 h and 48 h (Figure 4.5). Decrease in the absorbances by time, especially at 72 h, was an indication of the corruption of the stability of the nanoparticles. Thus, biosynthesis reactions should not be carried out more than 24 h.

The pH of the reaction affects the synthesis of ZnO NPs because it changes the structure of the molecules that act as capping and stabilizing agents for NPs. Bioactive compounds including amino, sulfate, carboxyl and hydroxyl groups etc. might play a

significant role in the reduction stage of NPs, especially at pH 7.5. On the other hand, the inactivation of functional groups in the supernatant decreases the formation of nanoparticles at low and high pH values (Al-Kordy et al, 2021). Various studies showed that optimum pH for biosynthesis ZnO NPs may vary depending on the conditions and microorganisms used. Ebadi et al. (2019) have obtained maximum ZnO NPs biosynthesis from the *Cyanobacter Nostoc* sp. at pH 9.0. Iqteqar et al. (2020) observed that alkaline pH (pH 9) favored ZnO NPs synthesis when used the supernatant of the *B. cereus* MN181367. Moreover Al-Kordy et al. (2021) found maximum biosynthesis of ZnO NPs at pH 8 by using *Alkalibacillus* sp. W7 that is similar to current study. Hence slight alkaline or neutral conditions are favorable for the biosynthesis. Saleh et al. (2021) have also observed small ZnO NPs (25 – 50 nm) being formed at pH 7 by *Bacillus subtilis* supernatant.

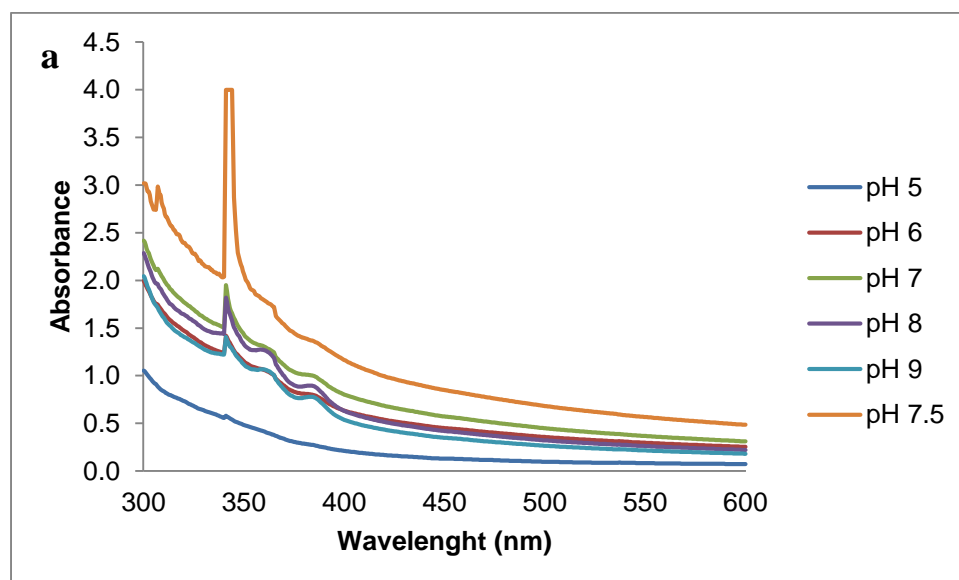


Figure 4.4. UV-VIS spectra of ZnO NPs biosynthesized at various pH values. a) 24 h, b) 48 h, c) 72 h.

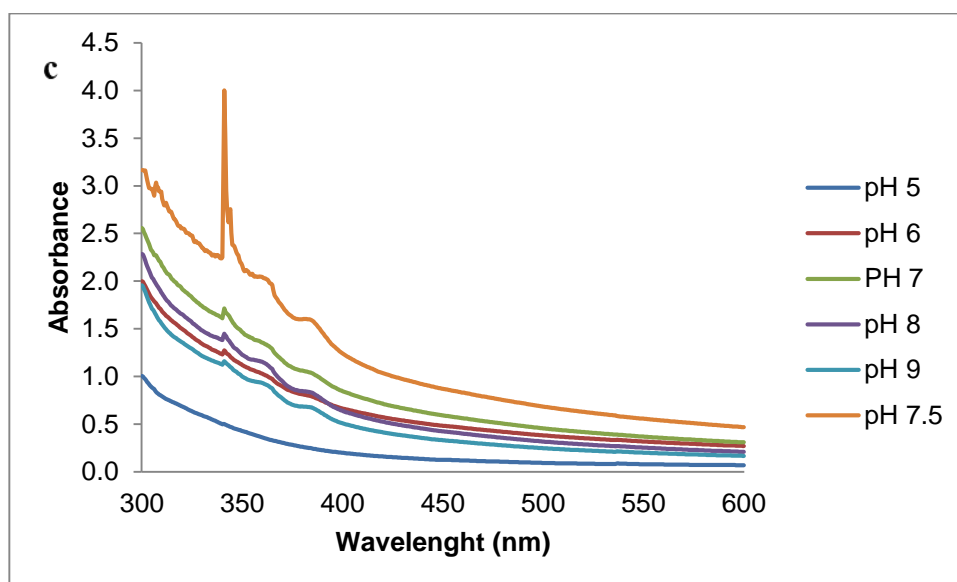
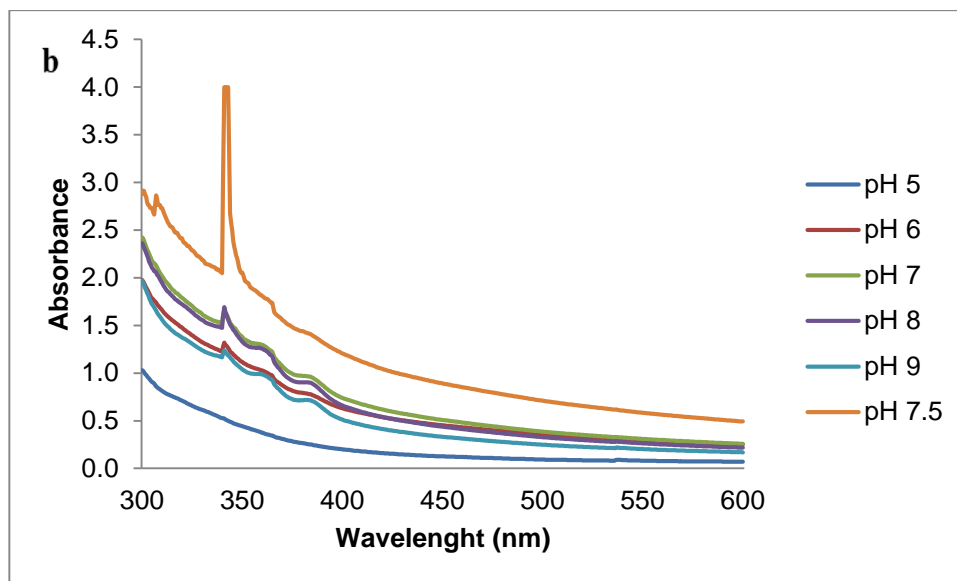


Figure 4.4. (Continued) UV-VIS spectra of ZnO NPs biosynthesized at various pH values. a) 24 h, b) 48 h, c) 72 h.

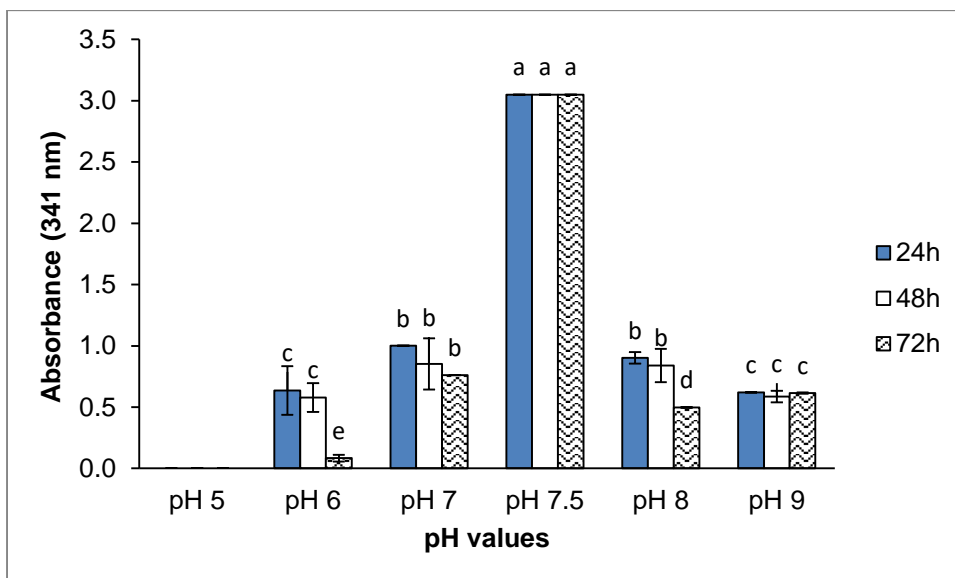


Figure 4.5. Effect of pH on ZnO NPs synthesis.

- The different letters refer to significant differences at $P < 0.05$ and statistical analysis was performed for each day individually.

- Sample diluted (1:2 v/v)

4.5. Effect of Incubation Temperature on ZnO NPs Synthesis

One of the main effectors in the production of nanoparticles is known to be temperature. Nanoparticle biosynthesis studies were carried out at four different temperatures (30, 33, 37 and 40°C). Absorbance values of the samples taken at 24 and 48 h were measured at 341 nm and the results are given in Figure 4.6. It was determined that high temperatures cause the decrease in the biosynthesis rate. The biosynthesis of ZnO NPs at 33 °C led to a dramatic increase in absorption and a strong peak at 341 nm.

Reported studies from the literature showed that optimum biosynthesis temperature is depending on the strain used. Fatholahi et al. (2021) reported the synthesis of ZnO NPs from zinc solution (zinc sulfate) using *Bacillus subtilis* at 37°C. ZnO NPs were synthesized by *Bacillus megaterium* through biological route with 37 °C and 24 h (Saravanan et al, 2018). ZnO NPs were synthesized using *Aeromonas hydrophila* at 30 °C for 24 h (Jayaseelan et al, 2012). Kundu et al. (2014) also investigated the synthesis of biogenic ZnO NPs in the presence of 0.1 M $ZnSO_4 \cdot H_2O$ using *Rhodococcus pyridinivorans* at 30 °C. The optimum conditions for the synthesis of ZnO NPs by *B. cereus* were found to be pH 9, using $(NH_2)_2SO_4$ at 37 °C within 48 h under light conditions (Iqtedar et al, 2020).

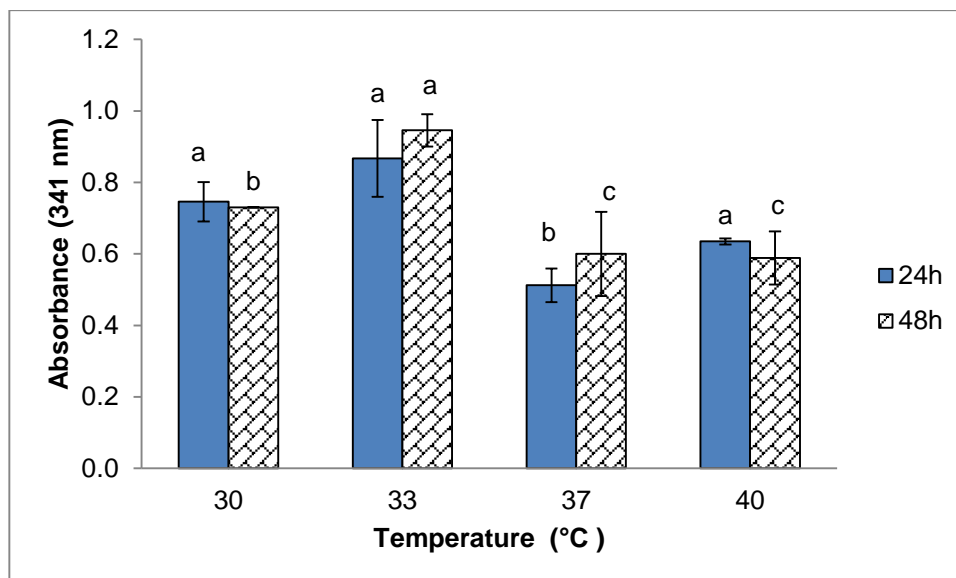


Figure 4.6. Effect of temperature on ZnO NPs synthesis.

- The different letters refer to significant differences at $P < 0.05$ and statistical analysis was performed for each day individually.
- Sample diluted (1:2 v/v)

4.6. Biosynthesis of Nisin Loaded Zinc Oxide NPs

The advantage of nisin loading nanoparticles is to improve sustained antimicrobial activity of ZnO NPs. Moreover, nanoparticle delivery systems can be designed easily and inexpensively allowing their use in a wide range of commercial products (Bernela et al, 2014). In order to increase the performance, especially antimicrobial activity of ZnO NPs, biosynthesis reactions were carried out by adding nisin into the biosynthesis medium. For this purpose, various concentrations (5, 10 and 15 mg/mL) of nisin were added and the reactions were performed at the optimized conditions determined for ZnO NPs (pH 7.5, 8 mM $ZnSO_4 \cdot 7H_2O$ and 33 °C). Figure 4.7 shows the absorbances of the samples measured at 341 nm 48h of the incubation period. Surface plasmon resonance peak intensity increased with the increased concentrations of nisin. However, the absorbance values decreased when the concentration was increased to 15 mg/mL. Unlike the sole biosynthesis of ZnO NPs, biosynthesis of nisin loaded ZnO NPs (N-ZnO NPs) increased after 48 h. This can be attributed to the preservation of nanoparticles with help of the nisin.

To improve the efficacy of the antimicrobial of metal nanoparticles, alternative methods are also introduced antimicrobial peptides with silver nanoparticles to

increase the stability and efficacy against *E. coli* cells (Pal et al, 2016). Nisin and heat have also been investigated to enhance the antibacterial action of MgO nanoparticles (NPs); the combination of nisin with MgO NPs increased the distortion and damage of the cell. As a result, the morphology of bacterial cells changes with the decreased bacterial number (Mirhosseini, 2016). Cationic peptide-conjugated silver NPs exhibited significant antimicrobial inhibition against *E. coli* and *C. albicans* comparing with peptide-conjugated gold NPs and unconjugated gold/silver nanoparticles (Bajaj et al, 2018). Jin and Gurtler (2011), inactivated *Salmonella* spp. in liquid egg white by coated jars with nisin, allyl isothiocyanate, and ZnO NPs. At the same time, the use of a combination of chitosan-zinc oxide nanocomposite and nisin allowed inducing a synergistic effect, therefore completely inactivated *L. monocytogenes* in white cheese under storage at 4 °C for two weeks (Divsalar et al, 2018). Zhao and Kuipers (2021), reported bactericidal activity of silver-nisin nanoparticles against clinically isolated multidrug resistance strains from wound infections including *A. baumannii*, *P. aeruginosa*, *E. coli*, *K. pneumoniae* and *S. aureus*. Significant antibacterial activity has been observed by the nisin-loaded chitosan NPs against pathogenic Gram-positive and Gram-negative bacteria.

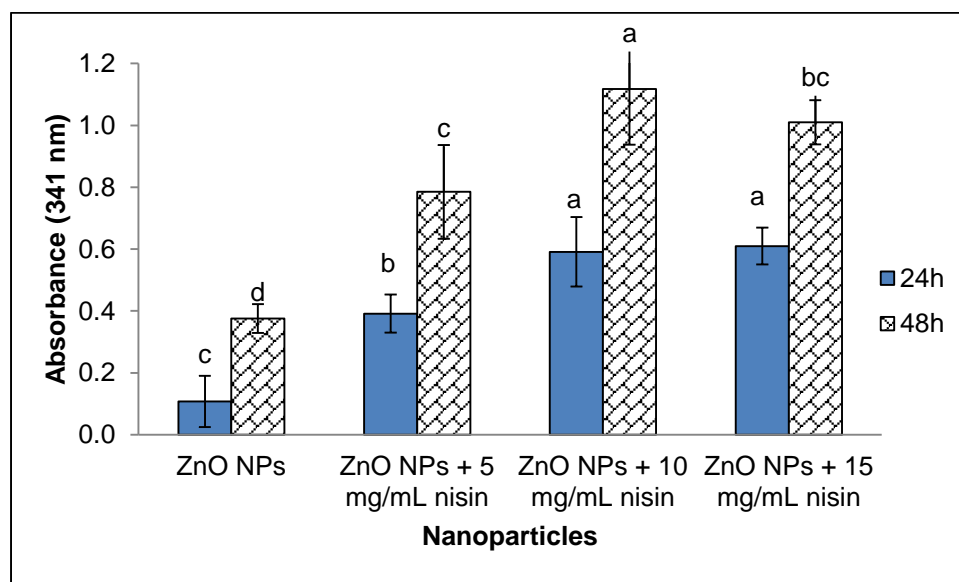


Figure 4.7. Nisin conjugation ZnO NPs synthesis with different concentrations of nisin after 24 h and 48 h.

- The different letters refer to significant differences at $P < 0.05$ and statistical analysis was performed for each day individually.
- Sample diluted (1:6 v/v)

4.7. Characterization of Nanoparticles

Nanoparticle characterization studies were performed using nanoparticles obtained at the optimized biosynthesis conditions.

4.7.1. Transmission electron microscopy

Transmission electron microscopy was used to determine the size and shape of ZnO NPs. When optimum conditions were applied quasi-spherical ZnO NPs with diameters ranging from 14-45 nm were obtained with the average of 26 nm (Figure 4.8a). All the nanoparticles were smaller than 100 nm and the size distribution histogram revealed that 60 % of nanoparticles sizes were between 20-30 nm as shown in (Figure 4.8b). TEM micrograph of N-ZnO NPs powder showed that they consisted of quasi spherical nanoparticles quite similar to ZnO NPs both in shape and size (Figure 4.9a). Nanoparticles sizes varied between 14 and 40 nm, and average diameter was calculated 23 nm using ImageJ software. The distribution observed from the histogram shows that almost 57 % of the particles were in the range of 20 and 30 nm (Figure 4.9b).

The current study was agreed with the literature at which generally small ZnO NPs (<100 nm) were reported. Madhumitha et al. (2019) used the *Pithecellobium dulce* peel in the synthesis of ZnO NPs, the TEM micrographs indicated that the particle size of ZnO NPs was 30 nm with spherically shaped. The TEM images results obtained by Yashni et al. (2021) for biosynthesized ZnO NPs using *Corriandrum sativum* leaf extract have shown quasi-spherical clusters of the nanoparticles. Barani et al. (2021) reported the synthesis of spherical ZnO NPs via aquatic *Vibrio* sp. VLA strain and the average size was determined as 20.26 nm.

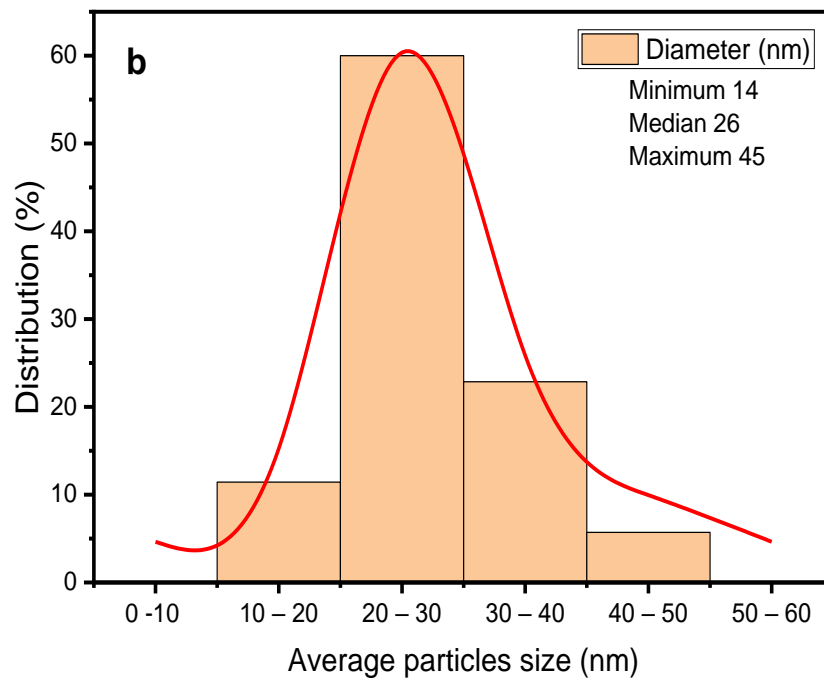
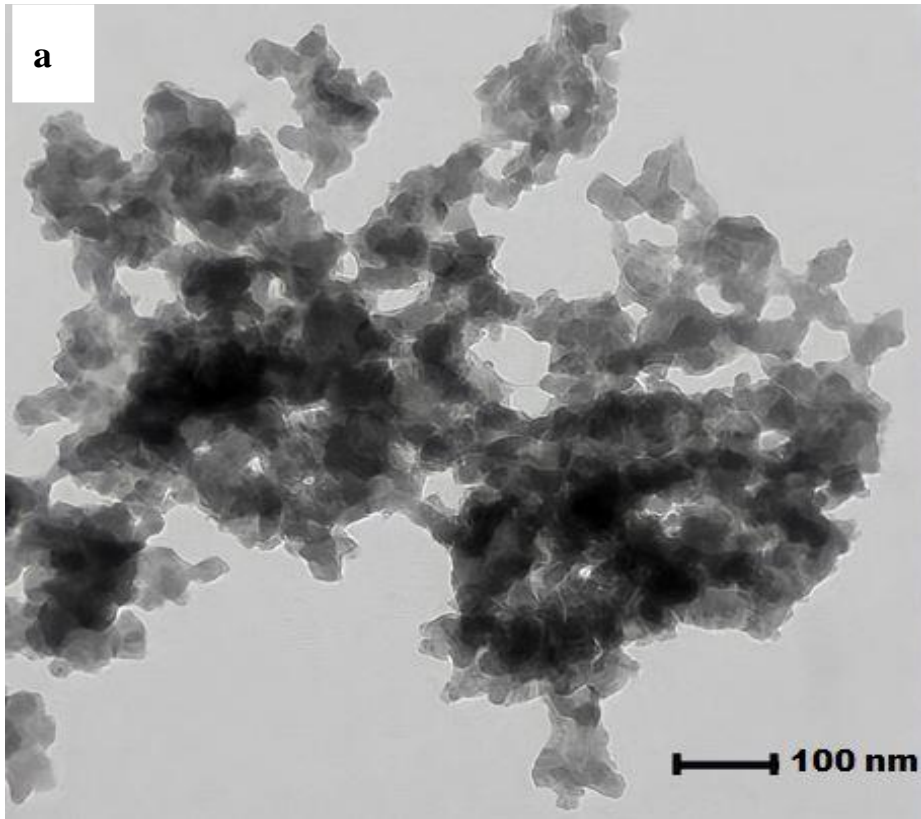


Figure 4.8. TEM micrograph ZnO NPs (a) and average distribution of ZnO NPs (b).

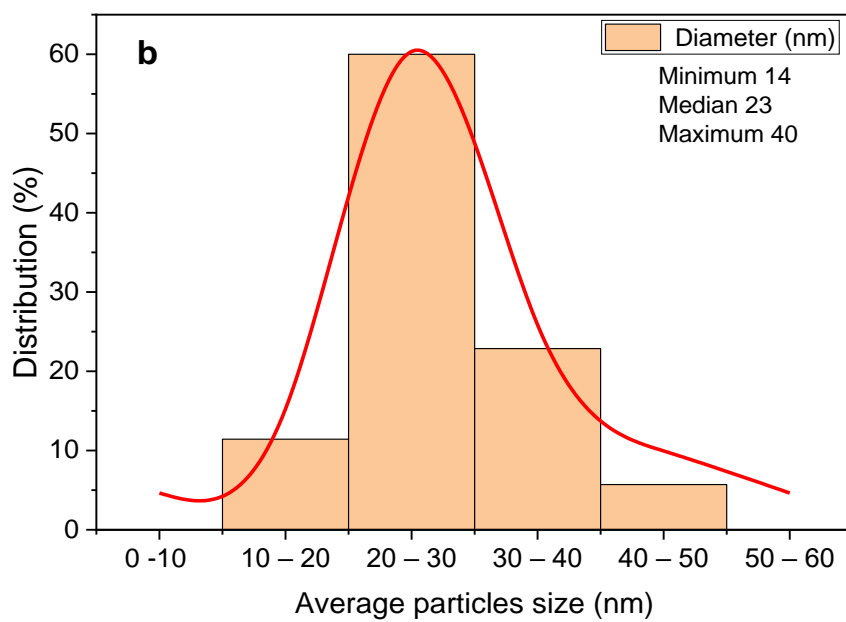
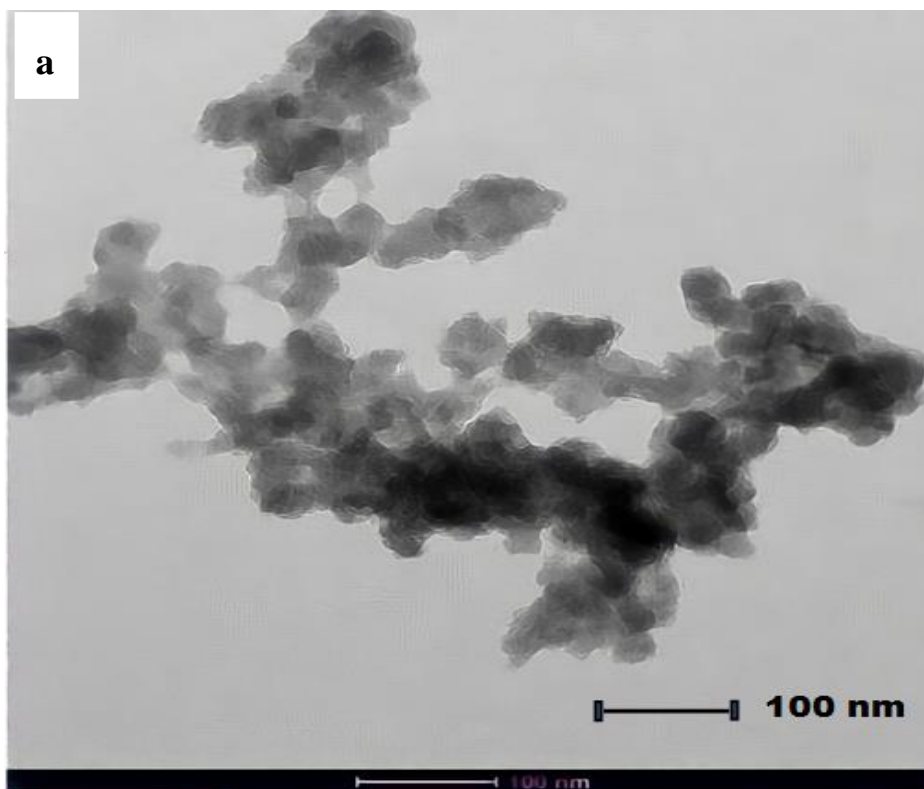


Figure 4.9. TEM micrograph N-ZnO NPs (a) and average distribution of N-ZnO NPs (b).

4.7.2. Field emission scanning electron microscopy

The synthesized ZnO NPs were also investigated for their morphology with FESEM. Figure (4.10a) shows the spherically or quasi-spherically shaped ZnO NPs and agglomeration has been detected. The particle size of ZnO NPs demonstrated the uniform size distribution of nanoparticles ranging from 21 to 59 nm with an average diameter of 35 nm. The size distribution histogram revealed that 50% of nanoparticle sizes were between 30-40 nm as shown in Figure 4.10b.

FESEM was used to study the morphology of the nisin-loaded ZnO NPs at a magnification of 200,000X (Figure 4.11). Non-clear nanoparticles and smooth surface can be seen from the figure. In the case of N-ZnO NPs, ZnO NPs embedded in the nisin which showed an irregular rougher surface with holes because the nisin peptide acts as a network and fully covers ZnO NPs surface. As the nanoparticles were not clear, particles size was not determined.

Various studies showed that the size and shape of the ZnO NPs were almost similar to the findings obtained in the current study. Jayabalan et al. (2019) reported the formation of spherical ZnO NPs by *Pseudomonas putida* with size ranging between 25 and 45 nm with FESEM. Similarly, Sangeetha, et al. (2011) biosynthesized spherical ZnO NPs with particle sizes ranging from 25 to 40 nm using *Aloe barbadensis miller* leaf extract. SEM and TEM micrographs indicated that the particle size of ZnO NPs was observed as ~20 nm and smooth spherically shaped, which were fabricated using the green route (Imade et al, 2022). The FETEM images showed that the probiotic bacteria *Lactobacillus plantarum* VITES07 produced ZnO NPs that appear roughly spherical in shape and smaller (Selvarajan and Mohanasrinivasan, 2013).

Zheng et al. (2018), synthesized ZnO NPs using *Glycyrrhiza glabra* seed aqueous extract and they found the morphology of the ZnO NPs quite similar to this study. Ahmed et al. (2021) reported spherically synthesized ZnO NPs by *B. cereus* with a size ranging from 21 to 35 nm. Sorbiun et al. (2018), successfully synthesized spherical ZnO NPs using an aqueous extract of *Oak* fruit hull with an average particle size of 34 nm.

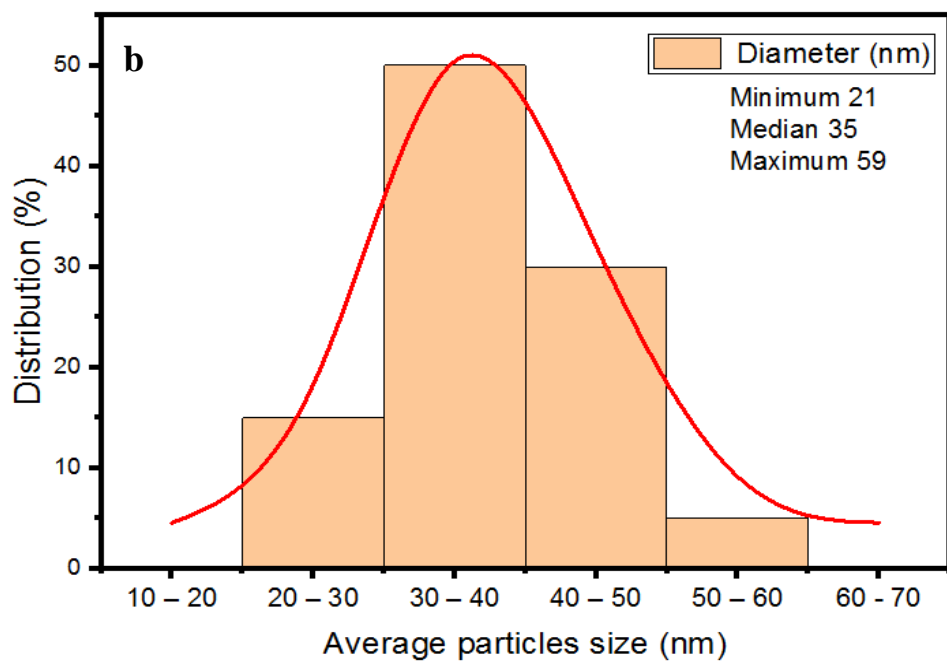
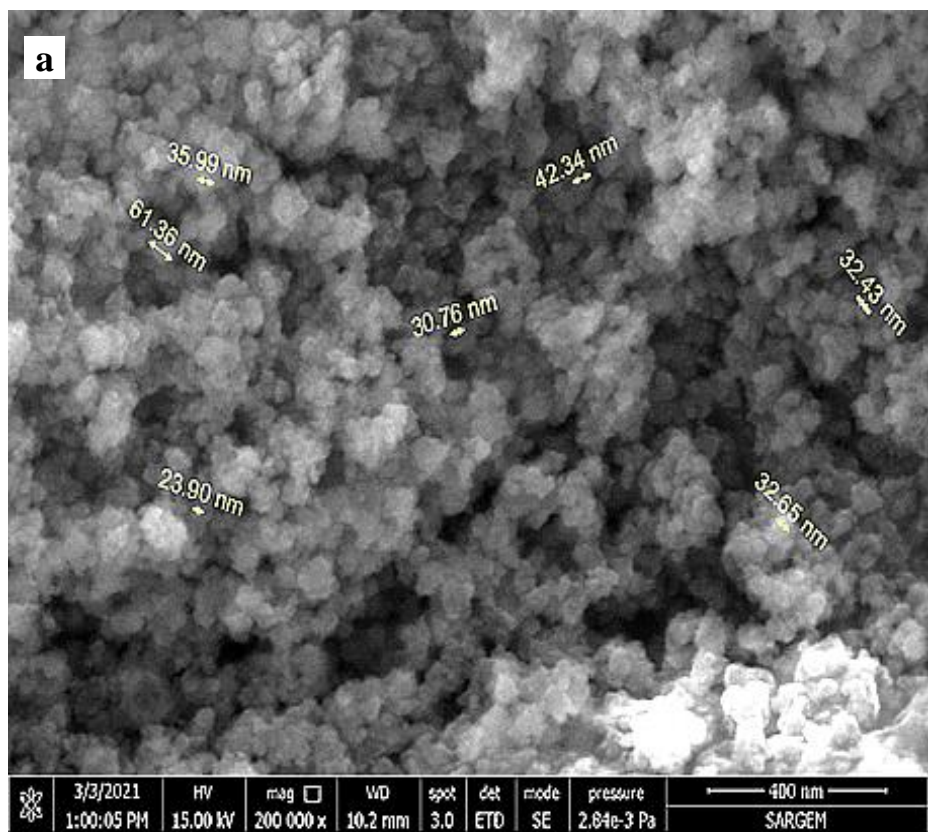


Figure 4.10. FESEM image of biosynthesized ZnO NPs (a) and particle size distribution (b) of ZnO NPs synthesized by *Bacillus subtilis* ZBP4.

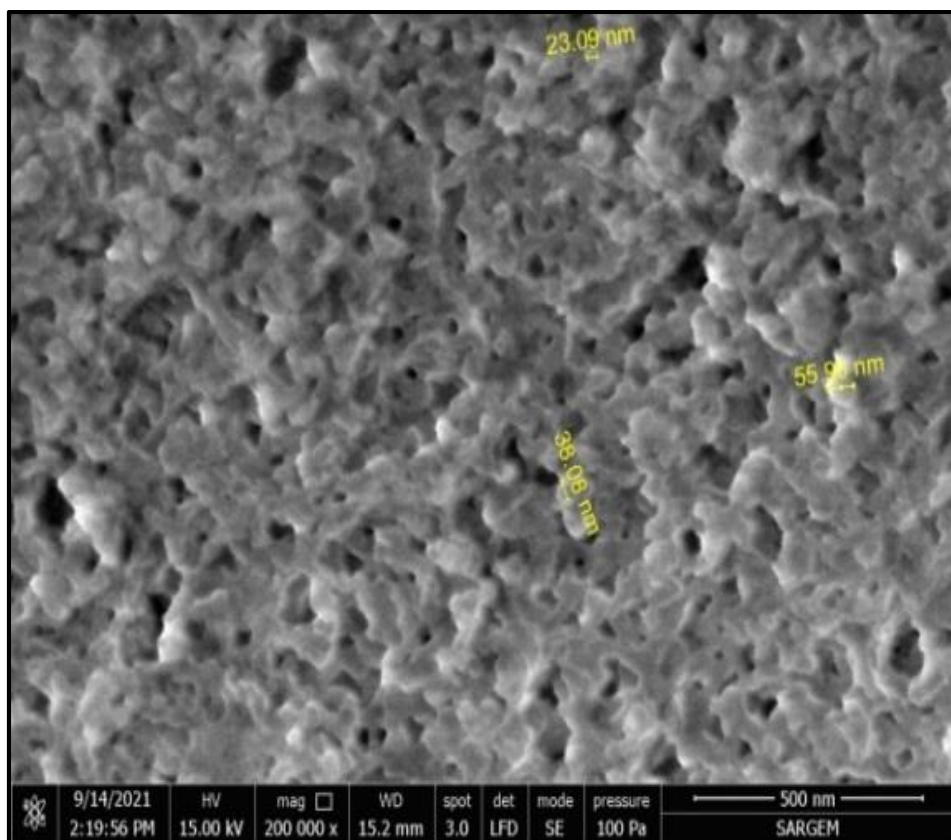


Figure 4.11. FESEM image of N-ZnO NPs.

4.7.3. Energy dispersive x-ray spectrometer

The biosynthesized ZnO NPs were analyzed by EDS to identify chemical compositions in the sample (Figure 4.12). EDS analysis confirmed the presence Zn atom along the peak at 1 KeV which characteristic for Zn atom with EDS. Also, a signal peak around 0.5 keV is characteristic of the oxygen atom. The weight percentages of zinc and oxygen atoms were 8.48 % and 23.54 % respectively (Table 4.1). There are some peaks between 0 and 2.5 KeV which are attributed to organic substances in the samples including C and P atoms.

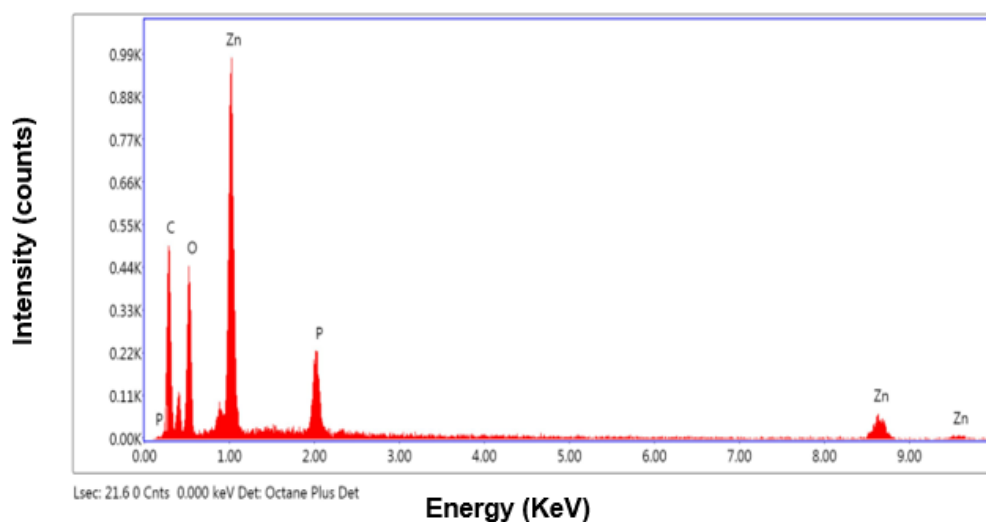
EDS spectra shown in Figure (4.13) are used to analyze the purity of the prepared N-ZnO NPs and prove the presence N, Zn and O in the samples. The EDS spectrum of pure N-ZnO is composed of N, Zn and O elements with corresponding contents of 16.93%, 9.39 % and 23.6 %, respectively (Table 4.2).

Table 4.1. Weight and atomic percentage composition of prepared ZnO NPs.

| Elements | Weight % | Atomic % | Net Int. |
|----------|----------|----------|----------|
| C K | 43.21 | 64.94 | 132.11 |
| O K | 20.87 | 23.54 | 114.17 |
| P K | 5.20 | 3.03 | 87.82 |
| Zn K | 30.72 | 8.48 | 43.19 |

Table 4.2. Weight and atomic percentage composition of 10 mg nisin loaded-ZnO NPs.

| Elements | Weight % | Atomic % | Net Int. |
|----------|----------|----------|----------|
| C K | 28.67 | 45.68 | 46.98 |
| N K | 12.39 | 16.93 | 13.31 |
| O K | 19.73 | 23.60 | 59.81 |
| Zn L | 32.07 | 9.39 | 134.00 |
| P K | 6.33 | 3.91 | 57.83 |
| S K | 0.82 | 0.49 | 7.55 |

**Figure 4.12.** Energy dispersive X-ray spectrum of the ZnO NPs.

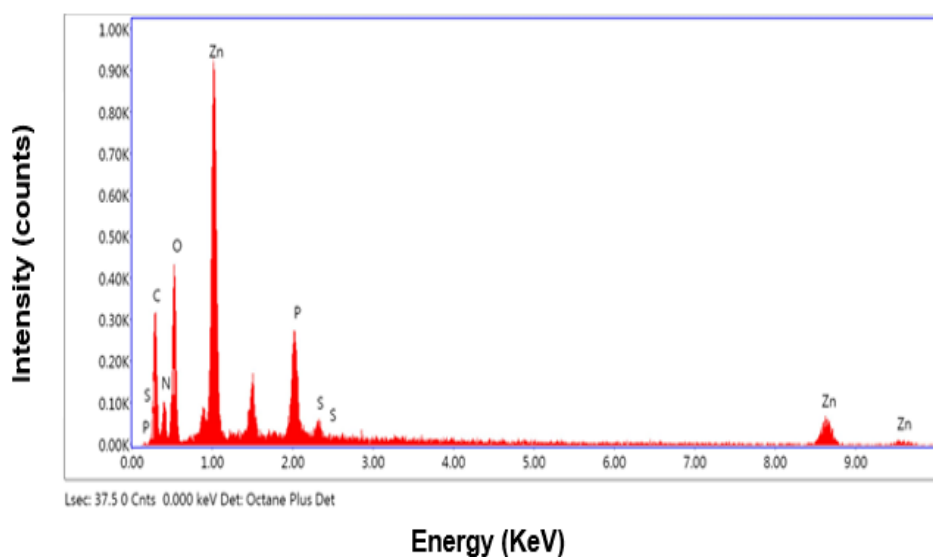


Figure 4.13. Energy dispersive X-ray spectrum of the N-ZnO NPs.

4.7.4. X-ray diffraction spectroscopy

Figure 4.16 illustrates the wide range of XRD diffractograms of the ZnO and N-ZnO NPs synthesized through the green method with optimum conditions. The results showed the XRD pattern for ZnO NPs, which is indexed as a crystal structure as shown in Figure 4.14. Also, The XRD results of N-ZnO NPs appeared amorphous and alone broad peaks at 2θ angles ($2\theta = 26.99^\circ$).

The XRD analysis of ZnO is in line with previous reports, they obtained the crystal structure of ZnO NPs created by plant extracts (Arumugam et al, 2021a; Varadavenkatesan et al, 2019). Our results matched with results of Shanmugasundaram and Balagurunathan (2017), which were biosynthesized crystal ZnO NPs using *Streptomyces* sp.

The amorphous structure of N-ZnO NPs is probably attributed to the presence of nisin on the surface of zinc nanoparticles. Nisin is act as a network covering all ZnO NPs as confirmed by FESEM images.

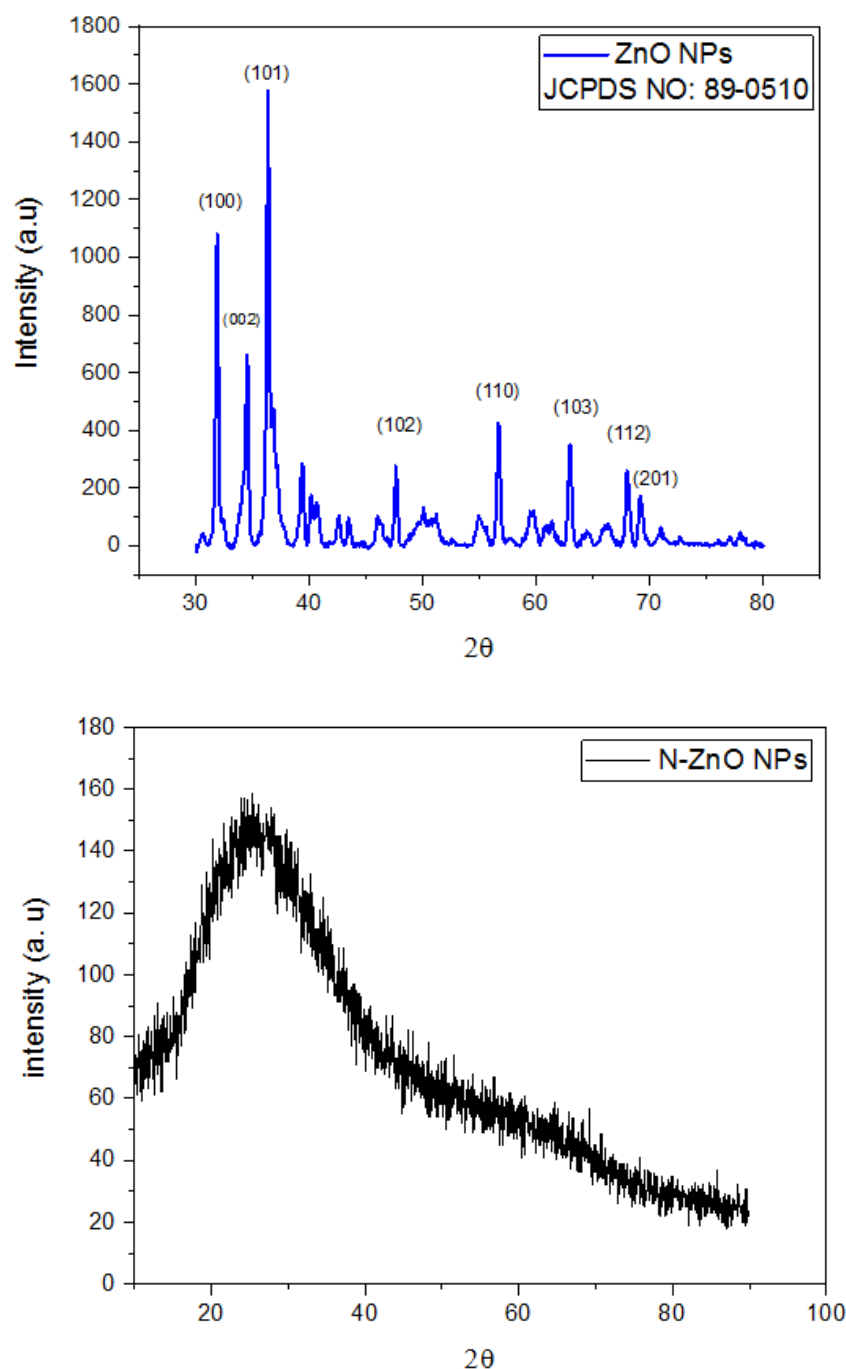


Figure 4.14. X-ray diffraction pattern of ZnO and N-ZnO NPs.

4.7.5. Fourier transform infrared spectroscopy

Measurements using the Fourier transform infrared spectroscopy technique were performed to locate possible biomolecules involved in the effective stabilization and capping of biosynthesized NPs. FTIR spectrum of ZnO NPs powder show different bands positioned at 3311 to 3312, 1638, 1407 to 1408, 1048 to 1051, and 569 cm^{-1} (Figure 4.15 and Table 4.3). Also, FTIR spectrum of nisin and N-ZnO NPs shows different bands positioned at at 3277 to 3281, 1637, 1406 to 1407, 1044 to 1045 and

558 cm^{-1} bands (Table 4.3). In the range of 3000-4000 cm^{-1} , the spectrum shows broad peaks at nearly 3000 cm^{-1} and 3400 cm^{-1} which correspond to the stretching vibration of amide I of proteins/enzymes and carbohydrates bonded O-H bonds (Santhoshkumar et al, 2017). The C = O stretch is shown around 1637 cm^{-1} for ZnO NPs and N-ZnO NPs respectively (Ebadi et al, 2019). The primary amines are shown around 1536 cm^{-1} , while extending vibration at 1407-1408 and 1406-1407 cm^{-1} for ZnO NPs and N-ZnO NPs respectively, which are attributed to C-N groups of amino acids substances (Muhammad et al, 2019). Intense peaks at 1048-1051 and 1044-1045 cm^{-1} for ZnO NPs and N-ZnO NPs respectively, which are associated with the C-O-C groups (El-Belely et al, 2021). The peaks were observed in this region at 569 and 558 cm^{-1} are allotted to Zn-O and N-ZnO NPs bonds respectively (Figure 4.15).

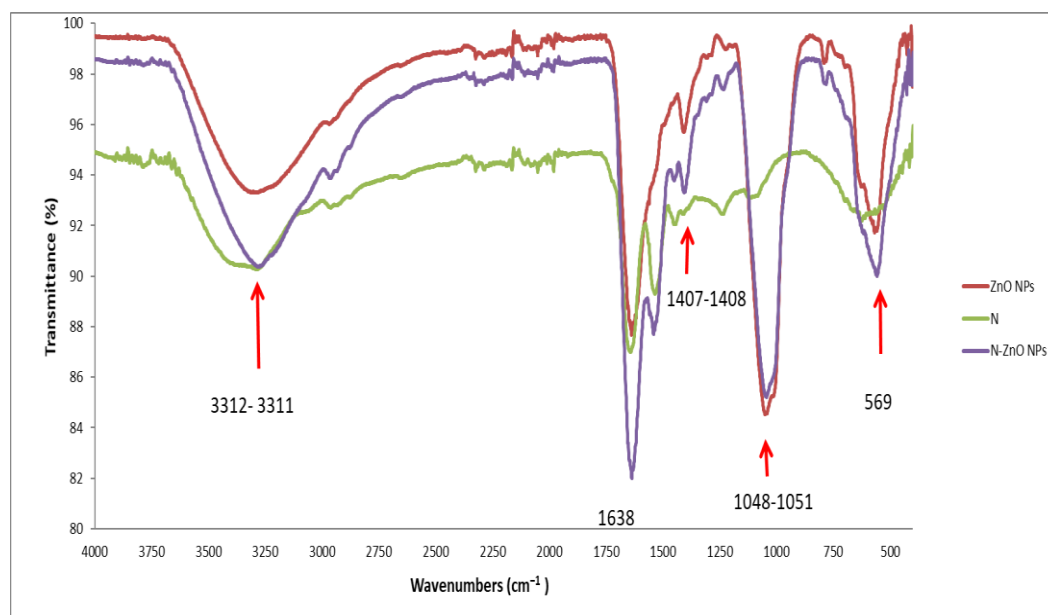


Figure 4.15. The Fourier transforms infrared (FTIR) spectroscopy measurement of ZnO NPs, nisin and N-ZnO NPs.

Table 4.3. Assignment of different peaks in the FTIR spectra of ZnO NPs, nisin loaded ZnO NPs.

| Possible assignment | Frequency (cm) ⁻¹ | | |
|--------------------------------|------------------------------|-----------|------------|
| | ZnO NPs | nisin | N- ZnO NPs |
| O – H stretching vibration | 3311-3312 | 3283-3286 | 3277-3281 |
| C = O stretching vibration | 1638 | 1643 | 1637 |
| Primary amines | - | 1536 | 1541 |
| C - N stretching in amino acid | 1407-1408 | 1446-1450 | 1406-1407 |
| C- O - C stretching vibration | 1048-1051 | - | 1044-1045 |
| Zn-O bond | 569 | - | - |
| N-Zn-O bond | - | - | 558 |

4.7.6. Zeta potential

The electrostatic potential at the particle interface between the colloidal particles' compact layer and diffuse layer is known as the zeta potential. It measures the electric potential between the particle interface and the stage of continuous phase distant from the interface (Kumar and Kumbhat, 2016; Ostolska and Wiśniewska, 2014). One of the parameters influencing the stability of particle dispersion is the zeta potential, with a value close to zero indicating a less stable dispersion. Zeta potential measurements reveal the potential stability of biogenic nanoparticles between - 30 mV and +30 mV. According to the triple measurements, the zeta potential of ZnO NPs biosynthesized by *Bacillus subtilis* ZBP4 ranged from -18.26 to -20.40 mV, and the calculated average zeta potential values of this nanoparticle was -19.0 mV (Figure 4.16a). Measurements of zeta potential of N-ZnO NPs exhibited again negative surface charge (-17.7 mV), which indicated that the particles are moderately stable (Figure 4.16b).

The zeta potential results of the current study are in accord with values reported by the other researchers. Barani et al. (2021) reported the zeta potential value of ZnO NPs biosynthesized by *Marinobacter* sp. 2C8 and *Vibrio* sp as -20.54 ± 7.15 and -23.87 ± 2.29 mV, respectively. A similar result was obtained by Balraj et al. (2017) as -21.8 mV for moderately stable ZnO NPs.

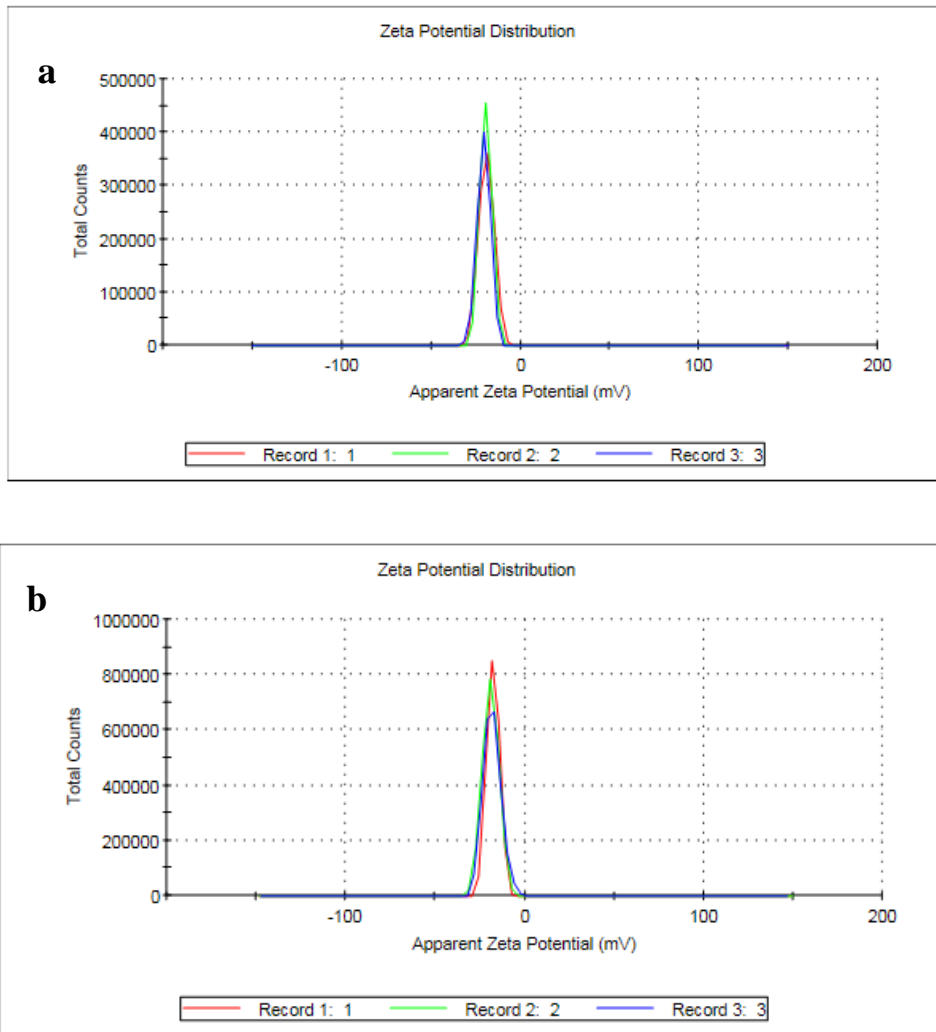


Figure 4.16. Zeta potential distribution of ZnO NPs (a) and N-ZnO NPs at 10 mg/mL (b).

4.7.7. Energy bandgap of nanoparticles

The amount of photon energy required by an electron to excite from the valence level to the lowest conduction level is known as the bandgap energy (Ekennia et al, 2021; Makuła et al, 2018). The bandgap of NPs is calculated by Tauc's plot equation, the graph was plotted using the data obtained from the absorption spectrum of NPs ($\alpha h\nu$)² with the photon energy ($h\nu$), and the value of the direct bandgap (E_g) was inferred at the intercept of ($\alpha h\nu$)² liner extrapolation with the x-axis. E_g was determined as 3.37 eV and 3.38 eV for ZnO NPs and N-ZnO NPs which were biosynthesized at the optimal conditions, respectively. These results indicated the semi-conductive property of NPs (Figure 4.17).

In other to further understand the bandgap properties of the NPs obtained using different concentrations of ZnSO₄.7H₂O and pH values, the calculated values of E_g

ranged from 3.30 to 3.33 eV to varying concentrations of salt (Appendix A). The highest values of the direct bandgap were found to be 3.41 eV for pH 7 after 24 h of incubation (Appendix B). Based on the observations above, we can briefly summarize that the precursor concentration and pH value can slightly change in the energy bandgap of nanoparticles.

The presence of ZnO NPs was validated in prior investigations on the production of ZnO NPs by metabolites of *Euphorbia sanguinea* (absorption peak at 356-378 nm); the direct bandgap was determined to be 2.72-4.37 eV (Ekennia et al, 2021). However the ZnO NPs obtained using various phytochemicals present in the extract gave the closest band gap energy to 3.37 eV (Mirgane et al, 2021). Another study synthesized ZnO NPs using *Rhodococcus pyridinivorans* bacteria; they obtained band energies of 3.31 eV (Kundu et al., 2014). Various researchers also observed similar results in the absorption band. The bandgap energies were found about 3.37 eV for synthesized ZnO NPs (Azizi et al, 2017; Quevedo-robles et al, 2022).

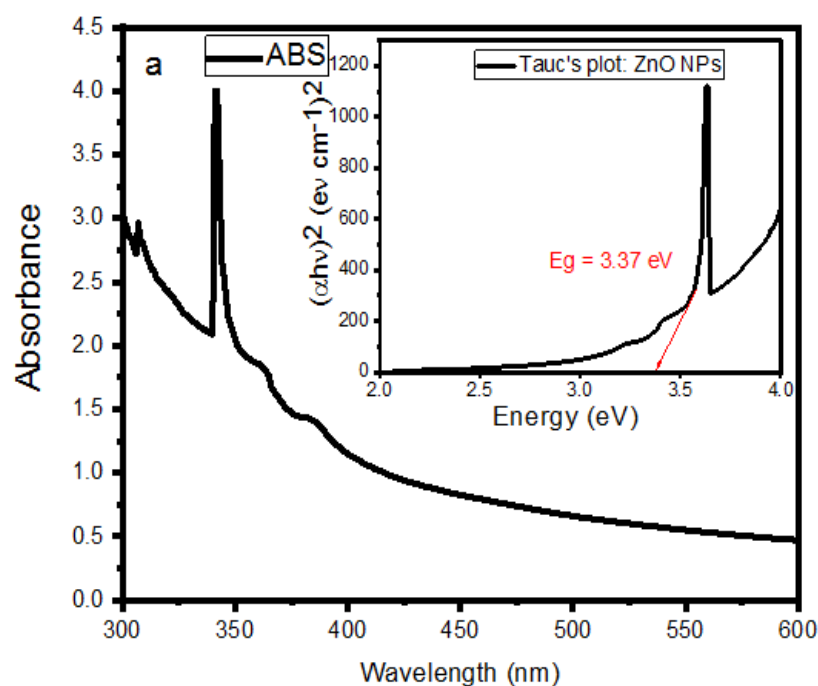


Figure 4.17. UV–VIS absorption spectrum of ZnO NPs and Tauc's plot of ZnO NPs (a) and N-ZnO NPs (b) deduced from the spectrum.

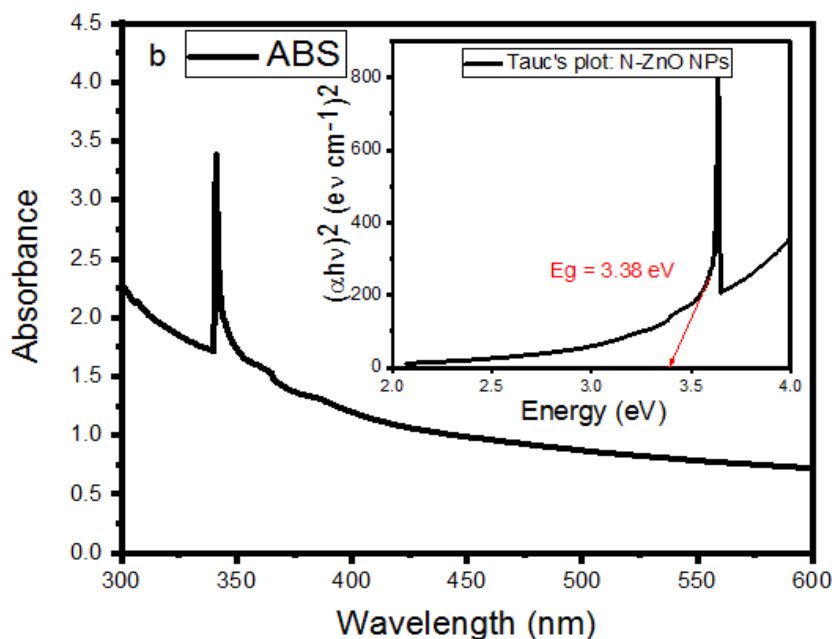


Figure 4.17. (Continued) UV–VIS absorption spectrum of ZnO NPs and Tauc's plot of ZnO NPs (a) and N-ZnO NPs (b) deduced from the spectrum.

4.8. Antimicrobial Activity of ZnO NPs

4.8.1. Antimicrobial activity of ZnO NPs against Gram positive bacteria

The effectiveness of ZnO NPs were determined in certain concentrations against three types of Gram-positive bacteria including *B. cereus*, *L. monocytogenes* ATCC 7644, and *S. aureus* ATCC 25923 as shown in Figure 4.18. The ZnO NPs were inhibited all the bacterial isolates under study with different inhibition zone diameters (IZD). The maximum IZD of *B. cereus*, *L. monocytogenes* ATCC 7644 and *S. aureus* ATCC 25923 were 12, 11 and 11.5 mm respectively. This result is in good agreement with Alizadeh-Sani (2020) who reported that ZnO NPs that inhibited *L. monocytogenes* and MIC value was found to be 1.5 mg/mL.

The lower activity of nanoparticles in this study could be due to agglomerates of nanoparticles generated in the suspension with greater diameters, which reduce adhesion and penetration of these nanoparticles into bacterial cells to kill them (Panpaliya et al, 2019). The results of the current study contradicted with Chennimalai et al. (2021), who explained the antibacterial activity of ZnO NPs against *S. aureus*, and *B. cereus* were 17 and 18 mm.

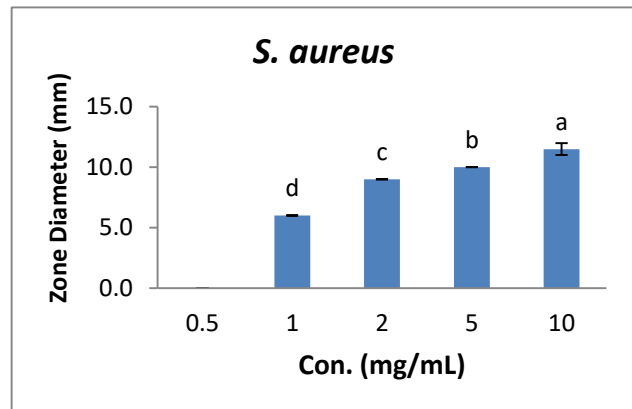
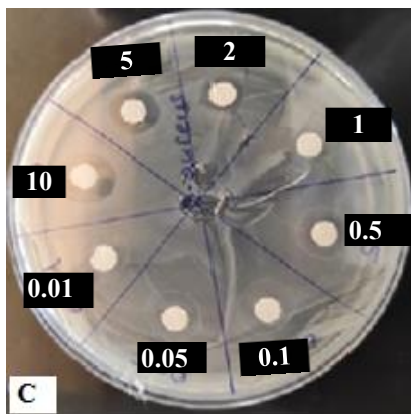
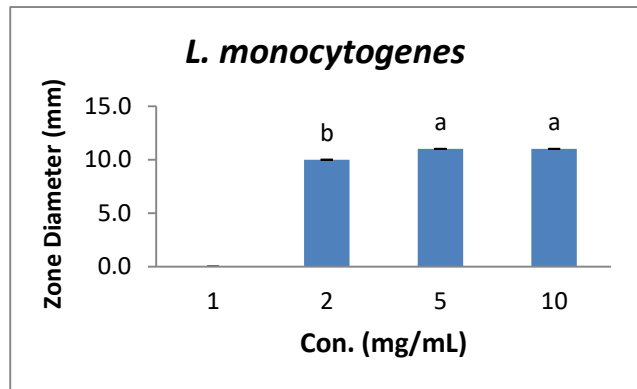
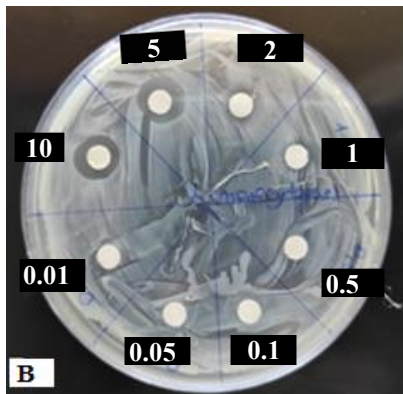
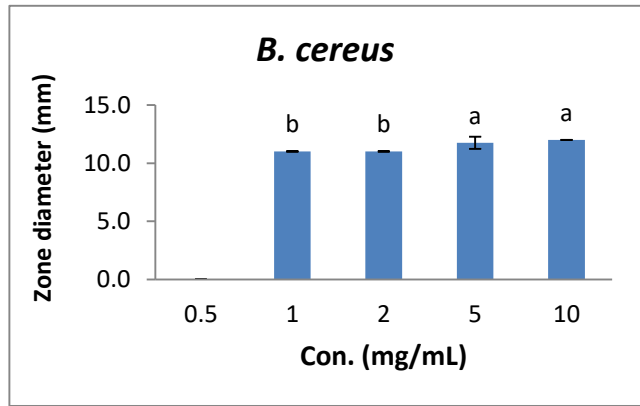
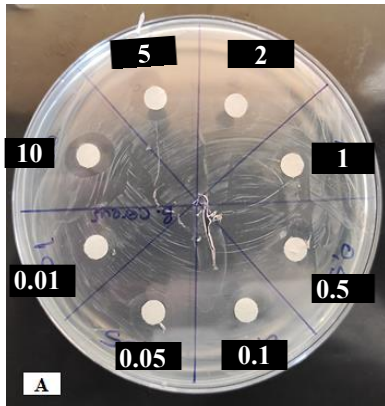


Figure 4.18. Antimicrobial activity of ZnO NPs. 0.01 mg/mL, 0.05 mg/mL, 0.1 mg/mL, 0.5 mg/mL, 1 mg/mL, 2 mg/mL, 5 mg/mL, 10 mg/mL used disc diffusion test (A) *B. cereus*, (B) *L. monocytogenes* ATCC 7644, (C) *S. aureus* ATCC 25923.

The different letters refer to significant differences at $P < 0.05$.

4.8.2. Antimicrobial activity of ZnO NPs against Gram negative bacteria

Biogenic ZnO NPs synthesized by *Bacillus subtilis* ZBP4 strain have been evaluated for their antibacterial activity against some Gram negative bacteria using the disc diffusion method (Figure 4.19). The ZnO NPs have the maximum zone of inhibition against the *S. Typhimurium* (13.3 mm), while the *P. aeruginosa* and *E. coli* Type 1 showed lowest affected with NPs at 10 mg/mL. Whereas, ZnO NPs at 1 mg were recorded lowest IZD (10 mm) towards *P. aeruginosa*, *E. coli* Type 1 and *E. coli* O157:H7 NCTC 12900 (Figure 4.19, Table 4.4). It was found that, at a concentration of 10 mg/mL, Gram-negative bacteria showed the largest inhibition zone in *S. Typhimurium* produced by ZnO NPs fabricated by *Bacillus subtilis* ZBP4, compared with the effect of the same nanoparticles on Gram-positive bacteria. Since Gram-positive bacteria cell wall is made up of a thicker peptidoglycan layer than Gram-negative bacteria, the difference in their cell wall composition may be the cause of variance in the effect of nanoparticles on bacteria. (Ali et al, 2018). In contrast to our study, Al-Radadi et al. (2022), who mentioned that isolates (*E. coli* and *S. aureus*) were more susceptible to synthesized ZnO NPs using ginger plant (*Zingiber officinale*). The results has converged with Chennimalai et al. (2021), who showed inhibition zones 13 mm against *E. coli*.

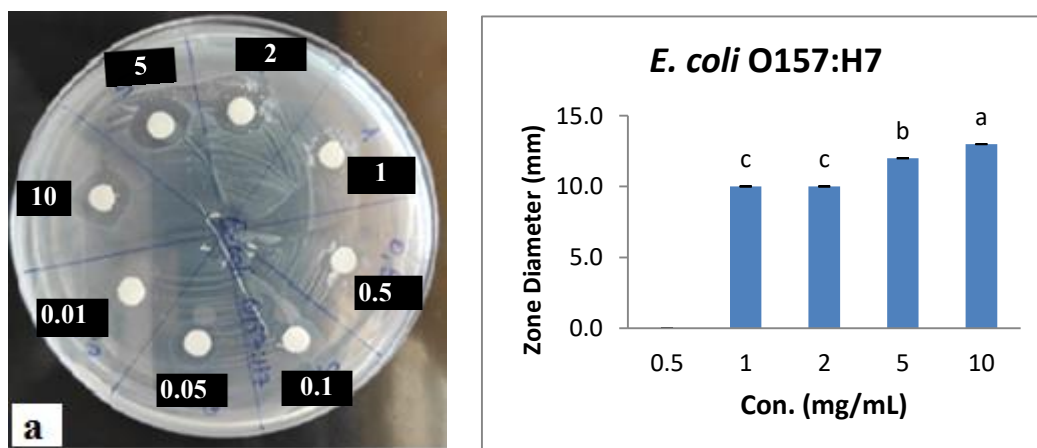


Figure 4.19. Antibacterial activity of ZnO NPs. 0.01 mg/mL, 0.05 mg/mL, 0.1 mg/mL, 0.5 mg/mL, 1 mg/mL, 2 mg/mL, 5 mg/mL, 10 mg/mL used disc diffusion test (a) *E. coli* O157:H7 NCTC 12900, (b) *P. aeruginosa*, (c) *S. Typhimurium*, (d) *E. coli* Type 1.

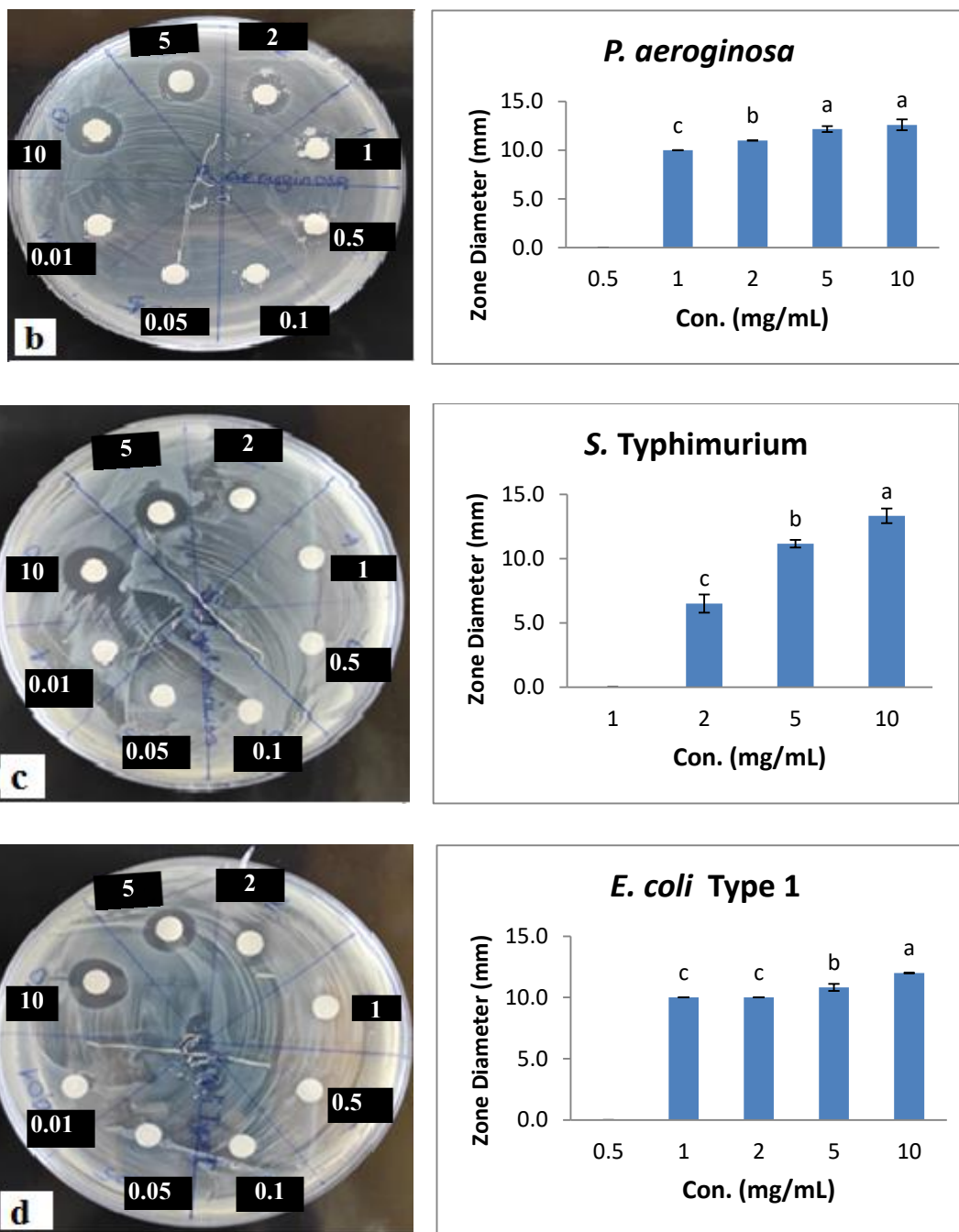


Figure 4.19. (Continued) Antibacterial activity of ZnO NPs. 0.01 mg/mL, 0.05 mg/mL, 0.1 mg/mL, 0.5 mg/mL, 1 mg/mL, 2 mg/mL, 5 mg/mL, 10 mg/mL used disc diffusion test (a) *E. coli* O157:H7 NCTC 12900, (b) *P. aeruginosa*, (c) *S. Typhimurium*, (d) *E. coli* Type 1.

The different letters refer to significant differences at $P < 0.05$.

4.8.3. Antifungal activity of ZnO NPs against *Candida albicans*

The antimicrobial activity of biosynthesized ZnO NPs was studied against the *C. albicans* using a standard zone of inhibition and is depicted in Figure 4.20. The maximum zone of inhibition was observed in the ZnO NPs (10 mg/mL) against *C.*

albicans (12 mm). On the other hand, the minimum zone of inhibition was observed in ZnO NPs (2 mg/mL) against *C. albicans* (10 mm). Pillai et al. (2020) investigated the effects ZnO NPs synthesized by *Cinnamomum verum* (PA1) on the growth *C. albicans*. Interestingly, nanoparticles exhibited a great effect against *C. albicans* (8 mm), while no inhibition showed on *A. niger*. These results are similar to a study conducted by Sharma and Ghose (2015) who observed that ZnO NPs has effective against *C. albicans* and the inhibition zone diameter of 20 mg/mL of ZnO NPs was 11.4 mm.

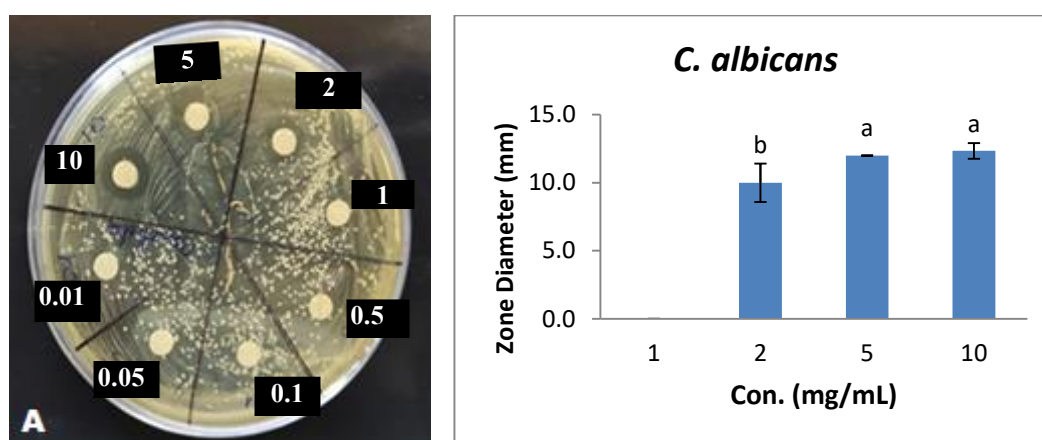


Figure 4.20. Antifungal activity of ZnO NPs against *C. albicans*. 0.01 mg/mL, 0.05 mg/mL, 0.1 mg/mL, 0.5 mg/mL, 1 mg/mL, 2 mg/mL, 5 mg/mL, 10 mg/mL used disc diffusion test.

The different letters refer to significant differences at $P < 0.05$.

4.9. Minimum Inhibitory Concentration (MIC) of ZnO NPs

Minimum inhibitory concentration value for the synthesized nanoparticles varied depending on bacterial isolates. The results in Table (4.4) were observed the effect of different concentrations of ZnO NPs on inhibition of various bacterial isolates. The MIC results proved the MIC value of ZnO NPs against *B. cereus*, *S. aureus* ATCC 25923, *E. coli* O157:H7 NCTC 12900, *E. coli* Type 1 and *P. aeruginosa* bacteria was 1 mg/mL, while it was 2 mg/mL for *L. monocytogenes* ATCC 7644, *S. Typhimurium* and *C. albicans*. From the results gained and summarized in Table (4.4), the ZnO NPs synthesized using *Bacillus subtilis* ZBP4 has exhibited strong antimicrobial activity against both Gram-positive and Gram-negative bacteria as well as *C. albicans*. The

results were contrasted with Lal et al. (2022), who found that MIC values of plant mediated ZnO NPs were 0.062 mg/mL for *S. aureus* and 0.125 mg/mL for *P. aeruginosa* and *E. coli* respectively. The present result goes in agreement with previous study by Aljelehawy et al. (2021).

Table 4.4. Antimicrobial activity of varying amounts of ZnO NPs synthesized at pH 7.5, 33 °C using 8 mM ZnSO₄.H₂O.

| ZnO NPs (mg/mL) | Zone of inhibition (mm) | | | | | | | | |
|-----------------|--------------------------|-------------------------|--------------------------|------------------------|---------------------------|--------------------------|--------------------------|---------------------------|-------------------------|
| | <i>B. cereus</i> | <i>L. monocytogenes</i> | <i>S. aureus</i> | <i>E. coli</i> O157:H7 | <i>P. aeruginosa</i> | <i>S. Typhimurium</i> | <i>E. coli</i> Type 1 | <i>S. Enteritidis</i> | <i>C. albicans</i> |
| 0.5 | - | - | - | - | - | - | - | - | - |
| 1 | 11 ^{Ba} ± 0 | - | 6 ^{Dc} ± 0 | 10 ^{Cb} ± 0 | 10 ^{Cb} ± 0 | - | 10 ^{Cb} ± 0 | 11 ^{Ba} ± 0 | - |
| 2 | 11 ^{Ba} ± 0 | 10 ^{Bb} ± 0 | 9 ^{Cc} ± 0 | 10 ^{Cb} ± 0 | 11 ^{Ba} ± 0 | 6.5 ^{Cd} ± 0.7 | 10 ^{Cb} ± 0 | 11 ^{Ba} ± 0.7 | 10 ^{Bb} ± 1.4 |
| 5 | 11.8 ^{Aa} ± 0.5 | 11 ^{Ab} ± 0 | 10 ^{Bc} ± 0 | 12 ^{Ba} ± 0 | 12.2 ^{Aa} ± 0.3 | 11.2 ^{Bb} ± 0.3 | 10.8 ^{Bb} ± 0.3 | 12.6 ^{Aa} ± 0.6 | 12 ^{Aa} ± 0 |
| 10 | 12 ^{Abc} ± 0 | 11 ^{Ad} ± 0 | 11.5 ^{Ac} ± 0.5 | 13 ^{Aa} ± 0 | 12.6 ^{Aab} ± 0.5 | 13.3 ^{Aa} ± 0.6 | 12 ^{Abc} ± 0 | 12.6 ^{Aab} ± 0.6 | 12 ^{Abc} ± 0.6 |

-No inhibition zone

-The different letters (capital letters) in the column refer to significant differences at 0.05.

-The different letters (small letters) in the row refer to significant differences at 0.05.

4.10. Antibacterial Activity of Nisin or Nisin-ZnO NPs

The exact antibacterial mechanism of N-ZnO NPs is not completely clear. nisin antibiotic peptide is capable of interacting with negative charges biomolecules especially lipid bilayer in the plasma membrane of vegetative cells and hydrophilic-hydrophobic force play an important role in parallel adsorption of nisin with lipids (Santos et al, 2018). The practical application of nisin is limited because the outer membrane of Gram-negative bacteria acts as a defense wall to bacteriocins, thus Gram-positive bacteria are sustainable more than Gram-negative bacteria (Abee et al, 1994; Pol et al, 2000). Pore formation is thought to produce fast transmembrane electrostatic potential dissipation, resulting in strongly deform membrane permeabilization and facilitate of penetrate of nanoparticles inside cell (Arakha et al, 2016; Prince et al, 2016).

4.11. Antibacterial Activity of Nisin and N-ZnO NPs

4.11.1. Antibacterial activity of nisin or nisin-ZnO NPs against Gram positive bacteria

In vitro antibacterial activity of nisin was carried out and nisin conjugated with the ZnO NPs against pathogenic Gram-positive bacteria including *B. cereus*, *L. monocytogenes* ATCC 7644 and *S. aureus* ATCC 25923. The results showed the high inhibition activity of N-ZnO NPs against these bacterial pathogens. The diameter of the inhibition zone of *B. cereus*, *L. monocytogenes* ATCC 7644 and *S. aureus* ATCC 25923 as follows 12.9, 13.8 and 14.8 mm for nisin conjugated with ZnO NPs. It was found that the nisin enhanced the action rates of the ZnO NPs in a synergistic mode as well as in its own way on these pathogens. In contrast, the antimicrobial activity was ineffective with free nisin corresponding to the same concentrations used as illustrated in Figure 4.21. This result is in agreement with the report given by Morsy et al. (2018) reveals that the *L. monocytogenes* strains were more susceptible to ZnO NPs combined with nisin (nisin: ZnO-NPs; 1:1, v/v); the reason attributed to the membrane of *L. monocytogenes* is sensitive to damage and pore formation. Consequently, their combination may enable an attack on several targets at once. Additionally, N-ZnO NPs was the most active combination against *B. Cereus*, *L. monocytogenes* ATCC 7644 and *S. aureus* ATCC 25923.

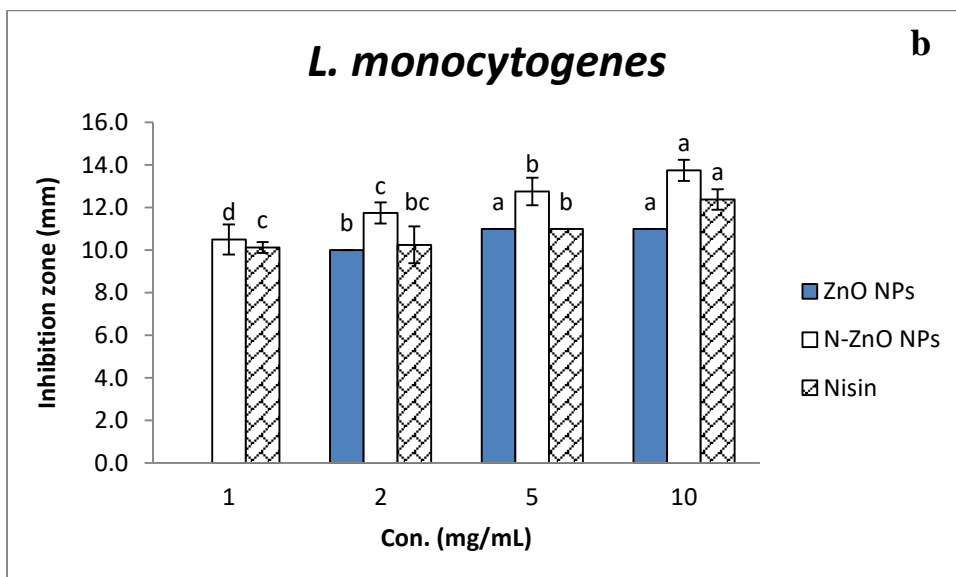
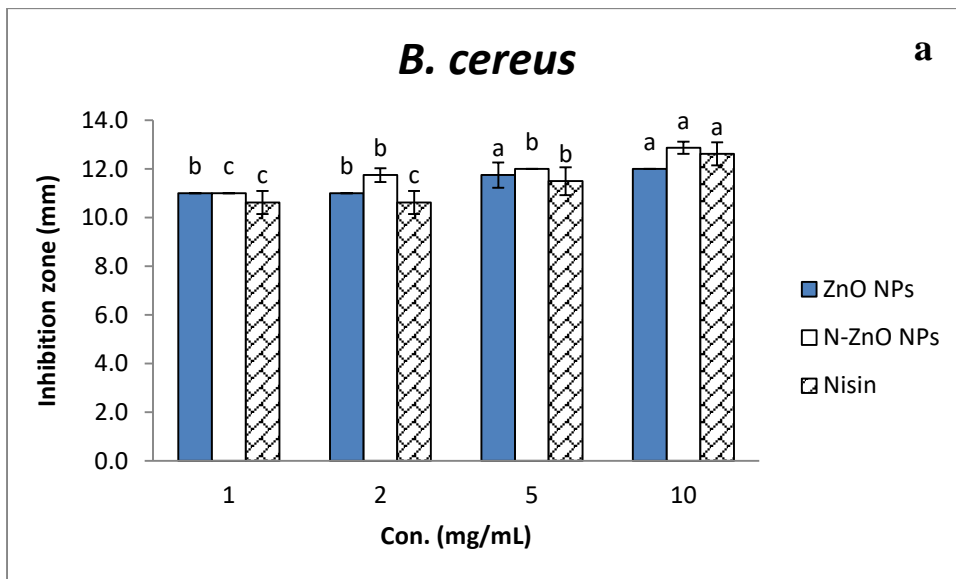


Figure 4.21. Antibacterial activity of ZnO NPs, nisin and nisin loaded ZnO NPs. 1 mg/mL, 2 mg/mL, 5 mg/mL, 10 mg/mL used disc diffusion test (a) *B. cereus*, (b) *L. monocytogenes* ATCC 7644, (c) *S. aureus* ATCC 25923.

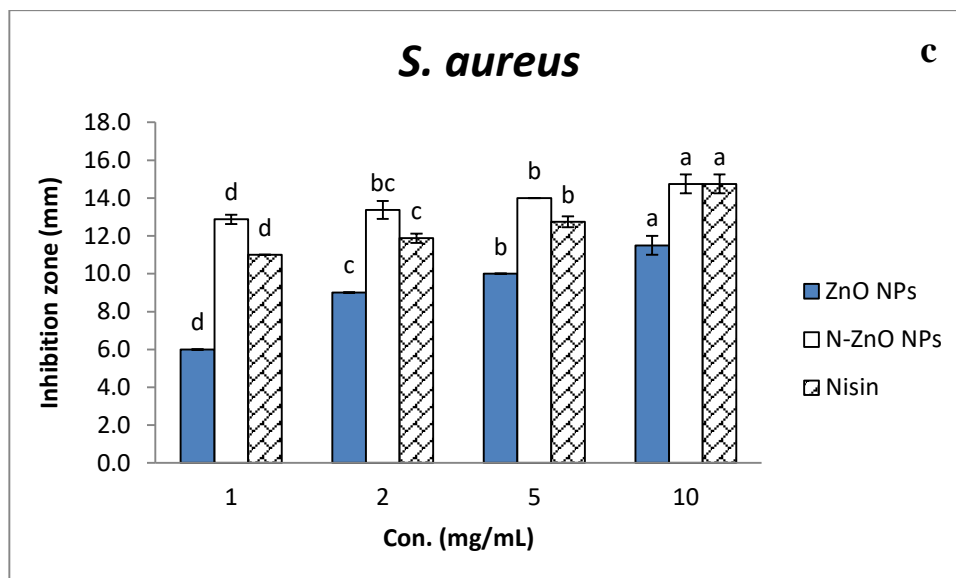


Figure 4.21. (Continued) Antibacterial activity of ZnO NPs, nisin and nisin loaded ZnO NPs. 1 mg/mL, 2 mg/mL, 5 mg/mL, 10 mg/mL used disc diffusion test (a) *B. cereus*, (b) *L. monocytogenes* ATCC 7644, (c) *S. aureus* ATCC 25923.

- The different letters refer to significant differences at $P < 0.05$ and Statistical analysis was performed for each day individually.

4.11.2. Antibacterial activity of nisin or nisin-ZnO NPs against Gram negative bacteria

To investigate the effect of different concentrations of nisin and biosynthesized N-ZnO NPs on Gram-negative bacteria growth, antibacterial activity was assessed against different pathogenic bacteria using the disc diffusion method as shown in Figure 4.22. The results showed the synergistic effect of nisin with ZnO NPs at different concentrations against bacterial isolates. Nisin loaded ZnO NPs showed high efficacy against bacterial isolations compared to the action of nisin alone; the inhibition zones formed by N-ZnO NPs at 10 mg/mL against Gram-negative bacteria were 16 mm and 15.8 mm for *S. Enteritidis* ATCC 13076 and *P. aeruginosa* respectively, Also bioconjugation of ZnO NPs with bacteriocin resulted in a significant reduction of MIC values. Results appeared that the MIC for N-ZnO NPs were 0.05 mg/mL for *S. Enteritidis* ATCC 13076, and 2 mg/mL for *S. Typhimurium* and *E. coli* O157:H7 NCTC 12900. At the same time, the MIC for free nisin were 0.1 mg/mL for *S. Enteritidis* ATCC 13076. The nisin peptide did not show antibacterial activity toward each *E. coli* O157: H7 NCTC 12900, *S. Typhimurium* and *E. coli* Type 1. The results

indicated that N-ZnO NPs have better inhibitory effects against some species of Gram negative (*S. Enteritidis* ATCC 13076 and *P. aeruginosa*) and Gram positive bacteria (*B. cereus*, *L. monocytogenes* ATCC 7644 and *S. aureus* ATCC 25923) than those caused by free ZnO NPs or free nisin. Zinc oxide NPs did not show synergistic effects with nisin against *E. coli* O157: H7 NCTC 12900, *S. Typhimurium* and *E. coli* Type 1 compared with ZnO NPs alone. The our results agreed with findings (Morsy et al, 2018).

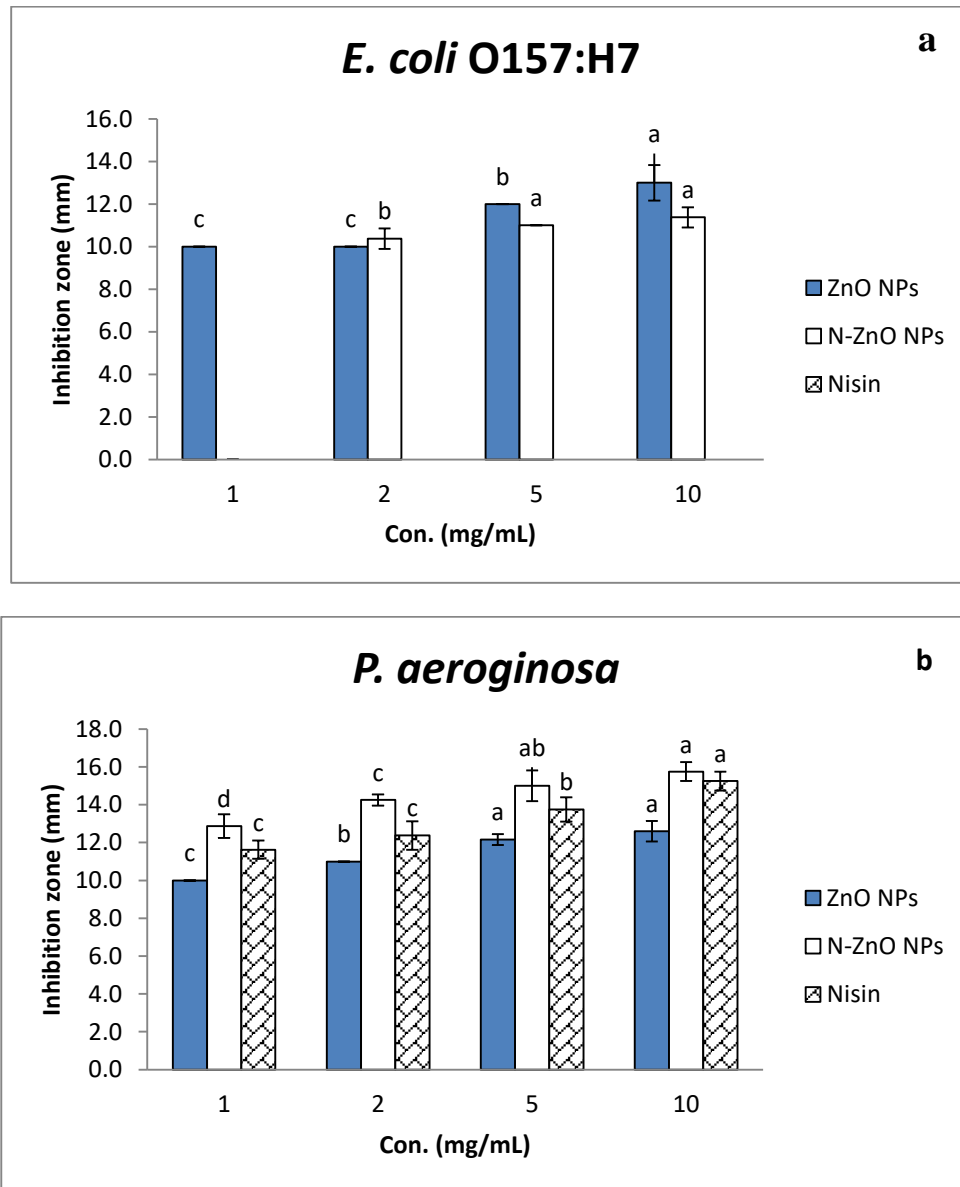


Figure 4.22. Antibacterial activity of ZnO NPs, nisin and nisin loaded ZnO NPs. 1 mg/mL, 2 mg/mL, 5 mg/mL, 10 mg/mL used disc diffusion test (a) *E. coli* O157:H7 NCTC 12900, (b) *P. aeruginosa*, (c) *S. Typhimurium*, (d) *E. coli* Type 1, (e) *S. Enteritidis* ATCC 13076.

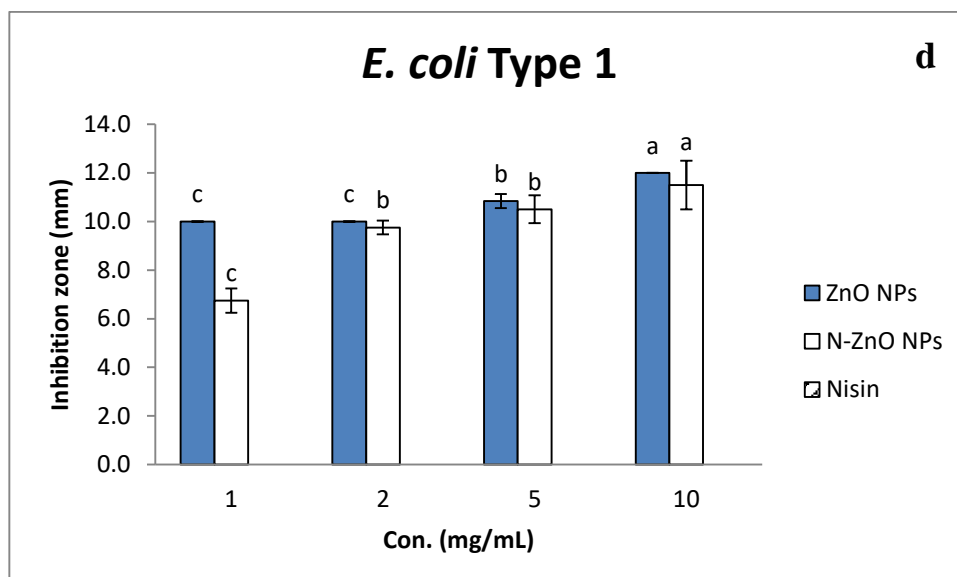
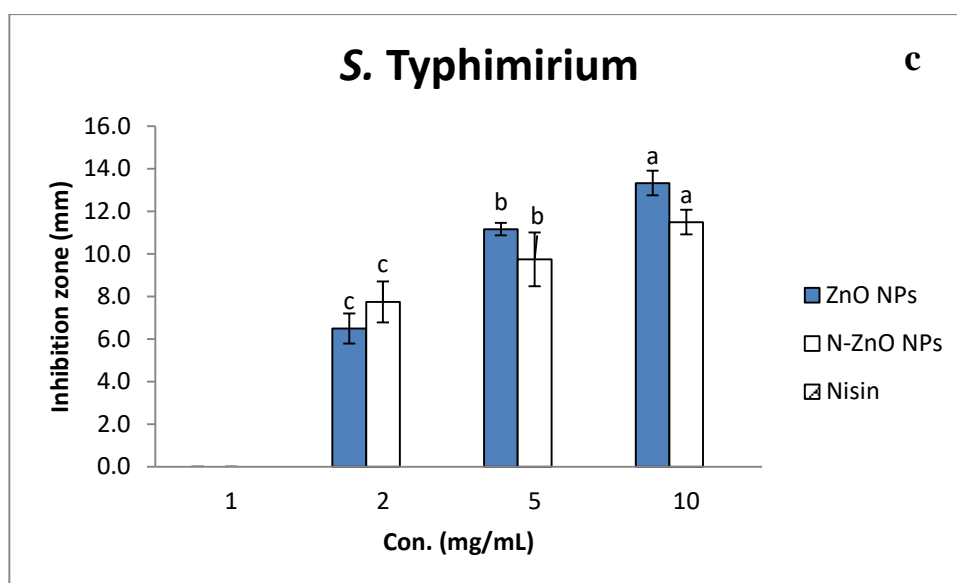


Figure 4.22. (Continued) Antibacterial activity of ZnO NPs, nisin and nisin loaded ZnO NPs. 1 mg/mL, 2 mg/mL, 5 mg/mL, 10 mg/mL used disc diffusion test (a) *E. coli* O157:H7 NCTC 12900, (b) *P. aeruginosa*, (c) *S. Typhimurium*, (d) *E. coli* Type 1, (e) *S. Enteritidis* ATCC 13076.

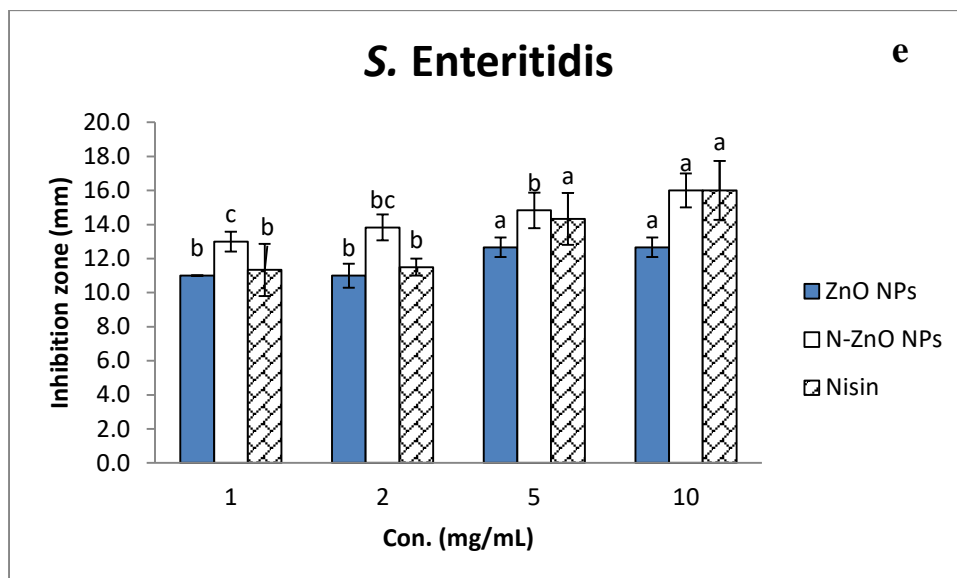


Figure 4.22. (Continued) Antibacterial activity of ZnO NPs, nisin and nisin loaded ZnO NPs. 1 mg/mL, 2 mg/mL, 5 mg/mL, 10 mg/mL used disc diffusion test (a) *E. coli* O157:H7 NCTC 12900, (b) *P. aeruginosa*, (c) *S. Typhimurium*, (d) *E. coli* Type 1, (e) *S. Enteritidis* ATCC 13076.

- The different letters refer to significant differences at $P < 0.05$ and statistical analysis was performed for each day individually.

4.12. Antimicrobial Activity of ZnO NPs in Liquid Medium

The measurement of the minimum exposure time curve was used to estimate the effective bactericidal impact of ZnO NPs on two model bacteria. Briefly, ZnO NPs were added to bacterial suspensions in TSB during the exponential growth phase, and we measured the MFU at 0, 1, 2, 3, 4, 5, 6, 7, 8, 22, 23, and 24 h of culture to following bacterial growth. This study showed that bacterial growth was delayed at low concentrations (100 and 250 $\mu\text{g/mL}$) and both bacteria treated with 100 and 250 $\mu\text{g/mL}$ of ZnO NPs showed nearly similar inhibitory effects. ZnO NPs at a concentration of 500 $\mu\text{g/mL}$ demonstrated potent inhibition of bacterial growth after 5 h of incubation (Figure 4.23).

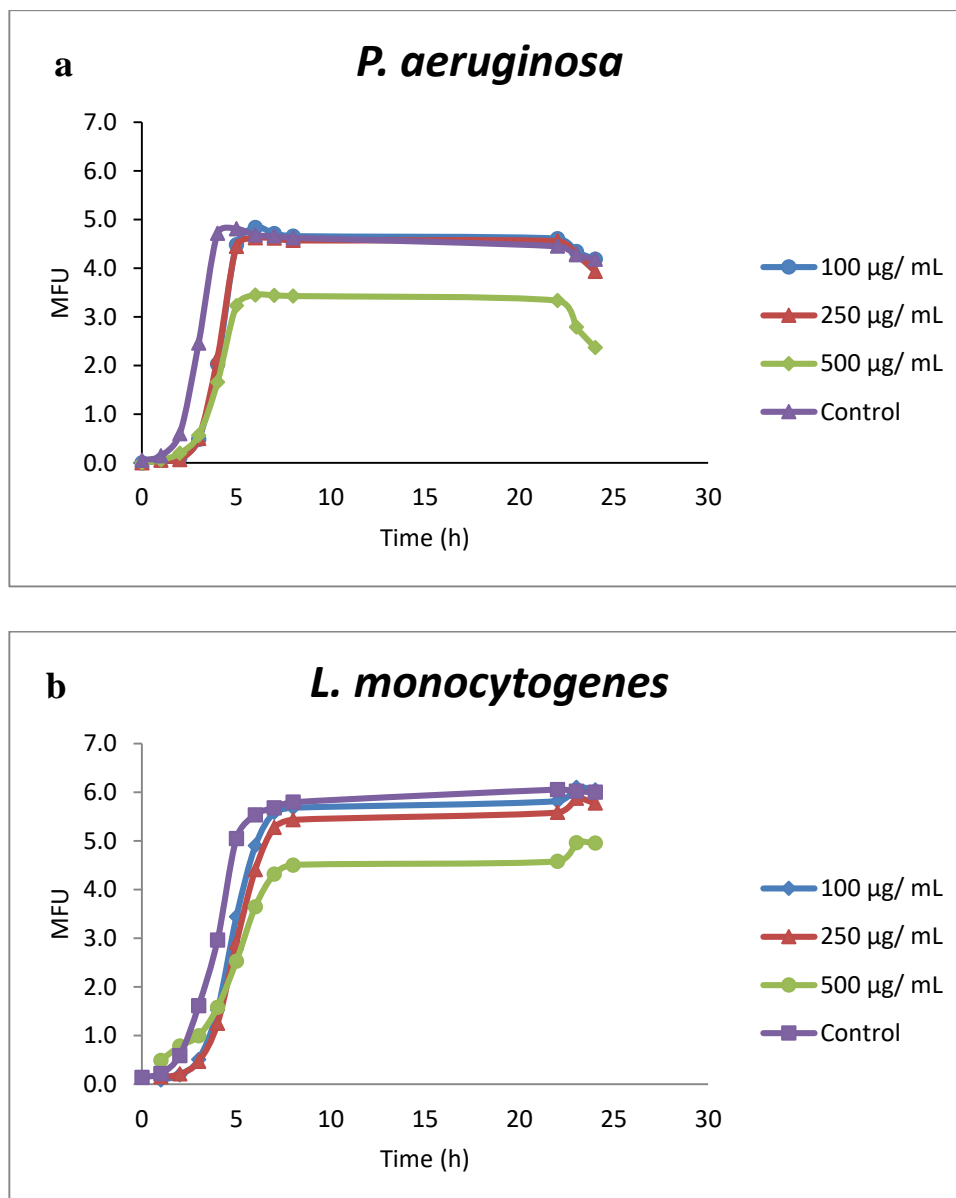


Figure 4.23. Growth curve of *P. aeruginosa* (a) and *L. monocytogenes* ATCC 7644 (b) in tryptic soy broth in the presence of various concentrations of ZnO NPs.

4.13. Growth Inhibition Curves of ZnO NPs, Nisin and N-ZnO NPs in Liquid Medium

The effects of different concentrations of nisin and ZnO NPs alone or in conjugations with nisin on *L. monocytogenes* ATCC 7644 and *S. aureus* ATCC 25923 were illustrated in Figures 4.24 and 4.25. Therefore, the influences of NPs on bacterial growth were measured at different times (0, 1, 2, 3, 4, 5, 6, 7, 8, 9, 10 and 24 h). The antibacterial activity was determined through the determination of the optical density (OD) of the culture. The results showed that the OD values of high concentration ZnO

NPs (150 µg/mL) synthesized by bacteria were decreased and *L. monocytogenes* ATCC 7644 bacteria were more sensitive to ZnO NPs, On another hand, ZnO NPs do not exhibit cell killing or growth arresting properties against *S. aureus* ATCC 25923 at 30 and 75 µg/mL. Under the absence of NPs, *L. monocytogenes* ATCC 7644 and *S. aureus* ATCC 25923 reached the exponential phase (log phase) rapidly. While, treated with 30, 75 and 150 µg/mL of N-ZnO NPs, bacterial cells were lagged to 24 h. With the increasing concentration of NPs, the delay was more evident (Figure 4.24 c and 4.25 c). Results also illustrated that the bacterial isolates delayed replication at 30 and 75 µg/mL (bacteriostatic effect) and completely inhibited *S. aureus* at 150 µg/mL (bactericidal effect). Zinc Oxide show strong synergistic effects with nisin, It might be also a novel route to use ZnO NP with nisin for bacterial control.

Table 4.5 shows the inhibition percentage of each of ZnO NPs, nisin and nisin- ZnO NPs against *L. monocytogenes* ATCC 7644 and *S. aureus* ATCC 25923 at 6 hours. The results showed that nisin functionalized ZnO NPs are more effective against *L. monocytogenes* ATCC 7644 and *S. aureus* ATCC 25923 than ZnO NPs alone. Results revealed that contact times (6 h) were enough for 94.98 and 96.79 % reduction (MFU) in the viable population of *L. monocytogenes* ATCC 7644 and *S. aureus* ATCC 25923 at 150 µg/ mL. But a decrease in growth was not observed in ZnO NPs treated culture (30 µg/ mL, 75 µg/ mL and 150 µg/ mL) which proved the bacteria slightly was susceptible compared to N-ZnO NPs treated.

Zinc oxide nanoparticles were evaluated on *S. aureus* ATCC 25923 and *S. Typhimurium*, the viability of these bacteria decreased after 3 h of the incubation period (Navale et al, 2015). Another study showed that *S. aureus* growth was inhibited by ZnO NPs, and time-dependent alterations in bacterial growth were measured using a spectrophotometer (Agarwal et al, 2019). In a similar study conducted by Zhao and Kuipers (2021) Ag-nisin NP has strong bactericidal activity against all pathogenic bacteria, which killed each of the *E. coli*, *K. pneumoniae*, and *S. aureus* within 1 hour of treatment, while *P. aeruginosa* cells were killed in 4 h after treatment, which is matched with the current findings. Thus, zinc oxide shows strong synergistic effects with nisin, and it may open new vistas to using ZnO NP with nisin for bacterial control. *S. aureus* cells lose their ability to grow, indicating that the integrity or structure of the bacterial membrane may have been affected, leading to cell death (Mirhosseini and Afzali, 2016). This study is the first of its kind, we achieved the high antibacterial

efficacy of N-ZnO NPs with comparable to ZnO NPs. The reason may be attributed to the high concentration of peptides on the surface of NPs, as a result it gets the massive area of touch of nisin-capped NPs with the bacterial cell (Peng et al, 2016).

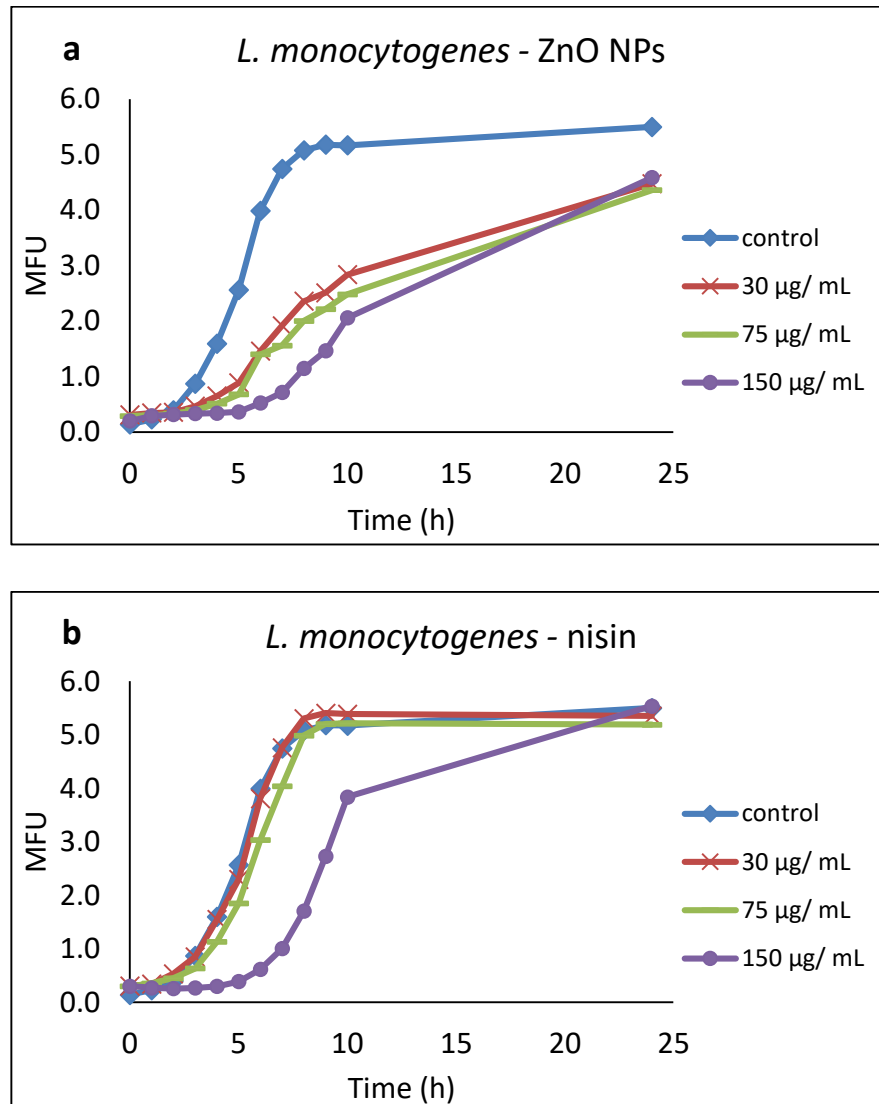


Figure 4.24. Bacterial growth curve of *L. monocytogenes* ATCC 7644 in TSB.

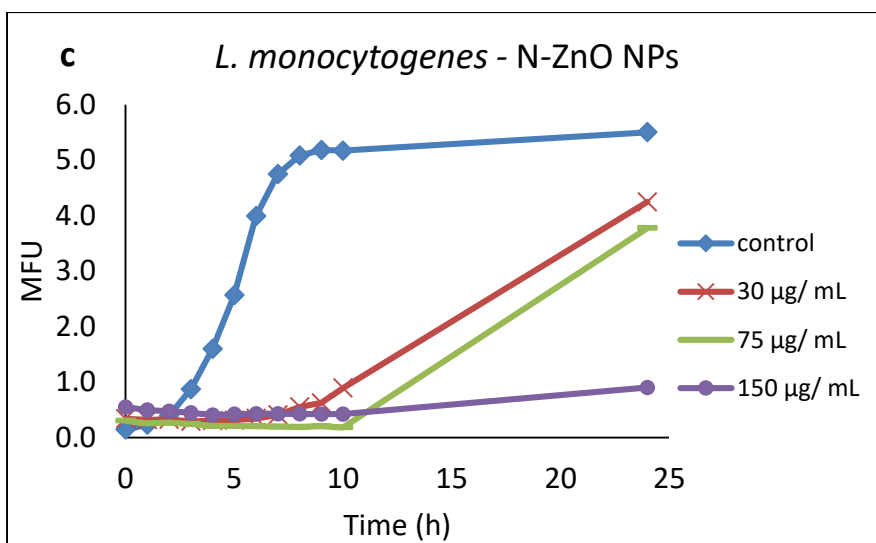


Figure 4.24. (Continued) Bacterial growth curve of *L. monocytogenes* ATCC 7644 in TSB.

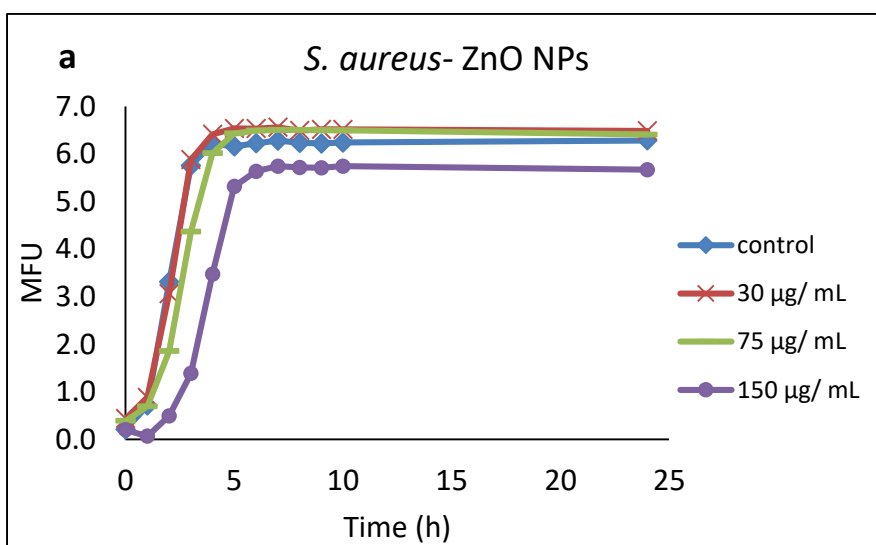


Figure 4.25. Bacterial growth curve of *S. aureus* ATCC 25923 in TSB.

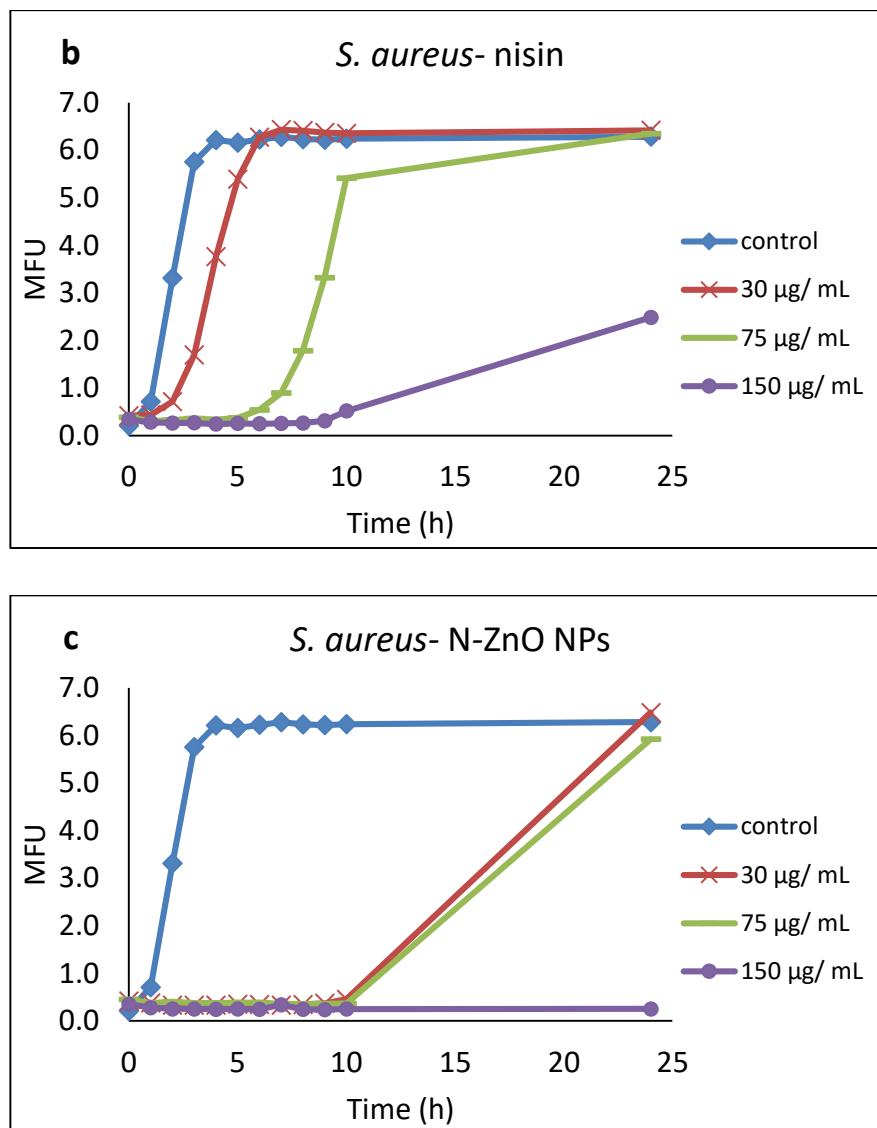


Figure 4.25. (Continued) Bacterial growth curve of *S. aureus* ATCC 25923 in TSB.

Table 4.5. The inhibition percentage of ZnO NPs, free nisin and nisin- ZnO NPs against *L. monocytogenes* ATCC 7644 and *S. aureus* ATCC 25923 at 6 hours.

| Type of bacteria | | Inhibition % (6 hours) | | | |
|------------------|-------------------------|------------------------|-----------|-----------|------------|
| | | control | 30 µg/ mL | 75 µg/ mL | 150 µg/ mL |
| ZnO NPs | <i>L. monocytogenes</i> | 0 | 63.41 | 64.92 | 87.47 |
| | <i>S. aureus</i> | 0 | 0 | 0 | 10.12 |
| Free nisin | <i>L. monocytogenes</i> | 0 | 4.52 | 24.07 | 84.96 |
| | <i>S. aureus</i> | 0 | 0 | 91.74 | 96.79 |
| N-ZnO NPs | <i>L. monocytogenes</i> | 0 | 91.48 | 94.98 | 94.98 |
| | <i>S. aureus</i> | 0 | 94.55 | 94.55 | 96.79 |

4.14. Antioxidant Activity of ZnO NPs and N-ZnO NPs

Figure 4.26 presents the DPPH radical scavenging activity of ZnO NPs and N-ZnO NPs synthesized using *Bacillus subtilis* ZBP4. In this test, the NPs convert the purple radical (picrylhydrazyl) to the equivalent light yellow hydrazine (picrylhydrazyl). With time, the peak intensity at 517 nm gradually decreases with increased nanoparticles concentration, resulting in inhibition percentages of N-ZnO NPs 28.6, 28.8, 31.8, 33.7 and 34.6 % at 1500, 2000, 2500, 3000 and 3500 µg/mL respectively. The results also clearly indicated that the addition of the nisin peptide could significantly improve the DPPH radical scavenging activities of the ZnO NPs, the highest DPPH radical scavenging activity up to 34.6 % was recorded for 3500 µg/mL of nisin loaded ZnO NPs, while the ZnO NPs exhibited the lowest activity (15.3 %).

The IC₅₀ value was determined from the plotted graph of scavenging activity against the different concentrations of ZnO and N-ZnO NPs. The percentage of DPPH reduction expressed the scavenging activity after 30 min of reaction as displayed in Table (4.6).

According to Arumugam et al. (2021b), ZnO NPs synthesized from *Syzygium cumini* (Java plum) aqueous leaf extract demonstrated 64.5 % DPPH activity at 100 µg /mL and the activity was higher when compared to the achieved result. The results were contrasted with Ananthalakshmi et al. (2019), who mentioned significant antioxidant activity (% 80.99) of ZnO NPs at 1000 µg/mL. In DPPH, The concentration of the migrated electron from the oxygen atom to the odd electron on the nitrogen atom may be a reason for the low antioxidant activity of N-ZnO NPs (Das et al, 2013).

Table 4.6. Free radical scavenging activity of ZnO NPs and N-ZnO NPs determined by DPPH assay.

| Sample No | Nanoparticle Concentration ($\mu\text{g/mL}$) | Antioxidant Activity of ZnO NPs | | Antioxidant Activity of N-ZnO NPs | |
|-----------|---|---------------------------------|------------------|-----------------------------------|------------------|
| | | Inhibition (%) | IC ₅₀ | Inhibition (%) | IC ₅₀ |
| 1 | 1500 | 9.1 | | 28.6 | |
| 2 | 2000 | 11.5 | | 28.8 | |
| 3 | 2500 | 11.8 | 15544.69 | 31.8 | 7925.5882 |
| 4 | 3000 | 13.7 | | 33.7 | |
| 5 | 3500 | 15.3 | | 34.6 | |

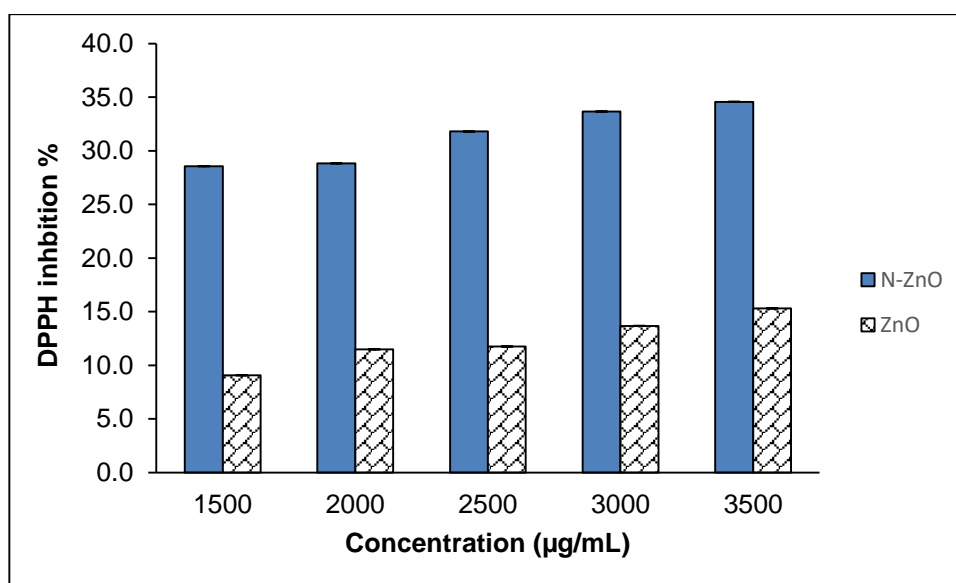


Figure 4.26. DPPH Scavenging activity of ZnO NPs and N-ZnO NPs synthesized using *Bacillus subtilis* ZBP4.

4.15. Effect Storage on Shelf Life of Nanoparticles

The effect of storage on the stability or the shelf life of synthesized NPs by *Bacillus subtilis* ZBP4 showed in Figure 4.27. The stability of the synthesized NPs was monitored for 120 days by using UV–VIS spectral analysis. The UV–visible spectra of ZnO NPs did not show an absorption peak after 120 days of storage in the refrigerator. Results showed that N-ZnO NPs synthesized by *Bacillus* remained stable without color change. Keeping the N-ZnO NPs for 120 days has a minimal effect on

the stability of NPs synthesized by nonpathogenic bacteria. Figure 4.27c presents an absorption peak observed at 341 nm, indicating the stable of 10 mg nisin conjugated with ZnO NPs and no remarkable differences between the colors of NPs during this storage period. Current study findings suggest that the conjugation of nisin with ZnO NPs helps increase the shelf life of ZnO NPs for 4 months of storage at 4 °C.

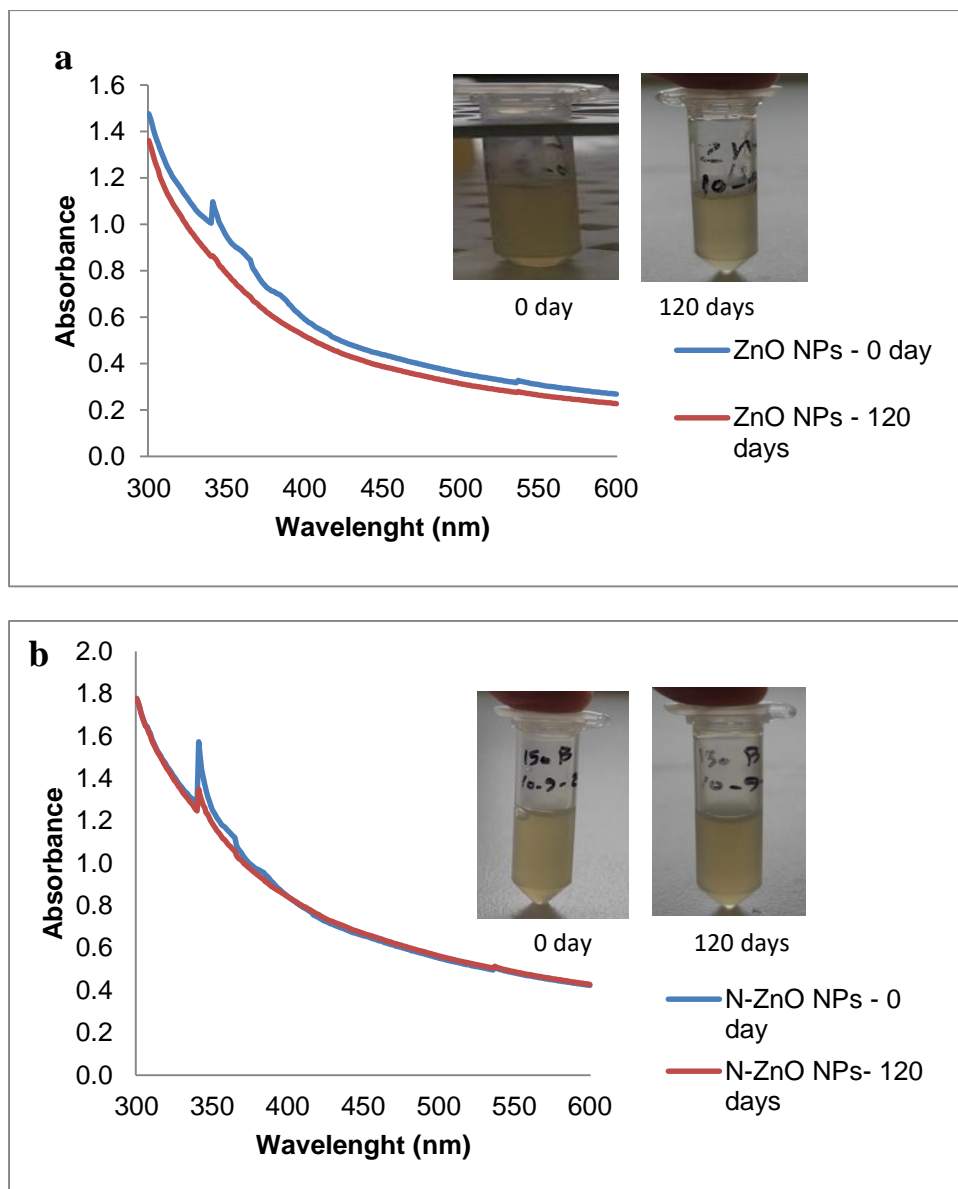


Figure 4.27. UV–Visible Spectra of ZnO NPs, nisin loaded ZnO NPs after storage for 120 days a) ZnO NPs; b) nisin loaded ZnO NPs at 5 mg /mL; c) nisin loaded ZnO NPs at 10 mg /mL; d) nisin loaded ZnO NPs at 15 mg /mL.

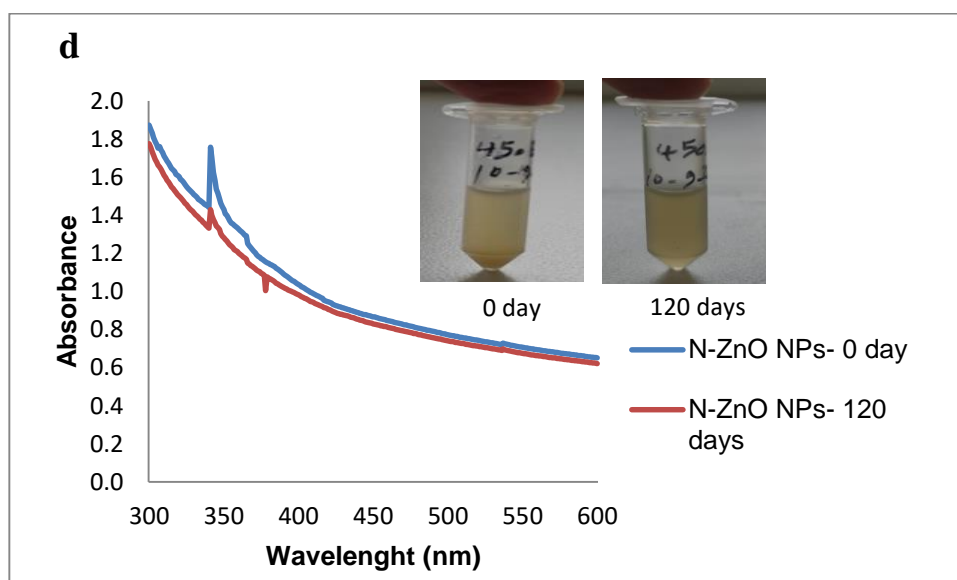
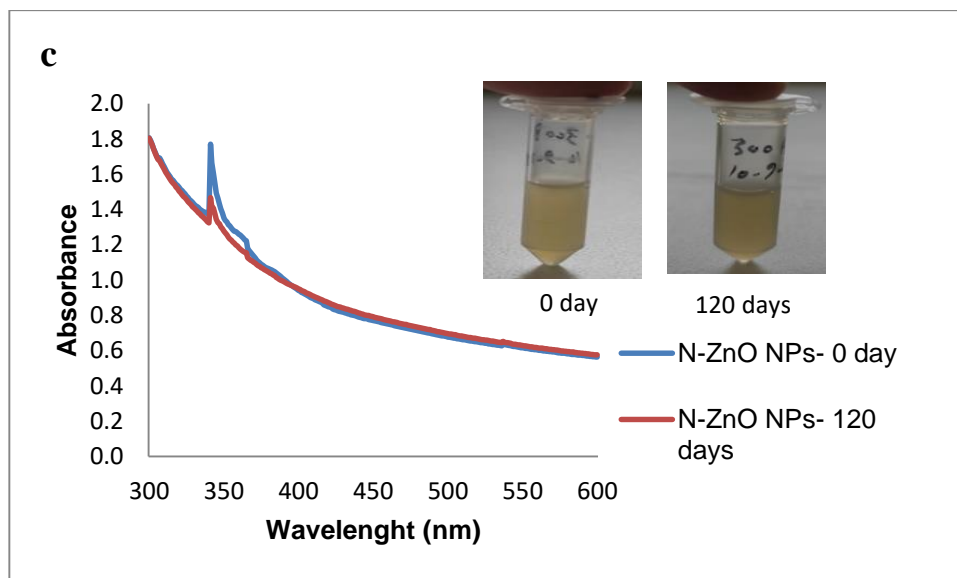


Figure 4.27. (Continued) UV–Visible Spectra of ZnO NPs, nisin loaded ZnO NPs after storage for 120 days a) ZnO NPs; b) nisin loaded ZnO NPs at 5 mg /mL; c) nisin loaded ZnO NPs at 10 mg /mL; d) nisin loaded ZnO NPs at 15 mg /mL.

4.16. Cytotoxicity assay

MTT assay is one of the common first steps in assessing mitochondrial function, which is based on reducing MTT into a blue formazan compound, in addition, the number of dead cells and metabolic activities can be identified (Fouda et al, 2018). According to our findings, in vitro the cytotoxic effect of biosynthesized nisin-loaded ZnO NPs (10 mg/mL) exhibited significantly inhibit dependent on time and dose, the morbidity rate significantly increased with increasing NPS concentrations (Figure 4.28). After 72 h, The findings showed that adding N-ZnO NPs reduced the viability of epithelial cells and that this reduction was closely correlated with concentrations ($P < 0.05$). The percentage of decreasing viability was (71.972 ± 0.048 , 50.705 ± 0.068 , 6.097 ± 0.032 , 6.291 ± 0.011 , 5.798 ± 0.025 , 6.141 ± 0.042 and 3.731 ± 0.002) in concentration (1, 10, 50, 250, 500, 750 and 1000 $\mu\text{g/mL}$) respectively. Figure 4.29 demonstrated that the half-maximal inhibitory concentrations of NPs, the IC_{50} was achieved as 7.371 and 5.961 $\mu\text{g/mL}$ for the N-ZnO NPs following 48 and 72 h exposure, respectively.

Despite the incompatibility of N-ZnO NPs with Vero cells, the nanoparticles have a unique advantage in their ability to quickly destroy pathogens after contacting them in a short period. Mohd Yusof et al. (2020) demonstrated that the MTT assay results confirming the in vitro cytotoxicity effect of ZnO NPs synthesized by supernatant of *Lactobacillus plantarum* against the Vero cell, the biocompatibility decreased significantly with increased concentration. After 24 h of incubation, the cell viability at 62.5, 125, 250, 500, and 1000 $\mu\text{g/mL}$ were 46.17%, 41.45%, 37.90%, 36.79%, and 29.94%, respectively. Similar report of cytotoxicity was discussed by Abdelmigid et al. (2022), However the cytotoxicity effect of biosynthesized ZnO NPs using *Punica granatum* L. peel (PPE) and coffee grounds (CE) on proliferation of Vero cells. The NPs demonstrated cytotoxicity effect at various concentration (100, 120, 140, 160, 180 and 200 $\mu\text{g/mL}$) after 72 h of exposure.

Mohamed et al. (2019) revealed that the rod and hexagonal ZnO NPs shows different viability percentage towards the Caco-2 as cancer cell line, Clone-9 and Vero cell lines as normal cells, whereby fifty percentage of cell death, which estimated as IC_{50} values of rod ZnO NPs and hexagonal ZnO NPs on the animal Vero cell line were 127.2 and 20.1 ppm respectively, the reason might be attributed to the physical and chemical properties and their stability of nanorod shape more than hexagonal shape ZnO NPs. Another pattern was observed that the same nanoparticles had an IC_{50} value of 50.81

g/mL against Caco-2 cells, indicating they were significantly more sensitive than cancer cells (A549) and normal lung epithelial cells (WI38) to the ZnO.NPs' most effective cytotoxic ability (Selim et al, 2020). The previous study indicated that the cytotoxicity effect of L-Cysteine capped ZnO NPs less than ZnO NPs in A549 and L929 cell lines, after 3h of exposure at low concentrations. The percentage cell viability in the A549 and L929 cell lines, when treated with 320 $\mu\text{g/mL}$ were 11.04 ± 0.55 and 11.71 ± 3.58 respectively (Arathi et al, 2022). Our results agree with the previous work of Saranya et al. (2017), which concluded that ZnO NPs have a cytotoxic effect on Vero normal cells, with this might be a result of the nanoparticles' ability to create reactive oxygen species (ROS). Increased ROS levels cause damage to cells' DNA, which inhibits the cell cycle and eventually leads to cell death. The results are in agreement with several studies that ZnO NPs showed cytotoxic effects against Vero cells in whereby dose-dependent manner, the IC_{50} value was found to be 20 $\mu\text{g/mL}$ (Majeed et al, 2017). Another similar pattern study that reported the biosynthesized Zinc NPs using *Pseudomonas hibiscicola* had IC_{50} value of 6.24 mg/mL (Punjabi et al, 2018).

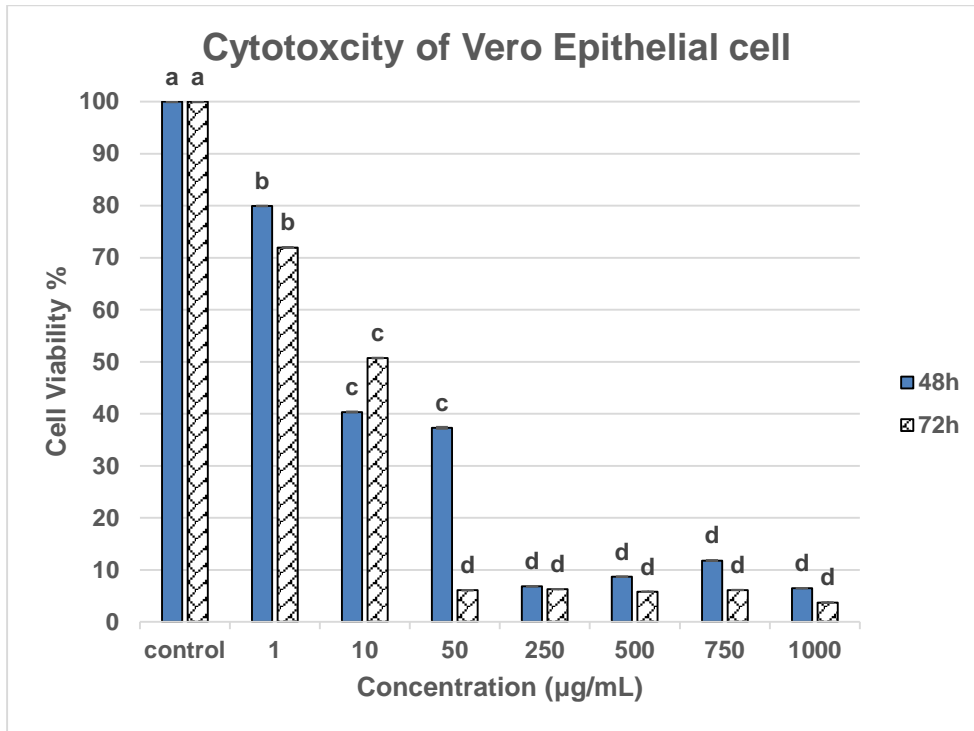


Figure 4.28. Cytotoxicity of various concentrations of N-ZnO NPs on epithelial cells using the MTT assay.

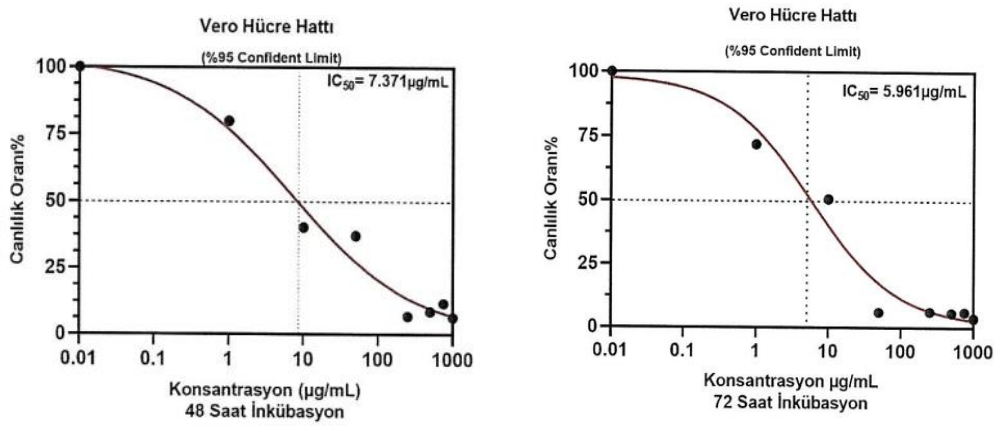


Figure 4.29. Calculation of IC₅₀ values in Graph Pad Software.

5. CONCLUSIONS AND RECOMMENDATIONS

This study investigated 45 different *Bacillus* isolates for the extracellular synthesis of zinc and N-ZnO NPs. As a result, most bacteria had not produced ZnO NPs, but *Bacillus subtilis* (ZBP4) that was isolated from a soil sample taken from Geyve province. It was determined that the ZBP4 strain was capable of producing ZnO NPs. ZBP4 strain has been selected for synthesis nanoparticles.

Nanoparticle biosynthesis was performed extracellularly with the use of CFS. A maximum absorption peak (λ_{max}) obtained at 341 nm indicated the successful biosynthesis of ZnO NPs and white precipitate. The optimization studies confirmed that the optimum condition for the synthesis of ZnO NPs by using CFS of *Bacillus subtilis* ZBP4 was at pH 7.5 for 24 h, 33 °C, and 8 mM of ZnSO₄·7H₂O.

Different concentration of nisin was investigated to conjugate with ZnO NPs. The absorption spectrum was recorded at 341 nm and validating the optical observation. The highest aggregation of optimum concentration was 10 mg /mL CFS after 24 h of incubation.

TEM analysis of the ZnO NPs synthesized under optimum conditions was performed. ZnO NPs have been determined that the dimensions are mainly in the range of 14-45 nm with quasi-spherical shapes. The crystal structure of ZnO NPs was determined by XRD spectroscopy. Also, N-ZnO NPs identified as having quasi-spherical shapes with an average diameter of about 23 nm. The XRD results of N-ZnO NPs appeared amorphous and alone broad peaks. Additionally, stability of N-ZnO NPs were detected after storage for 120 days at 0-10 °C. The nanoparticles were characterized by FESEM, EDS, FTIR and zeta potential measurement. Also, the results indicated that scavenging activity of N-ZnO NPs at all concentration more than ZnO NPs alone.

Results illustrated that nisin functionalized ZnO NPs have bacteriostatic and bactericidal effect in liquid media. The ZnO NPs were inhibitory effect on all the microorganisms tested and having the maximum zone of inhibition against the *S. Typhimurium*. According to some previous reports, ZnO NPs have cytotoxic effects

on a variety of cell lines. However, the cytotoxic effects of NPs are strongly dependent on a variety of factors, such as the properties of NPs (size and shape), production techniques, the type of cell line and incubation time used. The N-ZnO NPs could be a good antibacterial agent against pathogenic bacteria especially Gram positive bacteria, furthermore some types of Gram negative bacteria such as *P. aeruginosa* and *S. Enteritidis* ATCC 13076, that can help to avoid infection of bacteria.

The present investigation concluded that the green synthesis of ZnO NPs and N-ZnO NPs, using a supernatant of *Bacillus subtilis* ZBP4 as a reducing and capping agent, has advantages such as ease in availability, eco-friendly with which the process can be scaled up economic viability. The synthesis conditions have been optimized, providing rapid and large scale production of NPs. Proteins and enzymes contained in the supernatant may be responsible for the green synthesis of ZnO NPs and N-ZnO NPs. To elucidate the precise mechanisms and to comprehend the entire procedure behind the green synthesis of NPs, further study is required to investigate the activity of NPs invitro and invivo against pathogenic bacteria especially antibiotic resistant bacteria as well as pathogenic fungi. Also checking the activity of synthesized nanoparticles against cancer cells.

REFERENCES

- Abdelmigid, H. M., Hussien, N. A., Alyamani, A. A., Morsi, M. M., AlSufyani, N. M., & Kadi, H. A. (2022). Green Synthesis of Zinc Oxide Nanoparticles Using Pomegranate Fruit Peel and Solid Coffee Grounds vs. Chemical Method of Synthesis, with Their Biocompatibility and Antibacterial Properties Investigation. *Molecules*, 27(4), 1236.
- Abee, T., Rombouts, F. M., Hugenholtz, J., Guihard, G., & Letellier, L. (1994). Mode of action of nisin Z against *Listeria monocytogenes* Scott A grown at high and low temperatures. *Applied and Environmental Microbiology*, 60(6), 1962-1968.
- Agarwal, H., Menon, S., Kumar, S. V., & Rajeshkumar, S. (2018). Mechanistic study on antibacterial action of zinc oxide nanoparticles synthesized using green route. *Chemico-biological Interactions*, 286, 60-70. <https://doi.org/10.1016/j.cbi.2018.03.008>
- Agarwal, H., Nakara, A., Menon, S., & Shanmugam, V. (2019). Eco-friendly synthesis of zinc oxide nanoparticles using *Cinnamomum Tamala* leaf extract and its promising effect towards the antibacterial activity. *Journal of Drug Delivery Science and Technology*, 53, 101212. <https://doi.org/10.1016/j.jddst.2019.101212>
- Ahmed, T., Wu, Z., Jiang, H., Luo, J., Noman, M., Shahid, M., ... & Li, B. (2021). Bioinspired green synthesis of zinc oxide nanoparticles from a native *Bacillus cereus* strain RNT6: characterization and antibacterial activity against rice panicle blight pathogens *Burkholderia glumae* and *B. gladioli*. *Nanomaterials*, 11(4), 884. <https://doi.org/10.3390/nano11040884>
- Al-daimy, F. H. (2022). Biosynthesis of Ag and ZnO nanoparticles using Truffles and their antimicrobial and anticancer effects [PhD thesis]. University of Al-Qadisiyah
- Akbarian, M., Mahjoub, S., Elahi, S. M., Zabihi, E., & Tashakkorian, H. (2020). Green synthesis, formulation and biological evaluation of a novel ZnO nanocarrier loaded with paclitaxel as drug delivery system on MCF-7 cell line. *Colloids and Surfaces B: Biointerfaces*, 186, 110686. <https://doi.org/10.1016/j.colsurfb.2019.110686>
- Akçay, F. A. (2017). *Investigation of the productions of copper, zinc, and selenium nanoparticles by some Bacillus strains* [Master's thesis]. Sakarya University

- Alghair, Z. K., Fernig, D. G., & Ebrahimi, B. (2019). Enhanced inhibition of influenza virus infection by peptide–noble-metal nanoparticle conjugates. *Beilstein Journal of Nanotechnology*, *10*(1), 1038-1047. <https://doi.org/10.3762/bjnano.10.104>
- Ali, J., Irshad, R., Li, B., Tahir, K., Ahmad, A., Shakeel, M., ... & Khan, Z. U. H. (2018). Synthesis and characterization of phytochemical fabricated zinc oxide nanoparticles with enhanced antibacterial and catalytic applications. *Journal of Photochemistry and Photobiology B: Biology*, *183*, 349-356. <https://doi.org/10.1016/j.jphotobiol.2018.05.006>
- Alizadeh-Sani, M., Hamishehkar, H., Khezerlou, A., Maleki, M., Azizi-Lalabadi, M., Bagheri, V., ... & Ehsani, A. (2020). Kinetics analysis and susceptibility coefficient of the pathogenic bacteria by titanium dioxide and zinc oxide nanoparticles. *Advanced Pharmaceutical Bulletin*, *10*(1), 56. <https://doi.10.15171/apb.2020.007>
- Aljelehwany, Q., Karimi, N., & Alavi, M. (2021). Comparison of antibacterial and cytotoxic activities of phytosynthesized ZnONPs by leaves extract of *Daphne mucronata* at different salt sources. *Materials Technology*, *36*(12), 747-759. <https://doi.org/10.1080/10667857.2020.1794280>
- Al-Kordy, H. M., Sabry, S. A., & Mabrouk, M. E. (2021). Statistical optimization of experimental parameters for extracellular synthesis of zinc oxide nanoparticles by a novel haloaliphilic *Alkalibacillus* sp. W7. *Scientific Reports*, *11*(1), 1-14. <https://doi.org/10.1038/s41598-021-90408-y>
- Al-Radadi, N. S., Faisal, S., Alotaibi, A., Ullah, R., Hussain, T., Rizwan, M., ... & Ali, Z. (2022). Zingiber officinale driven bioproduction of ZnO nanoparticles and their anti-inflammatory, anti-diabetic, anti-alzheimer, anti-oxidant, and anti-microbial applications. *Inorganic Chemistry Communications*, *140*, 109274. <https://doi.org/10.1016/j.inoche.2022.109274>
- AL-Tamimi, B. Y. H. (2021). *Green synthesis of zinc and nickel oxides nanoparticles and study of their biological applications* [Master's thesis]. University of Anbar
- Amarasekara, H., Oshaben, K. M., Jeans, K. B., Rezvan Sangsari, P., Morgan, N. Y., O'Farrell, B., & Appella, D. H. (2022). Cyclopentane peptide nucleic acid: Gold nanoparticle conjugates for the detection of nucleic acids in a microfluidic format. *Biopolymers*, *113*(3), e23481. <https://doi.org/10.1002/bip.23481>
- Amin, M., Rakhisi, Z., & Ahmady, A. Z. (2015). Isolation and identification of *Bacillus* species from soil and evaluation of their antibacterial properties. *Avicenna Journal of Clinical Microbiology and Infection*, *2*(1), e23233. <https://doi.org/10.17795/ajcmi-23233>
- Amjadi, S., Emaminia, S., Nazari, M., Davudian, S. H., Roufegarinejad, L., & Hamishehkar, H. (2019). Application of reinforced ZnO nanoparticle-incorporated gelatin bionanocomposite film with chitosan nanofiber for packaging of chicken fillet and cheese as food models. *Food and Bioprocess Technology*, *12*(7), 1205-1219. <https://doi.org/10.1007/s11947-019-02286-y>
- Ananthalakshmi, R., Rajarathinam, S. R. X. & Sadiq, A. M. (2019). Antioxidant activity of ZnO nanoparticles synthesized using *Luffa acutangula* peel extract. *Research Journal of Pharmacy and Technology*, *12*(4), 1569-1572. <https://doi.org/10.5958/0974-360X.2019.00260.9>

- Arakha, M., Borah, S. M., Saleem, M., Jha, A. N., & Jha, S. (2016). Interfacial assembly at silver nanoparticle enhances the antibacterial efficacy of nisin. *Free Radical Biology and Medicine*, *101*, 434-445. <https://doi.org/10.1016/j.freeradbiomed.2016.11.016>
- Arathi, A., Joseph, X., Akhil, V., & Mohanan, P. V. (2022). L-Cysteine capped zinc oxide nanoparticles induced cellular response on adenocarcinomic human alveolar basal epithelial cells using a conventional and organ-on-a-chip approach. *Colloids and Surfaces B: Biointerfaces*, *211*, 112300.
- Arumugam, J., Thambidurai, S., Suresh, S., Selvapandiyan, M., Kandasamy, M., Pugazhenthiran, N., ... & Quero, F. (2021a). Green synthesis of zinc oxide nanoparticles using *Ficus carica* leaf extract and their bactericidal and photocatalytic performance evaluation. *Chemical Physics Letters*, *783*, 139040. <https://doi.org/10.1016/j.cplett.2021.139040>
- Arumugam, M., Manikandan, D. B., Dhandapani, E., Sridhar, A., Balakrishnan, K., Markandan, M., & Ramasamy, T. (2021b). Green synthesis of zinc oxide nanoparticles (ZnO NPs) using *Syzygium cumini*: Potential multifaceted applications on antioxidants, cytotoxic and as nanonutrient for the growth of *Sesamum indicum*. *Environmental Technology & Innovation*, *23*, 101653. <https://doi.org/10.1016/j.eti.2021.101653>
- Asif, A. K. M. A. H., and Hasan, M. Z. (2018). Application of nanotechnology in modern textiles: A review. *International Journal of Current Engineering and Technology*, *8*(2), 227-231. <https://doi.org/10.14741/ijcet/v.8.2.5>
- Avcı, A., Çağrı-Mehmetoğlu, A., & Arslan, D. (2017). Production of antimicrobial substances by a novel *Bacillus* strain inhibiting *Salmonella* Typhimurium. *LWT*, *80*, 265-270. <https://doi.org/10.1016/j.lwt.2017.02.030>
- Azharuddin, M., Zhu, G. H., Das, D., Ozgur, E., Uzun, L., Turner, A. P., & Patra, H. K. (2019). A repertoire of biomedical applications of noble metal nanoparticles. *Chemical Communications*, *55*(49), 6964-6996. <https://doi.org/10.1039/C9CC01741K>
- Azizi, S., Mohamad, R., & Mahdavi Shahri, M. (2017). Green microwave-assisted combustion synthesis of zinc oxide nanoparticles with *Citrullus colocynthis* (L.) Schrad: characterization and biomedical applications. *Molecules*, *22*(2), 301. <https://doi.org/10.3390/molecules22020301>
- Bacaksiz, E. M. İ. N., Parlak, M., Tomakin, M. U. R. A. T., Özçelik, A., Karakız, M., & Altunbaş, M. (2008). The effects of zinc nitrate, zinc acetate and zinc chloride precursors on investigation of structural and optical properties of ZnO thin films. *Journal of Alloys and Compounds*, *466*(1-2), 447-450. <https://doi.org/10.1016/j.jallcom.2007.11.061>
- Baek, S. K., and Song, K. B. (2018). Development of Gracilaria vermiculophylla extract films containing zinc oxide nanoparticles and their application in smoked salmon packaging. *Lwt*, *89*, 269-275. <https://doi.org/10.1016/j.lwt.2017.10.064>

- Bai Aswathanarayan, J., Rai Vittal, R., & Muddegowda, U. (2018). Anticancer activity of metal nanoparticles and their peptide conjugates against human colon adenorectal carcinoma cells. *Artificial Cells, Nanomedicine, and Biotechnology*, 46(7), 1444-1451. <https://doi.org/10.1080/21691401.2017.1373655>
- Bajaj, M., Pandey, S. K., Nain, T., Brar, S. K., Singh, P., Singh, S., ... & Sharma, R. K. (2017). Stabilized cationic dipeptide capped gold/silver nanohybrids: Towards enhanced antibacterial and antifungal efficacy. *Colloids and Surfaces B: Biointerfaces*, 158, 397-407. <https://doi.org/10.1016/j.colsurfb.2017.07.009>
- Bajaj, M., Pandey, S. K., Wangoo, N., & Sharma, R. K. (2018). Peptide functionalized metallic nanoconstructs: Synthesis, structural characterization, and antimicrobial evaluation. *ACS Biomaterials Science & Engineering*, 4(2), 739-747. <https://doi.org/10.1021/acsbiomaterials.7b00729>
- Balraj, B., Senthilkumar, N., Siva, C., Krithikadevi, R., Julie, A., Potheher, I. V., & Arulmozhi, M. (2017). Synthesis and characterization of zinc oxide nanoparticles using marine *Streptomyces* sp. with its investigations on anticancer and antibacterial activity. *Research on Chemical Intermediates*, 43(4), 2367-2376. DOI 10.1007/s11164-016-2766-6
- Bandeira, M., Giovanella, M., Roesch-Ely, M., Devine, D. M., & da Silva Crespo, J. (2020). Green synthesis of zinc oxide nanoparticles: A review of the synthesis methodology and mechanism of formation. *Sustainable Chemistry and Pharmacy*, 15, 100223. <https://doi.org/10.1016/j.scp.2020.100223>
- Baptista, P. V., McCusker, M. P., Carvalho, A., Ferreira, D. A., Mohan, N. M., Martins, M., & Fernandes, A. R. (2018). Nano-strategies to fight multidrug resistant bacteria—"A Battle of the Titans". *Frontiers in microbiology*, 9, 1441. <https://doi.org/10.3389/fmicb.2018.01441>
- Barani, M., Masoudi, M., Mashreghi, M., Makhdomi, A., & Eshghi, H. (2021). Cell-free extract assisted synthesis of ZnO nanoparticles using aquatic bacterial strains: Biological activities and toxicological evaluation. *International Journal of Pharmaceutics*, 606, 120878. <https://doi.org/10.1016/j.ijpharm.2021.120878>
- Baruzzi, F., Quintieri, L., Morea, M., & Caputo, L. (2011). Antimicrobial compounds produced by *Bacillus* spp. and applications in food. *Science Against Microbial Pathogens: Communicating Current Research and Technological Advances*, 2(1), 1102-1111.
- Batool, M., Khurshid, S., Qureshi, Z., & Daoush, W. M. (2021). Adsorption, antimicrobial and wound healing activities of biosynthesised zinc oxide nanoparticles. *Chemical Papers*, 75(3), 893-907. <https://doi.org/10.1007/s11696-020-01343-7>
- Bauer, A.W. (1966). Antibiotic susceptibility testing by a standardized single disc method. *Am J clin pathol*, 45, 149-158.
- Bayda, S., Adeel, M., Tuccinardi, T., Cordani, M., & Rizzolio, F. (2019). The history of nanoscience and nanotechnology: from chemical-physical applications to nanomedicine. *Molecules*, 25(1), 112. <https://doi.org/10.3390/molecules25010112>

- Becheri, A., Dürr, M., Lo Nostro, P., & Baglioni, P. (2008). Synthesis and characterization of zinc oxide nanoparticles: application to textiles as UV-absorbers. *Journal of Nanoparticle Research*, 10(4), 679-689. <https://doi.org/10.1007/s11051-007-9318-3>
- Bernela, M., Kaur, P., Chopra, M., & Thakur, R. (2014). Synthesis, characterization of nisin loaded alginate–chitosan–pluronic composite nanoparticles and evaluation against microbes. *LWT-Food Science and Technology*, 59(2), 1093-1099. <https://doi.org/10.1016/j.lwt.2014.05.061>
- Bhande, R. M., Khobragade, C. N., Mane, R. S., & Bhande, S. (2013). Enhanced synergism of antibiotics with zinc oxide nanoparticles against extended spectrum β -lactamase producers implicated in urinary tract infections. *Journal of nanoparticle research*, 15(1), 1-13. DOI 10.1007/s11051-012-1413-4
- Bhattacharjee, S. (Ed.). (2019). *Principles of Nanomedicine*. Jenny Stanford Publishing. <https://doi.org/10.1201/9780429031236>
- Bhattacharya, P., Swain, S., Giri, L., & Neogi, S. (2019). Fabrication of magnesium oxide nanoparticles by solvent alteration and their bactericidal applications. *Journal of Materials Chemistry B*, 7(26), 4141-4152. <https://doi.org/10.1039/C9TB00782B>
- Bindhu, M. R., and Umadevi, M. (2014). Antibacterial activities of green synthesized gold nanoparticles. *Materials Letters*, 120, 122-125. <https://doi.org/10.1016/j.matlet.2014.01.108>
- Bourgat, Y., Mikolai, C., Stiesch, M., Klahn, P., & Menzel, H. (2021). Enzyme-responsive nanoparticles and coatings made from alginate/peptide ciprofloxacin conjugates as drug release system. *Antibiotics*, 10(6), 653. <https://doi.org/10.3390/antibiotics10060653>
- Bratovčić, A., Odošić, A., Čatić, S., & Šestan, I. (2015). Application of polymer nanocomposite materials in food packaging. *Croatian Journal of Food Science and Technology*, 7(2), 86-94. <https://doi.org/10.17508/CJFST.2015.7.2.06>
- Busi, S., Rajkumari, J., Pattnaik, S., Parasuraman, P., & Hnamte, S. (2016). Extracellular synthesis of zinc oxide nanoparticles using *Acinetobacter schindleri* SIZ7 and its antimicrobial property against foodborne pathogens. *Journal of Microbiology, Biotechnology and Food Sciences*, 5, 407-411. <https://doi.org/10.15414/jmbfs.2016.5.5.407-411>
- Buzea, C., Pacheco, I. I., & Robbie, K. (2007). Nanomaterials and nanoparticles: sources and toxicity. *Biointerphases*, 2(4), MR17-MR71. <https://doi.org/10.1116/1.2815690>
- Chaari, M., and Matoussi, A. (2012). Electrical conduction and dielectric studies of ZnO pellets. *Physica B: Condensed Matter*, 407(17), 3441-3447. <https://doi.org/10.1016/j.physb.2012.04.056>
- Chamundeeswari, M., Sobhana, S. L., Jacob, J. P., Kumar, M. G., Devi, M. P., Sastry, T. P., & Mandal, A. B. (2010). Preparation, characterization and evaluation of a biopolymeric gold nanocomposite with antimicrobial activity. *Biotechnology and Applied Biochemistry*, 55(1), 29-35. <https://doi.org/10.1042/BA20090198>

- Chen, G., Svirskis, D., Lu, W., Ying, M., Huang, Y., & Wen, J. (2018). N-trimethyl chitosan nanoparticles and CSKSSDYQC peptide: N-trimethyl chitosan conjugates enhance the oral bioavailability of gemcitabine to treat breast cancer. *Journal of Controlled Release*, 277, 142-153. <https://doi.org/10.1016/j.jconrel.2018.03.013>
- Cheng, Y., Cao, Y., Ihsan, A. U., Khan, F. U., Li, X., Xie, D., ... & Zhou, X. (2019). Novel treatment of experimental autoimmune prostatitis by nanoparticle-conjugated autoantigen peptide T2. *Inflammation*, 42(3), 1071-1081. <https://doi.org/10.1007/s10753-019-00968-5>
- Chennimalai, M., Vijayalakshmi, V., Senthil, T. S., & Sivakumar, N. (2021). One-step green synthesis of ZnO nanoparticles using *Opuntia humifusa* fruit extract and their antibacterial activities. *Materials Today: Proceedings*, 47, 1842-1846. <https://doi.org/10.1016/j.matpr.2021.03.409>
- Crandall, A. D., and Montville, T. J. (1998). Nisin resistance in *Listeria monocytogenes* ATCC 700302 is a complex phenotype. *Applied and Environmental Microbiology*, 64(1), 231-237. <https://doi.org/10.1128/AEM.64.1.231-237.1998>
- Daniel, M. C., and Astruc, D. (2004). Gold nanoparticles: assembly, supramolecular chemistry, quantum-size-related properties, and applications toward biology, catalysis, and nanotechnology. *Chemical Reviews*, 104(1), 293-346. <https://doi.org/10.1021/cr030698+>
- Darwish, R. M., and Salama, A. H. (2022). Study the Effect of Conjugate Novel Ultra-Short Antimicrobial Peptide with Silver Nanoparticles against Methicillin Resistant *S. aureus* and ESBL *E. coli*. *Antibiotics*, 11(8), 1024. <https://doi.org/10.3390/antibiotics11081024>
- Das, D., Nath, B. C., Phukon, P., & Dolui, S. K. (2013). Synthesis of ZnO nanoparticles and evaluation of antioxidant and cytotoxic activity. *Colloids and Surfaces B: Biointerfaces*, 111, 556-560. <https://doi.org/10.1016/j.colsurfb.2013.06.041>
- Deljou, A., and Goudarzi, S. (2016). Green extracellular synthesis of the silver nanoparticles using thermophilic *Bacillus* sp. AZ1 and its antimicrobial activity against several human pathogenetic bacteria. *Iranian Journal of Biotechnology*, 14(2), 25. doi: 10.15171/ijb.1259
- Di Guglielmo, C., López, D. R., De Lapuente, J., Mallafre, J. M. L., & Suárez, M. B. (2010). Embryotoxicity of cobalt ferrite and gold nanoparticles: a first in vitro approach. *Reproductive Toxicology*, 30(2), 271-276. <https://doi.org/10.1016/j.reprotox.2010.05.001>
- Divsalar, E., Tajik, H., Moradi, M., Forough, M., Lotfi, M., & Kuswandi, B. (2018). Characterization of cellulosic paper coated with chitosan-zinc oxide nanocomposite containing nisin and its application in packaging of UF cheese. *International journal of biological macromolecules*, 109, 1311-1318. <https://doi.org/10.1016/j.ijbiomac.2017.11.145>
- Dizaj, S. M., Lotfipour, F., Barzegar-Jalali, M., Zarrintan, M. H., & Adibkia, K. (2014). Antimicrobial activity of the metals and metal oxide nanoparticles. *Materials Science and Engineering: C*, 44, 278-284. <https://doi.org/10.1016/j.msec.2014.08.031>

- Drexler, E. K. (1986). Engines of creation: the coming era of nanotechnology. Anchor Books, Doubleday. http://e-drexler.com/p/06/00/EOC_Cover.html
- Drexler, K. E. (1991). *Molecular machinery and manufacturing with applications to computation* [PhD thesis]. Massachusetts Institute of Technology
- Dykman, L. A., Staroverov, S. A., & Fomin, A. S. (2018). Effect of M2e peptide–gold nanoparticle conjugates on development of anti-influenza antibodies. *Gold Bulletin*, 51(4), 197-203. <https://doi.org/10.1007/s13404-018-0239-y>
- Ebadi, M., Zolfaghari, M. R., Aghaei, S. S., Zargar, M., & Noghabi, K. A. (2022). *Desertifilum* sp. EAZ03 cell extract as a novel natural source for the biosynthesis of zinc oxide nanoparticles and antibacterial, anticancer and antibiofilm characteristics of synthesized zinc oxide nanoparticles. *Journal of Applied Microbiology*, 132(1), 221-236. <https://doi.org/10.1111/jam.15177>
- Ebadi, M., Zolfaghari, M. R., Aghaei, S. S., Zargar, M., Shafiei, M., Zahiri, H. S., & Noghabi, K. A. (2019). A bio-inspired strategy for the synthesis of zinc oxide nanoparticles (ZnO NPs) using the cell extract of *cyanobacterium Nostoc* sp. EA03: from biological function to toxicity evaluation. *RSC Advances*, 9(41), 23508-23525. <https://doi.org/10.1039/C9RA03962G>
- Ekennia, A. C., Uduagwu, D. N., Nwaji, N. N., Oje, O. O., Emma-Uba, C. O., Mgbii, S. I., ... & Nwanji, O. L. (2021). Green synthesis of biogenic zinc oxide nanoflower as dual agent for photodegradation of an organic dye and tyrosinase inhibitor. *Journal of Inorganic and Organometallic Polymers and Materials*, 31(2), 886-897. <https://doi.org/10.1007/s10904-020-01729-w>
- El-Belely, E. F., Farag, M. M., Said, H. A., Amin, A. S., Azab, E., Gobouri, A. A., & Fouda, A. (2021). Green synthesis of zinc oxide nanoparticles (ZnO-NPs) using *Arthrospira platensis* (Class: Cyanophyceae) and evaluation of their biomedical activities. *Nanomaterials*, 11(1), 95. <https://doi.org/10.3390/nano11010095>
- EL-Ghwas, D. E. (2022). Characterization and biological synthesis of zinc oxide nanoparticles by new strain of *Bacillus foraminis*. *Biodiversitas Journal of Biological Diversity*, 23(1). <https://doi.org/10.13057/biodiv/d230159>
- Eltarahony, M., Zaki, S., ElKady, M., & Abd-El-Haleem, D. (2018). Biosynthesis, characterization of some combined nanoparticles, and its biocide potency against a broad spectrum of pathogens. *Journal of Nanomaterials*. 2018, 16. <https://doi.org/10.1155/2018/5263814>
- Fan, S., Zheng, Y., Liu, X., Fang, W., Chen, X., Liao, W., ... & Liu, J. (2018). Curcumin-loaded PLGA-PEG nanoparticles conjugated with B6 peptide for potential use in Alzheimer's disease. *Drug Delivery*, 25(1), 1091-1102. <https://doi.org/10.1080/10717544.2018.1461955>
- Farfán-Castro, S., García-Soto, M. J., Comas-García, M., Arévalo-Villalobos, J. I., Palestino, G., González-Ortega, O., & Rosales-Mendoza, S. (2021). Synthesis and immunogenicity assessment of a gold nanoparticle conjugate for the delivery of a peptide from SARS-CoV-2. *Nanomedicine: Nanotechnology, Biology and Medicine*, 34, 102372. <https://doi.org/10.1016/j.nano.2021.102372>

- Fatholahi, A., Khalaji, S., Hosseini, F., & Abbasi, M. (2021). Nano-Bio zinc synthesized by *Bacillus subtilis* modulates broiler performance, intestinal morphology and expression of tight junction's proteins. *Livestock Science*, *251*, 104660. <https://doi.org/10.1016/j.livsci.2021.104660>
- Forootanfar, H., Adeli-Sardou, M., Nikkhoo, M., Mehrabani, M., Amir-Heidari, B., Shahverdi, A. R., & Shakibaie, M. (2014). Antioxidant and cytotoxic effect of biologically synthesized selenium nanoparticles in comparison to selenium dioxide. *Journal of Trace Elements in Medicine and Biology*, *28*(1), 75-79. <https://doi.org/10.1016/j.jtemb.2013.07.005>
- Fouda, A., Saad, E. L., Salem, S. S., & Shaheen, T. I. (2018). In-Vitro cytotoxicity, antibacterial, and UV protection properties of the biosynthesized Zinc oxide nanoparticles for medical textile applications. *Microbial Pathogenesis*, *125*, 252-261.
- Freestone, I., Meeks, N., Sax, M., & Higgitt, C. (2007). The Lycurgus cup—a roman nanotechnology. *Gold Bulletin*, *40*(4), 270-277. <https://doi.org/10.1007/BF03215599>
- Fultz, B., and Howe, J. M. (2012). *Transmission electron microscopy and diffractometry of materials* (1st digital ed.). Springer Science & Business Media.
- Gakiya-Teruya, M., Palomino-Marcelo, L., Pierce, S., Angeles-Boza, A. M., Krishna, V., & Rodriguez-Reyes, J. C. F. (2020). Enhanced antimicrobial activity of silver nanoparticles conjugated with synthetic peptide by click chemistry. *Journal of Nanoparticle Research*, *22*(4), 1-11. <https://doi.org/10.1007/s11051-020-04799-6>
- García, M. A. (2011). Surface plasmons in metallic nanoparticles: fundamentals and applications. *Journal of Physics D: Applied Physics*, *44*(28), 283001. <https://doi.org/10.1088/0022-3727/44/28/283001>
- Gessner, I., and Neundorf, I. (2020). Nanoparticles modified with cell-penetrating peptides: Conjugation mechanisms, physicochemical properties, and application in cancer diagnosis and therapy. *International journal of molecular sciences*, *21*(7), 2536. <https://doi.org/10.3390/ijms21072536>
- Getie, S., Belay, A., Chandra Reddy, A. R., & Belay, Z. (2017). Synthesis and characterizations of zinc oxide nanoparticles for antibacterial applications. *J Nanomed Nanotechnol*, *8*(004). <https://doi.org/10.4172/2157-7439.S8-004>
- Ghadiri, E., Naghavi, N. S., & Ghaedi, K. (2021). Gene Production and Characterization of *Bacillus Subtilis* Cellulase Collected from Central-Northern Iran Forests. *Proceedings of the National Academy of Sciences, India Section B: Biological Sciences*, *91*(3), 543-548. <https://doi.org/10.1007/s40011-021-01241-2>
- Gong, Y., Andelman, T., Neumark, G. F., O'Brien, S., & Kuskovsky, I. L. (2007). Origin of defect-related green emission from ZnO nanoparticles: effect of surface modification. *Nanoscale Research Letters*, *2*(6), 297-302. <https://doi.org/10.1007/s11671-007-9064-6>

- Gothandam, K. M., Ranjan, S., Dasgupta, N., & Lichtfouse, E. (Eds.). (2020). *Environmental Biotechnology* Vol. 1. Springer International Publishing.
- Gurunathan, S., Kalishwaralal, K., Vaidyanathan, R., Venkataraman, D., Pandian, S. R. K., Muniyandi, J., ... & Eom, S. H. (2009). Biosynthesis, purification and characterization of silver nanoparticles using *Escherichia coli*. *Colloids and Surfaces B: Biointerfaces*, 74(1), 328-335. <https://doi.org/10.1016/j.colsurfb.2009.07.048>
- Gümüs, C., Ozkendir, O. M., Kavak, H., & Ufuktepe, Y. (2006). Structural and optical properties of zinc oxide thin films prepared by spray pyrolysis method. *Journal of Optoelectronics and Advanced Materials*, 8(1), 299.
- Hanumith, S., Mahalakshmi, V. and Abirami, S. (2018) 'Biosynthesis of Zinc Oxide Nanoparticles Using *Bacillus* Species Potentiates Anticancer and Antimicrobial Activity, *Int. J. Trend Sci. Res. Dev*, 2(5), 1797–1802.
- He, X., Deng, H., & Hwang, H. M. (2019). The current application of nanotechnology in food and agriculture. *Journal of food and drug analysis*, 27(1), 1-21. <https://doi.org/10.1016/j.jfda.2018.12.002>
- Hernández-Sánchez, H., and Gutiérrez-López, G. F. (2015). Food nanoscience and nanotechnology. Springer.
- Hernández-Sierra, J. F., Ruiz, F., Pena, D. C. C., Martínez-Gutiérrez, F., Martínez, A. E., Guillén, A. D. J. P., ... & Castañón, G. M. (2008). The antimicrobial sensitivity of *Streptococcus mutans* to nanoparticles of silver, zinc oxide, and gold. *Nanomedicine: Nanotechnology, Biology and Medicine*, 4(3), 237-240. <https://doi.org/10.1016/j.nano.2008.04.005>
- Huang, J., Li, Q., Sun, D., Lu, Y., Su, Y., Yang, X., ... & Chen, C. (2007). Biosynthesis of silver and gold nanoparticles by novel sundried *Cinnamomum camphora* leaf. *Nanotechnology*, 18(10), 105104. <https://doi.org/10.1088/0957-4484/18/10/105104>
- Hulla, J. E., Sahu, S. C., & Hayes, A. W. (2015). Nanotechnology: History and future. *Human & experimental toxicology*, 34(12), 1318-1321. <https://doi.org/10.1177/09603271155603588>
- Hussain, I., Singh, N. B., Singh, A., Singh, H., & Singh, S. C. (2016). Green synthesis of nanoparticles and its potential application. *Biotechnology Letters*, 38(4), 545-560. <https://doi.org/10.1007/s10529-015-2026-7>
- Hussein, E. A. M., Mohammad, A. A. H., Harraz, F. A., & Ahsan, M. F. (2019). Biologically synthesized silver nanoparticles for enhancing tetracycline activity against *Staphylococcus aureus* and *Klebsiella pneumoniae*. *Brazilian Archives of Biology and Technology*, 62. <https://doi.org/10.1590/1678-4324-2019180266>
- Imade, E. E., Ajiboye, T. O., Fadiji, A. E., Onwudiwe, D. C., & Babalola, O. O. (2022). Green synthesis of zinc oxide nanoparticles using *plantain* peel extracts and the evaluation of their antibacterial activity. *Scientific African*, 16, e01152. <https://doi.org/10.1016/j.sciaf.2022.e01152>

- Iqbal, T., Irfan, F., Afsheen, S., Zafar, M., Naeem, S., & Raza, A. (2021). Synthesis and characterization of Ag–TiO₂ nano-composites to study their effect on seed germination. *Applied Nanoscience*, *11*(7), 2043-2057. <https://doi.org/10.1007/s13204-021-01912-6>
- Iqbal, T., Raza, A., Zafar, M., Afsheen, S., Kebaili, I., & Alrobei, H. (2022). Plant-mediated green synthesis of zinc oxide nanoparticles for novel application to enhance the shelf life of tomatoes. *Applied Nanoscience*, *12*(2), 179-191. <https://doi.org/10.1007/s13204-021-02238-z>
- Iqtedar, M., Riaz, H., Kaleem, A., Abdullah, R., Aihetasham, A., Naz, S., & Sharif, S. (2020). Biosynthesis, optimization and characterization of ZnO nanoparticles using *Bacillus cereus* MN181367 and their antimicrobial activity against multidrug resistant bacteria. *Revista Mexicana de Ingeniería Química*, *19* (Sup. 1), 253-266. <https://doi.org/10.24275/RMIQ/BIO1605>
- Iravani, S. (2011). Green synthesis of metal nanoparticles using plants. *Green Chemistry*, *13*(10), 2638-2650. <https://doi.org/10.1039/C1GC15386B>
- Jain, P. K., Huang, X., El-Sayed, I. H., & El-Sayed, M. A. (2007). Review of some interesting surface plasmon resonance-enhanced properties of noble metal nanoparticles and their applications to biosystems. *Plasmonics*, *2*(3), 107-118. <https://doi.org/10.1007/s11468-007-9031-1>
- Janaki, A. C., Sailatha, E., & Gunasekaran, S. (2015). Synthesis, characteristics and antimicrobial activity of ZnO nanoparticles. *Spectrochimica Acta Part A: Molecular and Biomolecular Spectroscopy*, *144*, 17-22. <https://doi.org/10.1016/j.saa.2015.02.041>
- Jayabalan, J., Mani, G., Krishnan, N., Pernabas, J., Devadoss, J. M., & Jang, H. T. (2019). Green biogenic synthesis of zinc oxide nanoparticles using *Pseudomonas putida* culture and its In vitro antibacterial and anti-biofilm activity. *Biocatalysis and Agricultural Biotechnology*, *21*, 101327. <https://doi.org/10.1016/j.bcab.2019.101327>
- Jayaseelan, C., Rahuman, A. A., Kirthi, A. V., Marimuthu, S., Santhoshkumar, T., Bagavan, A., ... & Rao, K. B. (2012). Novel microbial route to synthesize ZnO nanoparticles using *Aeromonas hydrophila* and their activity against pathogenic bacteria and fungi. *Spectrochimica Acta Part A: Molecular and Biomolecular Spectroscopy*, *90*, 78-84. <https://doi.org/10.1016/j.saa.2012.01.006>
- Jiang, J., Pi, J., and Cai, J. (2018). The advancing of zinc oxide nanoparticles for biomedical applications. *Bioinorganic Chemistry and Applications*, *2018*, 1-18. <https://doi.org/10.1155/2018/1062562>
- Jin, T., and Gurtler, J. B. (2011). Inactivation of Salmonella in liquid egg albumen by antimicrobial bottle coatings infused with allyl isothiocyanate, nisin and zinc oxide nanoparticles. *Journal of Applied Microbiology*, *110*(3), 704-712. <https://doi.org/10.1111/j.1365-2672.2011.04938.x>
- Johnston, H. J., Hutchison, G., Christensen, F. M., Peters, S., Hankin, S., & Stone, V. (2010). A review of the in vivo and in vitro toxicity of silver and gold particulates: particle attributes and biological mechanisms responsible for the observed toxicity. *Critical Reviews in Toxicology*, *40*(4), 328-346. <https://doi.org/10.3109/10408440903453074>

- Jones, E., Salin, V., & Williams, G. W. (2005). *Nisin and the market for commercial bacteriocins* (No. 1406-2016-117331). TAMRC Consumer and Product. https://www.researchgate.net/publication/254389082_NISIN_and_the_Market_for_Commercial_Bacteriocins
- Kadhim, A. A., Salman, J. A. S., & Haider, A. (2018). Antibacterial and Anti virulence Factors activity of ZnO nanoparticles Biosynthesized by *Lactococcus lactis* ssp. Lactis. *Indian Journal of Public Health Research & Development*, 9(12), 1229-1233.
- Kadhim, A. A., Salman, J. A. S., Haider, A. J., Ibraheem, S. A., & ali Kadhim, H. (2019). Effect of zinc oxide nanoparticles biosynthesized by *leuconostoc mesenteroides* ssp. dextranicum against bacterial skin infections. In 2019 12th *International Conference on Developments in eSystems Engineering (DeSE)*, 755-760. IEEE. <https://doi.org/10.1109/DeSE.2019.00141>
- Kaviyarasu, K., Geetha, N., Kanimozhi, K., Magdalane, C. M., Sivaranjani, S., Ayeshamariam, A., ... & Maaza, M. (2017). In vitro cytotoxicity effect and antibacterial performance of human lung epithelial cells A549 activity of zinc oxide doped TiO₂ nanocrystals: investigation of bio-medical application by chemical method. *Materials Science and Engineering: C*, 74, 325-333.
- Khan, I., Saeed, K., & Khan, I. (2019). Nanoparticles: Properties, applications and toxicities. *Arabian Journal of Chemistry*, 12(7), 908-931. <https://doi.org/10.1016/j.arabjc.2017.05.011>
- Kharissova, O. V., Dias, H. R., Kharisov, B. I., Pérez, B. O., & Pérez, V. M. J. (2013). The greener synthesis of nanoparticles. *Trends in Biotechnology*, 31(4), 240-248. <https://doi.org/10.1016/j.tibtech.2013.01.003>
- Khusainov, R., Moll, G. N., & Kuipers, O. P. (2013). Identification of distinct nisin leader peptide regions that determine interactions with the modification enzymes NisB and NisC. *FEBS Open Bio*, 3, 237-242. <https://doi.org/10.1016/j.fob.2013.05.001>
- Kim, S. H., Lee, H. S., Ryu, D. S., Choi, S. J., & Lee, D. S. (2011). Antibacterial activity of silver-nanoparticles against *Staphylococcus aureus* and *Escherichia coli*. *Korean Journal of Microbiology and Biotechnology*, 39(1), 77-85.
- Kim, S., Lee, S. Y., & Cho, H. J. (2017). Doxorubicin-wrapped zinc oxide nanoclusters for the therapy of colorectal adenocarcinoma. *Nanomaterials*, 7(11), 354. <https://doi.org/10.3390/nano7110354>
- Korkin, A., Goodnick, S. and Nemanich, R. (2015). *Nanoscale materials and devices for electronics, photonics and solar energy*. Springer.
- Król, A., Railean-Plugaru, V., Pomastowski, P., Złoch, M., & Buszewski, B. (2018). Mechanism study of intracellular zinc oxide nanocomposites formation. *Colloids and Surfaces A: Physicochemical and Engineering Aspects*, 553, 349-358. <https://doi.org/10.1016/j.colsurfa.2018.05.069>
- Kulkarni, S. S., and Shirsat, M. D. (2015). Optical and structural properties of zinc oxide nanoparticles. *International Journal of Advanced Research in Physical Science*, 2(1), 14-18.
- Kumar, N., and Kumbhat, S. (2016). *Essentials in nanoscience and nanotechnology*. John Wiley & Sons.

- Kumar, S. S., Venkateswarlu, P., Rao, V. R., & Rao, G. N. (2013). Synthesis, characterization and optical properties of zinc oxide nanoparticles. *International Nano Letters*, 3(1), 1-6. <https://doi.org/10.1186/2228-5326-3-30>
- Kumar, S., Boro, J. C., Ray, D., Mukherjee, A., & Dutta, J. (2019). Bionanocomposite films of agar incorporated with ZnO nanoparticles as an active packaging material for shelf life extension of green grape. *Heliyon*, 5(6), e01867. <https://doi.org/10.1016/j.heliyon.2019.e01867>
- Kundu, D., Hazra, C., Chatterjee, A., Chaudhari, A., & Mishra, S. (2014). Extracellular biosynthesis of zinc oxide nanoparticles using *Rhodococcus pyridinivorans* NT2: multifunctional textile finishing, biosafety evaluation and in vitro drug delivery in colon carcinoma. *Journal of photochemistry and photobiology B: Biology*, 140, 194-204. <https://doi.org/10.1016/j.jphotobiol.2014.08.001>
- Lal, S., Verma, R., Chauhan, A., Dhatwalia, J., Guleria, I., Ghotekar, S., ... & Kumar, P. (2022). Antioxidant, antimicrobial, and photocatalytic activity of green synthesized ZnO-NPs from *Myrica esculenta* fruits extract. *Inorganic Chemistry Communications*, 141, 109518. <https://doi.org/10.1016/j.inoche.2022.109518>
- Lauster, D., Glanz, M., Bardua, M., Ludwig, K., Hellmund, M., Hoffmann, U., ... & Herrmann, A. (2017). Multivalent peptide–Nanoparticle conjugates for influenza-virus inhibition. *Angewandte Chemie International Edition*, 56(21), 5931-5936. <https://doi.org/10.1002/anie.201702005>
- Lee, E. H., Khan, I., & Oh, D. H. (2018). Evaluation of the efficacy of nisin-loaded chitosan nanoparticles against foodborne pathogens in orange juice. *Journal Of Food Science and Technology*, 55(3), 1127-1133. <https://doi.org/10.1007/s13197-017-3028-3>
- Lima, S. A. M., Sigoli, F. A., Jafellici Jr, M., & Davolos, M. R. (2001). Luminescent properties and lattice defects correlation on zinc oxide. *International Journal of Inorganic Materials*, 3(7), 749-754. [https://doi.org/10.1016/S1466-6049\(01\)00055-1](https://doi.org/10.1016/S1466-6049(01)00055-1)
- Liu, Q. (2021). Zeta Potential Measurements For Surface Modification Of Plastic Substrates For Nanofluidic Biosensors [PhD thesis]. Louisiana State University
- Luis, M., Pezzlo, M. T., Bittencourt, C. E., & Peterson, E. M. (3th Eds.). (2020). *Color atlas of medical bacteriology*. John Wiley & Sons.
- Luo, L., Wu, Y., Liu, C., Huang, L., Zou, Y., Shen, Y., & Lin, Q. (2019). Designing soluble soybean polysaccharides-based nanoparticles to improve sustained antimicrobial activity of nisin. *Carbohydrate Polymers*, 225, 115251. <https://doi.org/10.1016/j.carbpol.2019.115251>
- Luo, M. X., Hua, S., & Shang, Q. Y. (2021). Application of nanotechnology in drug delivery systems for respiratory diseases. *Molecular Medicine Reports*, 23(5), 1-17. <https://doi.org/10.3892/mmr.2021.11964>
- Madhumitha, G., Fowsiya, J., Gupta, N., Kumar, A., & Singh, M. (2019). Green synthesis, characterization and antifungal and photocatalytic activity of *Pithecellobium dulce* peel-mediated ZnO nanoparticles. *Journal of Physics and Chemistry of Solids*, 127, 43-51. <https://doi.org/10.1016/j.jpics.2018.12.005>

- Mahdi, Z. S., Talebnia Roshan, F., Nikzad, M., & Ezoji, H. (2021). Biosynthesis of zinc oxide nanoparticles using bacteria: a study on the characterization and application for electrochemical determination of bisphenol A. *Inorganic and Nano-Metal Chemistry*, 51(9), 1249-1257. <https://doi.org/10.1080/24701556.2020.1835962>
- Mahmoud, A., Kotb, E., Alqosaibi, A. I., Al-Karmalawy, A. A., Al-Dhuayan, I. S., & Alabkari, H. (2021). In vitro and in silico characterization of alkaline serine protease from *Bacillus subtilis* D9 recovered from Saudi Arabia. *Heliyon*, 7(10), e08148. <https://doi.org/10.1016/j.heliyon.2021.e08148>
- Majeed, S., Danish, M., Ismail, M. H. B., Ansari, M. T., & Ibrahim, M. N. M. (2019). Anticancer and apoptotic activity of biologically synthesized zinc oxide nanoparticles against human colon cancer HCT-116 cell line-in vitro study. *Sustainable Chemistry and Pharmacy*, 14, 100179.
- Makula, P., Pacia, M., & Macyk, W. (2018). How to correctly determine the band gap energy of modified semiconductor photocatalysts based on UV–VIS spectra. *The Journal of Physical Chemistry Letters*, 9(23), 6814-6817. <https://doi.org/10.1021/acs.jpcclett.8b02892>
- Mansoori, G. A., and Soelaiman, T. F. (2005). Nanotechnology--An introduction for the standards community. *Journal of ASTM International*. 2(6), JAI13110.
- Marín, R. R., Babick, F., & Hillemann, L. (2017). Zeta potential measurements for non-spherical colloidal particles—practical issues of characterisation of interfacial properties of nanoparticles. *Colloids and Surfaces A: Physicochemical and Engineering Aspects*, 532, 516-521. <https://doi.org/10.1016/j.colsurfa.2017.04.010>
- Markus, J., Mathiyalagan, R., Kim, Y. J., Abbai, R., Singh, P., Ahn, S., ... & Yang, D. C. (2016). Intracellular synthesis of gold nanoparticles with antioxidant activity by probiotic *Lactobacillus kimchicus* DCY51T isolated from Korean kimchi. *Enzyme and Microbial Technology*, 95, 85-93. <https://doi.org/10.1016/j.enzmictec.2016.08.018>
- Marsalek, R. (2014). Particle size and zeta potential of ZnO. *APCBEE procedia*, 9, 13-17. <https://doi.org/10.1016/j.apcbee.2014.01.003>
- Maza, L. M. D. L., Pezzlo, M. T., Shigei, J. T., Tan, G. L. and Peterson, E. M. (2013). *Color atlas of medical bacteriology*. ASM press.
- Mead, P. S., Slutsker, L., Dietz, V., McCaig, L. F., Bresee, J. S., Shapiro, C., ... & Tauxe, R. V. (1999). Food-related illness and death in the United States. *Emerging infectious diseases*, 5(5), 607. <https://doi.org/10.3201/eid0505.990502>
- Melencion, A. B., Gutierrez, W. M., Melencion, M. G., & Musuan, M. (2020). Antibacterial Activity of Zinc Oxide Nanoparticles Using *Banana Peel Extract* against Antibiotic-Resistant Bacteria. *CMU Journal of Science*, 24(1), 1-1.
- Mirgane, N. A., Shivankar, V. S., Kotwal, S. B., Wadhawa, G. C., & Sonawale, M. C. (2021). Degradation of dyes using biologically synthesized zinc oxide nanoparticles. *Materials Today: Proceedings*, 37, 849-853. <https://doi.org/10.1016/j.matpr.2020.06.037>

- Mirhosseini, M. (2016). Evaluation of antibacterial effect of magnesium oxide nanoparticles with nisin and heat in milk. *Mashhad University of Medical Sciences, Nanomed. J.*, 3(2): 135-142. <https://doi.org/10.7508/nmj.2016.02.007>
- Mirhosseini, M., and Afzali, M. (2016). Investigation into the antibacterial behavior of suspensions of magnesium oxide nanoparticles in combination with nisin and heat against *Escherichia coli* and *Staphylococcus aureus* in milk. *Food Control*, 68, 208-215. <https://doi.org/10.1016/j.foodcont.2016.03.048>
- Moghaddam, B. A., Moniri, M., Azizi, S., Abdul Rahim, R., Bin Ariff, A., Zuhainis Saad, W., ... & Mohamad, R. (2017). Biosynthesis of ZnO nanoparticles by a new *Pichia kudriavzevii* yeast strain and evaluation of their antimicrobial and antioxidant activities. *Molecules*, 22(6), 872. <https://doi.org/10.3390/molecules22060872>
- Moghaddas, S. M. T. H., Elahi, B., & Javanbakht, V. (2020). Biosynthesis of pure zinc oxide nanoparticles using Quince seed mucilage for photocatalytic dye degradation. *Journal of Alloys and Compounds*, 821, 153519. <https://doi.org/10.1016/j.jallcom.2019.153519>
- Mohamed, A. A., Fouda, A., Abdel-Rahman, M. A., Hassan, S. E. D., El-Gamal, M. S., Salem, S. S., & Shaheen, T. I. (2019). Fungal strain impacts the shape, bioactivity and multifunctional properties of green synthesized zinc oxide nanoparticles. *Biocatalysis and Agricultural Biotechnology*, 19, 101103.
- Mohammadi, F. M., and Ghasemi, N. (2018). Influence of temperature and concentration on biosynthesis and characterization of zinc oxide nanoparticles using cherry extract. *Journal of Nanostructure in Chemistry*, 8(1), 93-102. <https://doi.org/10.1007/s40097-018-0257-6>
- Mohd Yusof, H., Rahman, A., Mohamad, R., Zaidan, U. H., & Samsudin, A. A. (2020). Biosynthesis of zinc oxide nanoparticles by cell-biomass and supernatant of *Lactobacillus plantarum* TA4 and its antibacterial and biocompatibility properties. *Scientific Reports*, 10(1), 1-13.
- Morsy, M. K., Elsabagh, R., & Trinetta, V. (2018). Evaluation of novel synergistic antimicrobial activity of nisin, lysozyme, EDTA nanoparticles, and/or ZnO nanoparticles to control foodborne pathogens on minced beef. *Food Control*, 92, 249-254. <https://doi.org/10.1016/j.foodcont.2018.04.061>
- Mourdikoudis, S., Pallares, R. M., & Thanh, N. T. (2018). Characterization techniques for nanoparticles: comparison and complementarity upon studying nanoparticle properties. *Nanoscale*, 10(27), 12871-12934. <https://doi.org/10.1039/C8NR02278J>
- Muhammad, W., Ullah, N., Haroon, M., & Abbasi, B. H. (2019). Optical, morphological and biological analysis of zinc oxide nanoparticles (ZnO NPs) using *Papaver somniferum* L. *RSC Advances*, 9(51), 29541-29548. [10.1039/C9RA04424H](https://doi.org/10.1039/C9RA04424H)
- Muthuchamy, M., Muneeswaran, T., Rajivgandhi, G., Franck, Q., Muthusamy, A., & Ji-Ming, S. (2020). Biologically synthesized copper and zinc oxide nanoparticles for important biomolecules detection and antimicrobial applications. *Materials Today Communications*, 22, 100766. <https://doi.org/10.1016/j.mtcomm.2019.100766>

- Mydeen, S. S., Kumar, R. R., Kottaisamy, M., & Vasantha, V. S. (2020). Biosynthesis of ZnO nanoparticles through extract from *Prosopis juliflora* plant leaf: Antibacterial activities and a new approach by rust-induced photocatalysis. *Journal of Saudi Chemical Society*, 24(5), 393-406. <https://doi.org/10.1016/j.jscs.2020.03.003>
- Nadaroğlu, H., Güngör, A. A., & Selvi, İ. N. C. E. (2017). Synthesis of nanoparticles by green synthesis method. *International Journal of Innovative Research and Reviews*, 1(1), 6-9.
- Nagajyothi, P. C., Cha, S. J., Yang, I. J., Sreekanth, T. V. M., Kim, K. J., & Shin, H. M. (2015). Antioxidant and anti-inflammatory activities of zinc oxide nanoparticles synthesized using *Polygala tenuifolia* root extract. *Journal of Photochemistry and Photobiology B: Biology*, 146, 10-17. <https://doi.org/10.1016/j.jphotobiol.2015.02.008>
- Naik, E. I., Naik, H. B., Swamy, B. K., Viswanath, R., Gowda, I. S., Prabhakara, M. C., & Chetankumar, K. (2021). Influence of Cu doping on ZnO nanoparticles for improved structural, optical, electrochemical properties and their applications in efficient detection of latent fingerprints. *Chemical Data Collections*, 33, 100671. <https://doi.org/10.1016/j.cdc.2021.100671>
- Naseer, M., Aslam, U., Khalid, B., & Chen, B. (2020). Green route to synthesize Zinc Oxide Nanoparticles using leaf extracts of *Cassia fistula* and *Melia azadarach* and their antibacterial potential. *Scientific Reports*, 10(1), 1-10. <https://doi.org/10.1038/s41598-020-65949-3>
- Navale, G.R., Thripuranthaka, M. and Late, Dattatray J Shinde, S.S. (2015). Antimicrobial activity of ZnO nanoparticles against pathogenic bacteria and fungi. *Sci Med Central*, 3, 1033.
- Naveed Ul Haq, A., Nadhman, A., Ullah, I., Mustafa, G., Yasinzai, M., & Khan, I. (2017). Synthesis approaches of zinc oxide nanoparticles: the dilemma of ecotoxicity. *Journal of Nanomaterials*, 2017, 14. <https://doi.org/10.1155/2017/8510342>
- Naveed, M., Tianying, H., Wang, F., Yin, X., Chan, M. W. H., Ullah, A., ... & Khan, A. M. (2022). Isolation of lysozyme producing *Bacillus subtilis* Strains, identification of the new strain *Bacillus subtilis* BSN314 with the highest enzyme production capacity and optimization of culture conditions for maximum lysozyme production. *Current Research in Biotechnology*, 4, 290-301. <https://doi.org/10.1016/j.crbiot.2022.06.002>
- Neethirajan, S., and Jayas, D. S. (2011). Nanotechnology for the food and bioprocessing industries. *Food and Bioprocess Technology*, 4(1), 39-47. <https://doi.org/10.1007/s11947-010-0328-2>
- Ostolska, I., and Wiśniewska, M. (2014). Application of the zeta potential measurements to explanation of colloidal Cr₂O₃ stability mechanism in the presence of the ionic polyamino acids. *Colloid and Polymer Science*, 292(10), 2453-2464. <https://doi.org/10.1007/s00396-014-3276-y>
- Pachau, L. (2015). Recent developments in novel drug delivery systems for wound healing. *Expert Opinion on Drug Delivery*, 12(12), 1895-1909. <https://doi.org/10.1517/17425247.2015.1070143>

- Pal, I., Brahmkhatri, V. P., Bera, S., Bhattacharyya, D., Quirishi, Y., Bhunia, A., & Atreya, H. S. (2016). Enhanced stability and activity of an antimicrobial peptide in conjugation with silver nanoparticle. *Journal of Colloid and Interface Science*, *483*, 385-393. <https://doi.org/10.1016/j.jcis.2016.08.043>
- Pan, Y., Zuo, J., Hou, Z., Huang, Y., & Huang, C. (2020). Preparation of electrochemical sensor based on zinc oxide nanoparticles for simultaneous determination of AA, DA, and UA. *Frontiers in chemistry*, *8*, 592538. <https://doi.org/10.3389/fchem.2020.592538>
- Pandit, R., Rai, M., and Santos, C. A. (2017). Enhanced antimicrobial activity of the food-protecting nisin peptide by bioconjugation with silver nanoparticles. *Environmental Chemistry Letters*, *15*(3), 443-452. <https://doi.org/10.1007/s10311-017-0626-2>
- Panpaliya, N. P., Dahake, P. T., Kale, Y. J., Dadpe, M. V., Kendre, S. B., Siddiqi, A. G., & Maggavi, U. R. (2019). In vitro evaluation of antimicrobial property of silver nanoparticles and chlorhexidine against five different oral pathogenic bacteria. *The Saudi Dental Journal*, *31*(1), 76-83. <https://doi.org/10.1016/j.sdentj.2018.10.004>
- Papakostas, D., Rancan, F., Sterry, W., Blume-Peytavi, U., & Vogt, A. (2011). Nanoparticles in dermatology. *Archives of Dermatological Research*, *303*(8), 533-550. <https://doi.org/10.1007/s00403-011-1163-7>
- Parashar, M., Shukla, V. K., & Singh, R. (2020). Metal oxides nanoparticles via sol-gel method: a review on synthesis, characterization and applications. *Journal of Materials Science: Materials in Electronics*, *31*(5), 3729-3749. <https://doi.org/10.1007/s10854-020-02994-8>
- Pasquet, J., Chevalier, Y., Pelletier, J., Couval, E., Bouvier, D., & Bolzinger, M. A. (2014). The contribution of zinc ions to the antimicrobial activity of zinc oxide. *Colloids and Surfaces A: Physicochemical and Engineering Aspects*, *457*, 263-274. <https://doi.org/10.1016/j.colsurfa.2014.05.057>
- Pearnton, S. J., Norton, D. P., Ip, K., Heo, Y. W., & Steiner, T. (2003). Recent progress in processing and properties of ZnO. *Superlattices and Microstructures*, *34*(1-2), 3-32. [https://doi.org/10.1016/S0749-6036\(03\)00093-4](https://doi.org/10.1016/S0749-6036(03)00093-4)
- Peng, L. H., Huang, Y. F., Zhang, C. Z., Niu, J., Chen, Y., Chu, Y., ... & Mao, Z. W. (2016). Integration of antimicrobial peptides with gold nanoparticles as unique non-viral vectors for gene delivery to mesenchymal stem cells with antibacterial activity. *Biomaterials*, *103*, 137-149. <https://doi.org/10.1016/j.biomaterials.2016.06.057>
- Perkampus, H. H. (2013). *UV-VIS Spectroscopy and its Applications*. Springer Science & Business Media.
- Pfeiffer, W., Sattler, F., Vogler, S., Gerber, G., Grand, J. Y., & Möller, R. (1997). Rapid communication Photoelectron emission in femtosecond laser assisted scanning tunneling microscopy. *Applied Physics B*, *64*(2), 265-268.
- Pillai, A. M., Sivasankarapillai, V. S., Rahdar, A., Joseph, J., Sadeghfar, F., Rajesh, K., & Kyzas, G. Z. (2020). Green synthesis and characterization of zinc oxide nanoparticles with antibacterial and antifungal activity. *Journal of Molecular Structure*, *1211*, 128107. <https://doi.org/10.1016/j.molstruc.2020.128107>

- Pol, I. E., Mastwijk, H. C., Bartels, P. V., & Smid, E. J. (2000). Pulsed-electric field treatment enhances the bactericidal action of nisin against *Bacillus cereus*. *Applied and Environmental Microbiology*, 66(1), 428-430. <https://doi.org/10.1128/AEM.66.1.428-430.2000>
- Pomastowski, P., Król-Górniak, A., Railean-Plugaru, V., & Buszewski, B. (2020). Zinc oxide nanocomposites—Extracellular synthesis, physicochemical characterization and antibacterial potential. *Materials*, 13(19), 4347. <https://doi.org/10.3390/ma13194347>
- Prakash, A., Sharma, S., Ahmad, N., Ghosh, A., & Sinha, P. (2010). Bacteria mediated extracellular synthesis of metallic nanoparticles. *Int Res J Biotechnol*, 1(5), 071-079.
- Prince, A., Sandhu, P., Ror, P., Dash, E., Sharma, S., Arakha, M., ... & Saleem, M. (2016). Lipid-II independent antimicrobial mechanism of nisin depends on its crowding and degree of oligomerization. *Scientific Reports*, 6(1), 1-15. <https://doi.org/10.1038/srep37908>
- Punjabi, K., Mehta, S., Chavan, R., Chitalia, V., Deogharkar, D., & Deshpande, S. (2018). Efficiency of biosynthesized silver and zinc nanoparticles against multi-drug resistant pathogens. *Frontiers in Microbiology*, 9, 2207.
- Qian, J., Chen, Y., Wang, Q., Zhao, X., Yang, H., Gong, F., & Guo, H. (2021). Preparation and antimicrobial activity of pectin-chitosan embedding nisin microcapsules. *European Polymer Journal*, 157, 110676. <https://doi.org/10.1016/j.eurpolymj.2021.110676>
- Quevedo-Robles, R. V., Vilchis-Nestor, A. R., & Luque, P. A. (2022). Study of optical and morphological properties of nanoparticles semiconductors of zinc oxide synthesized using *Mimosa tenuiflora* extract for photodegradation of methyl orange. *Optical Materials*, 128, 112450. <https://doi.org/10.1016/j.optmat.2022.112450>
- Rai, A., Pinto, S., Velho, T. R., Ferreira, A. F., Moita, C., Trivedi, U., ... & Ferreira, L. (2016). One-step synthesis of high-density peptide-conjugated gold nanoparticles with antimicrobial efficacy in a systemic infection model. *Biomaterials*, 85, 99-110. <https://doi.org/10.1016/j.biomaterials.2016.01.051>
- Rai, M. K., Deshmukh, S. D., Ingle, A. P., & Gade, A. K. (2012). Silver nanoparticles: the powerful nanoweapon against multidrug-resistant bacteria. *Journal of Applied Microbiology*, 112(5), 841-852. <https://doi.org/10.1111/j.1365-2672.2012.05253.x>
- Rajamani, R., Kuppusamy, S., & Shanmugavadivu, M. (2013). Green synthesis of silver nanoparticles using *areca nut* extract for enhanced antibacterial activity. *Journal of Green Science and Technology*, 1(2), 102-106. <https://doi.org/10.1166/jgst.2013.1023>
- Rauf, M. A., Owais, M., Rajpoot, R., Ahmad, F., Khan, N., & Zubair, S. (2017). Biomimetically synthesized ZnO nanoparticles attain potent antibacterial activity against less susceptible *S. aureus* skin infection in experimental animals. *Rsc Advances*, 7(58), 36361-36373. <https://doi.org/10.1039/C7RA05040B>

- Rawat, K. (2021). *Nanotechnology in Food Production*. In *Nanotechnology* (1st Ed., pp. 333-368). Jenny Stanford Publishing.
- Rehman, S., Jermy, B. R., Akhtar, S., Borgio, J. F., Abdul Azeez, S., Ravinayagam, V., ... & Gani, A. (2019). Isolation and characterization of a novel thermophile; *Bacillus haynesii*, applied for the green synthesis of ZnO nanoparticles. *Artificial Cells, Nanomedicine, and Biotechnology*, 47(1), 2072-2082. <https://doi.org/10.1080/21691401.2019.1620254>
- Rezazadeh, N. H., Buazar, F., & Matroodi, S. (2020). Synergistic effects of combinatorial chitosan and polyphenol biomolecules on enhanced antibacterial activity of biofunctionalized silver nanoparticles. *Scientific Reports*, 10(1), 1-13. <https://doi.org/10.1038/s41598-020-76726-7>
- Roshanak, S., Shahidi, F., Yazdi, F. T., Javadmanesh, A., & Movaffagh, J. (2020). Evaluation of antimicrobial activity of Buforin I and Nisin and the synergistic effect of their combination as a novel antimicrobial preservative. *Journal of Food Protection*, 83(11), 2018-2025. <https://doi.org/10.4315/JFP-20-127>
- Sabir, S., Arshad, M., & Chaudhari, S. K. (2014). Zinc oxide nanoparticles for revolutionizing agriculture: synthesis and applications. *The Scientific World Journal*, 2014. <https://doi.org/10.1155/2014/925494>
- Sabir, S., Zahoor, M. A., Waseem, M., Siddique, M. H., Shafique, M., Imran, M., ... & Muzammil, S. (2020). Biosynthesis of ZnO nanoparticles using *bacillus subtilis*: characterization and nutritive significance for promoting plant growth in *Zea mays* L. *Dose-Response*, 18(3), 1559325820958911. <https://doi.org/10.1177/1559325820958911>
- Sadhukhan, P., Kundu, M., Chatterjee, S., Ghosh, N., Manna, P., Das, J., & Sil, P. C. (2019). Targeted delivery of quercetin via pH-responsive zinc oxide nanoparticles for breast cancer therapy. *Materials Science and Engineering: C*, 100, 129-140. <https://doi.org/10.1016/j.msec.2019.02.096>
- Sahani, S., and Sharma, Y. C. (2021). Advancements in applications of nanotechnology in global food industry. *Food Chemistry*, 342, 128318. <https://doi.org/10.1016/j.foodchem.2020.128318>
- Sahoo, S. K., Parveen, S., & Panda, J. J. (2007). The present and future of nanotechnology in human health care. *Nanomedicine: Nanotechnology, Biology and Medicine*, 3(1), 20-31. <https://doi.org/10.1016/j.nano.2006.11.008>
- Saleh, F., Kheirandish, F., Hosseini, F., & Yazdian, F. (2021). Evaluation the effect of ZnO nanoparticle derived *Bacillus subtilis* on the expression of efflux pump genes (AdeB AdeRS) in *Acinetobacter baumannii*. *Journal of Environmental Health Science and Engineering*, 19(1), 1133-1141. <https://doi.org/10.1007/s40201-021-00679-w>
- Salunke, B. K., Sawant, S. S., Lee, S. I., & Kim, B. S. (2015). Comparative study of MnO₂ nanoparticle synthesis by marine bacterium *Saccharophagus degradans* and yeast *Saccharomyces cerevisiae*. *Applied microbiology and biotechnology*, 99(13), 5419-5427. <https://doi.org/10.1007/s00253-015-6559-4>

- Salunke, B. K., Sawant, S. S., Lee, S. I., & Kim, B. S. (2016). Microorganisms as efficient biosystem for the synthesis of metal nanoparticles: current scenario and future possibilities. *World Journal of Microbiology and Biotechnology*, 32(5), 1-16. <https://doi.org/10.1007/s11274-016-2044-1>
- San Tang, K. (2019). The current and future perspectives of zinc oxide nanoparticles in the treatment of diabetes mellitus. *Life Sciences*, 239, 117011. <https://doi.org/10.1016/j.lfs.2019.117011>
- Sanaeimehr, Z., Javadi, I., & Namvar, F. (2018). Antiangiogenic and antiapoptotic effects of green-synthesized zinc oxide nanoparticles using *Sargassum muticum* algae extraction. *Cancer Nanotechnology*, 9(1), 1-16. <https://doi.org/10.1186/s12645-018-0037-5>
- Sangeetha, G., Rajeshwari, S., & Venckatesh, R. (2011). Green synthesis of zinc oxide nanoparticles by *aloe barbadensis miller* leaf extract: Structure and optical properties. *Materials Research Bulletin*, 46(12), 2560-2566. <https://doi.org/10.1016/j.materresbull.2011.07.046>
- Santhoshkumar, J., Kumar, S. V., & Rajeshkumar, S. (2017). Synthesis of zinc oxide nanoparticles using plant leaf extract against urinary tract infection pathogen. *Resource-Efficient Technologies*, 3(4), 459-465. <https://doi.org/10.1016/j.reffit.2017.05.001>
- Santos, J. C., Sousa, R. C., Otoni, C. G., Moraes, A. R., Souza, V. G., Medeiros, E. A., ... & Soares, N. F. (2018). Nisin and other antimicrobial peptides: Production, mechanisms of action, and application in active food packaging. *Innovative Food Science & Emerging Technologies*, 48, 179-194. <https://doi.org/10.1016/j.ifset.2018.06.008>
- Saranya, S., Vijayanai, K., Pavithra, S., Raihana, N., & Kumanan, K. (2017). In vitro cytotoxicity of zinc oxide, iron oxide and copper nanopowders prepared by green synthesis. *Toxicology Reports*, 4, 427-430.
- Saravanan, M., Gopinath, V., Chaurasia, M. K., Syed, A., Ameen, F., & Purushothaman, N. (2018). Green synthesis of anisotropic zinc oxide nanoparticles with antibacterial and cytofriendly properties. *Microbial pathogenesis*, 115, 57-63. <https://doi.org/10.1016/j.micpath.2017.12.039>
- Scherer, K., Wiedemann, I., Ciobanasu, C., Sahl, H. G., & Kubitscheck, U. (2013). Aggregates of nisin with various bactoprenol-containing cell wall precursors differ in size and membrane permeation capacity. *Biochimica et Biophysica Acta (BBA)-Biomembranes*, 1828(11), 2628-2636. <https://doi.org/10.1016/j.bbamem.2013.07.014>
- Schneider, C. A., Rasband, W. S., & Eliceiri, K. W. (2012). NIH Image to ImageJ: 25 years of image analysis. *Nature methods*, 9(7), 671-675. <https://doi.org/10.1038/nmeth.2089>
- Selim, Y. A., Azb, M. A., Ragab, I., & HM Abd El-Azim, M. (2020). Green synthesis of zinc oxide nanoparticles using aqueous extract of *Deverra tortuosa* and their cytotoxic activities. *Scientific Reports*, 10(1), 1-9.
- Selvarajan, E., & Mohanasrinivasan, V. (2013). Biosynthesis and characterization of ZnO nanoparticles using *Lactobacillus plantarum* VITES07. *Materials Letters*, 112, 180-182. <https://doi.org/10.1016/j.matlet.2013.09.020>

- Shamsuzzaman, A. A., Asif, M., Mashrai, A., & Khanam, H. (2014). Green synthesis of zno nanoparticles using *Bacillus subtilis* and their catalytic performance in the one-pot synthesis of steroidal thiophenes. *European Chemical Bulletin*, 3(9), 939-945.
- Shanmugasundaram, T., and Balagurunathan, R. (2017). Bio-medically active zinc oxide nanoparticles synthesized by using extremophilic actinobacterium, *Streptomyces* sp.(MA30) and its characterization. *Artificial Cells, Nanomedicine, and Biotechnology*, 45(8), 1521-1529. <https://doi.org/10.1080/21691401.2016.1260577>
- Sharma, R. K., and Ghose, R. (2015). Synthesis of zinc oxide nanoparticles by homogeneous precipitation method and its application in antifungal activity against *Candida albicans*. *Ceramics International*, 41(1), 967-975. <https://doi.org/10.1016/j.ceramint.2014.09.016>
- Shelar, S. B., Gawali, S. L., Barick, K. C., Kunwar, A., Mohan, A., Priyadarsini, I. K., & Hassan, P. A. (2020). Electrostatically bound lanreotide peptide-gold nanoparticle conjugates for enhanced uptake in SSTR2-positive cancer cells. *Materials Science and Engineering: C*, 117, 111272. <https://doi.org/10.1016/j.msec.2020.111272>
- Siddiqi, K. S., and Husen, A. (2018). Properties of zinc oxide nanoparticles and their activity against microbes. *Nanoscale Research Letters*, 13(1), 1-13. <https://doi.org/10.1186/s11671-018-2532-3>
- Singh, B. N., Rawat, A. K. S., Khan, W., Naqvi, A. H., & Singh, B. R. (2014). Biosynthesis of stable antioxidant ZnO nanoparticles by *Pseudomonas aeruginosa* rhamnolipids. *PLoS One*, 9(9), e106937. <https://doi.org/10.1371/journal.pone.0106937>
- Singh, M., Singh, S., Prasad, S., & Gambhir, I. S. (2008a). Nanotechnology in medicine and antibacterial effect of silver nanoparticles. *Digest Journal of Nanomaterials and Biostructures*, 3(3), 115-122.
- Singh, P. (2018). Nanotechnology in food preservation. *Food Sci*, 9(2), 435-441. <https://doi.org/10.15740/HAS/FSRJ/9.2/435-441>
- Singh, P., Kumar, A., & Kaur, D. (2008b). ZnO nanocrystalline powder synthesized by ultrasonic mist-chemical vapour deposition. *Optical Materials*, 30(8), 1316-1322. <https://doi.org/10.1016/j.optmat.2007.06.012>
- Skoglund, S., Hedberg, J., Yunda, E., Godymchuk, A., Blomberg, E., & Odnevall Wallinder, I. (2017). Difficulties and flaws in performing accurate determinations of zeta potentials of metal nanoparticles in complex solutions—Four case studies. *PLoS One*, 12(7), e0181735. <https://doi.org/10.1371/journal.pone.0181735>
- Sorbiun, M., Shayegan Mehr, E., Ramazani, A., & Taghavi Fardood, S. (2018). Green synthesis of zinc oxide and copper oxide nanoparticles using aqueous extract of oak fruit hull (jaft) and comparing their photocatalytic degradation of basic violet 3. *International Journal of Environmental Research*, 12(1), 29-37. <https://doi.org/10.1007/s41742-018-0064-4>

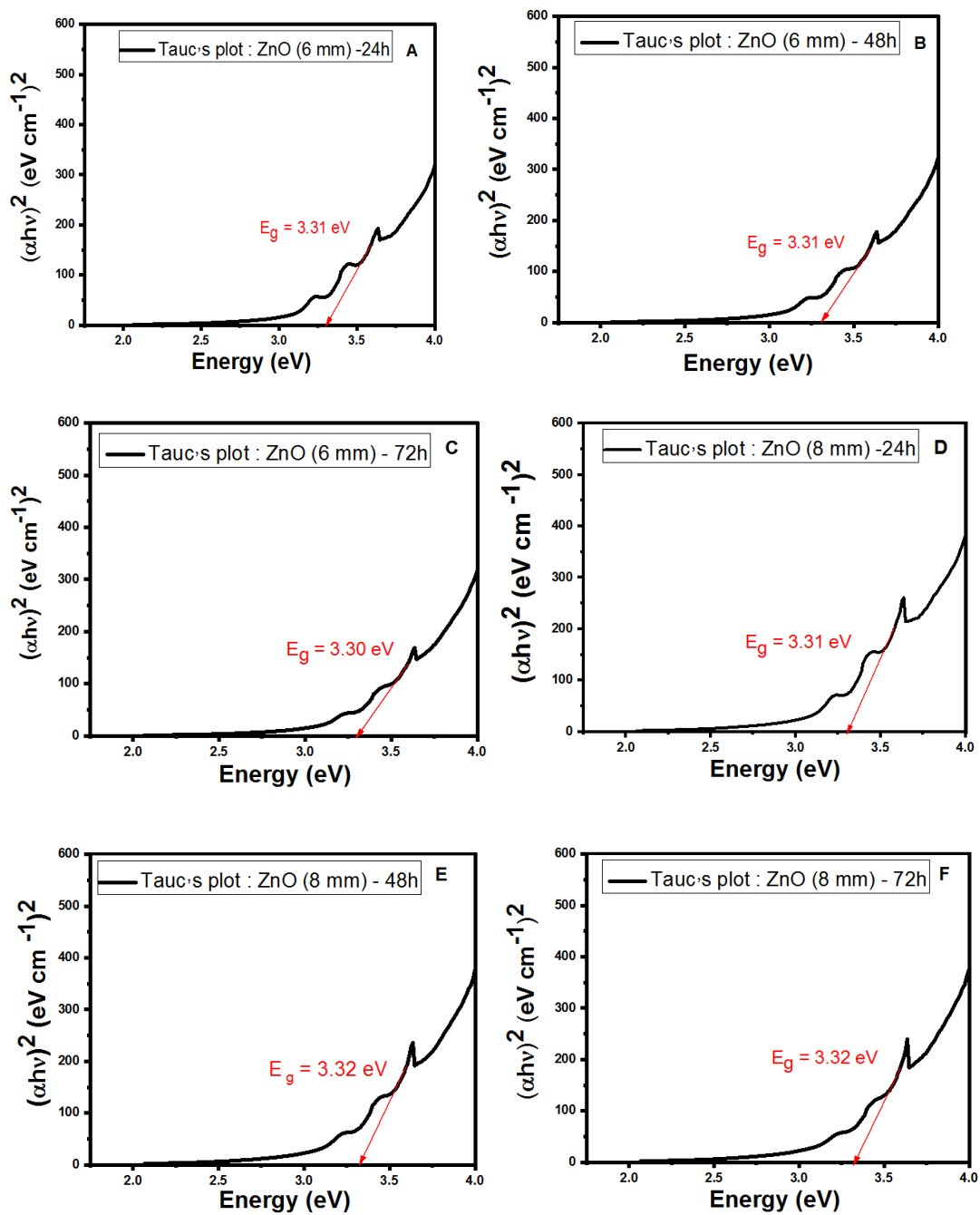
- Spirescu, V. A., Şuhan, R., Niculescu, A. G., Grumezescu, V., Negut, I., Holban, A. M., ... & Mogoantă, L. (2021). Biofilm-resistant nanocoatings based on ZnO nanoparticles and linalool. *Nanomaterials*, *11*(10), 2564. <https://doi.org/10.3390/nano11102564>
- Suba, S., Vijayakumar, S., Vidhya, E., Punitha, V. N., & Nilavukkarasi, M. (2021). Microbial mediated synthesis of ZnO nanoparticles derived from *Lactobacillus* spp: Characterizations, antimicrobial and biocompatibility efficiencies. *Sensors International*, *2*, 100104. <https://doi.org/10.1016/j.sintl.2021.100104>
- Suri, S. S., Fenniri, H., & Singh, B. (2007). Nanotechnology-based drug delivery systems. *Journal of Occupational Medicine and Toxicology*, *2*(1), 1-6. <https://doi.org/10.1186/1745-6673-2-16>
- Talaro, K. P., and Talaro, A. (1992). *Foundations in Microbiology*. WCB/McGraw-Hill.
- Taran, M., Rad, M., & Alavi, M. (2018). Biosynthesis of TiO₂ and ZnO nanoparticles by *Halomonas elongata* IBRC-M 10214 in different conditions of medium. *BioImpacts: BI*, *8*(2), 81. <https://doi.org/10.15171/bi.2018.10>
- Thakur, S., Shandilya, M., & Guleria, G. (2021). Appraisalment of antimicrobial zinc oxide nanoparticles through Cannabis *Jatropha curcusa Alovera* and *Tinosporacordifolia* leaves by green synthesis process. *Journal of Environmental Chemical Engineering*, *9*(1), 104882. <https://doi.org/10.1016/j.jece.2020.104882>
- Theron, J., Walker, J. A., & Cloete, T. E. (2008). Nanotechnology and water treatment: applications and emerging opportunities. *Critical reviews in microbiology*, *34*(1), 43-69. <https://doi.org/10.1080/10408410701710442>
- Tyagi, P. K., Gola, D., Tyagi, S., Mishra, A. K., Kumar, A., Chauhan, N., ... & Sirohi, S. (2020). Synthesis of zinc oxide nanoparticles and its conjugation with antibiotic: Antibacterial and morphological characterization. *Environmental Nanotechnology, Monitoring & Management*, *14*, 100391. <https://doi.org/10.1016/j.enmm.2020.100391>
- Van Cauteren, D., Le Strat, Y., Sommen, C., Bruyand, M., Tourdjman, M., Da Silva, N. J., ... & Desenclos, J. C. (2017). Estimated annual numbers of foodborne pathogen-associated illnesses, hospitalizations, and deaths, France, 2008–2013. *Emerging Infectious Diseases*, *23*(9), 1486. doi: 10.3201/eid2309.170081
- Varadavenkatesan, T., Lyubchik, E., Pai, S., Pugazhendhi, A., Vinayagam, R., & Selvaraj, R. (2019). Photocatalytic degradation of Rhodamine B by zinc oxide nanoparticles synthesized using the leaf extract of *Cyanometra ramiflora*. *Journal of Photochemistry and Photobiology B: Biology*, *199*, 111621. <https://doi.org/10.1016/j.jphotobiol.2019.111621>
- Velsankar, K., Sudhahar, S., Parvathy, G., & Kaliammal, R. (2020). Effect of cytotoxicity and antibacterial activity of biosynthesis of ZnO hexagonal shaped nanoparticles by *Echinochloa frumentacea* grains extract as a reducing agent. *Materials Chemistry and Physics*, *239*, 121976. <https://doi.org/10.1016/j.matchemphys.2019.121976>

- Vergara-Llanos, D., Koning, T., Pavicic, M. F., Bello-Toledo, H., Diaz-Gomez, A., Jaramillo, A., ... & Sánchez-Sanhueza, G. (2021). Antibacterial and cytotoxic evaluation of copper and zinc oxide nanoparticles as a potential disinfectant material of connections in implant provisional abutments: An in-vitro study. *Archives of Oral Biology*, 122, 105031.
- Wang, L., Hu, C., & Shao, L. (2017). The antimicrobial activity of nanoparticles: present situation and prospects for the future. *International journal of nanomedicine*, 12, 1227. <https://doi.org/10.2147/IJN.S121956>
- Wang, R., Tao, J., Du, K., Wang, Y., Ge, B., Li, F., ... and Duan, X. (2018). *Transmission electron microscopy*. In Progress in Nanoscale Characterization and Manipulation (pp. 69-203). Springer, Singapore.
- Wang, T., Sun, Z., Huang, D., Yang, Z., Ji, Q., Hu, N., ... & Zhang, Y. (2017). Studies on NH₃ gas sensing by zinc oxide nanowire-reduced graphene oxide nanocomposites. *Sensors and Actuators B: Chemical*, 252, 284-294. <https://doi.org/10.1016/j.snb.2017.05.162>
- Wang, Z. L. (2008). Splendid one-dimensional nanostructures of zinc oxide: a new nanomaterial family for nanotechnology. *ACS Nano*, 2(10), 1987-1992. <https://doi.org/10.1021/nn800631r>
- Webber, J. L., Namivandi-Zangeneh, R., Drozdek, S., Wilk, K. A., Boyer, C., Wong, E. H., ... & Beattie, D. A. (2021). Incorporation and antimicrobial activity of nisin Z within carrageenan/chitosan multilayers. *Scientific Reports*, 11(1), 1-15. <https://doi.org/10.1038/s41598-020-79702-3>
- Wiedemann, I., Breukink, E., van Kraaij, C., Kuipers, O. P., Bierbaum, G., de Kruijff, B., & Sahl, H. G. (2001). Specific binding of nisin to the peptidoglycan precursor lipid II combines pore formation and inhibition of cell wall biosynthesis for potent antibiotic activity. *Journal of Biological Chemistry*, 276(3), 1772-1779. <https://doi.org/10.1074/jbc.M006770200>
- Wojcieszak, D., Mazur, M., Kaczmarek, D., Poniedziałek, A., & Osękowska, M. (2017). An impact of the copper additive on photocatalytic and bactericidal properties of TiO₂ thin films. *Mater. Sci. Pol*, 35, 421-426. <https://doi.org/10.1515/msp-2017-0041>
- Wong, K. K., and Mann, S. (1996). Biomimetic synthesis of cadmium sulfide-ferritin nanocomposites. *Advanced Materials*, 8(11), 928-932. <https://doi.org/10.1002/adma.19960081114>
- Wood, R. W. (1902). XLII. On a remarkable case of uneven distribution of light in a diffraction grating spectrum. *The London, Edinburgh, and Dublin Philosophical Magazine and Journal of Science*, 4(21), 396-402. <https://doi.org/10.1080/14786440209462857>
- Xie, Y., He, Y., Irwin, P. L., Jin, T., & Shi, X. (2011). Antibacterial activity and mechanism of action of zinc oxide nanoparticles against *Campylobacter jejuni*. *Applied and Environmental Microbiology*, 77(7), 2325-2331. <https://doi.org/10.1128/AEM.02149-10>
- Yadwade, R., Gharpure, S., & Ankamwar, B. (2021). Nanotechnology in cosmetics pros and cons. *Nano Express*, 2(2), 022003. <https://doi.org/10.1088/2632-959X/abf46b>

- Yashni, G., Al-Gheethi, A., Mohamed, R., Shanmugan, V. A., & Al-Sahari, M. N. A. (2021). Phytotoxicity evaluation of ZnO nanoparticles synthesized from *Corriandrum sativum* leaf extract. *Materials Today: Proceedings*, 47, 1336-1340. <https://doi.org/10.1016/j.matpr.2021.02.816>
- Yıldırım, Ö.A. (2014) ‘Synthesis of Zinc Oxide Nanoparticles By Aqueous Methods [Ph.D thesis]. Middle East Technical University
- Yurtluk, T., Akçay, F. A., & Avcı, A. (2018). Biosynthesis of silver nanoparticles using novel *Bacillus* sp. SBT8. *Preparative Biochemistry & Biotechnology*, 48(2), 151-159. <https://doi.org/10.1080/10826068.2017.1421963>
- Zhang, C., Zheng, X., Wan, X., Shao, X., Liu, Q., Zhang, Z., & Zhang, Q. (2014). The potential use of H102 peptide-loaded dual-functional nanoparticles in the treatment of Alzheimer's disease. *Journal of Controlled Release*, 192, 317-324. <https://doi.org/10.1016/j.jconrel.2014.07.050>
- Zhang, Q. Y., Yan, Z. B., Meng, Y. M., Hong, X. Y., Shao, G., Ma, J. J., ... & Fu, C. Y. (2021). Antimicrobial peptides: mechanism of action, activity and clinical potential. *Military Medical Research*, 8(1), 1-25. <https://doi.org/10.1186/s40779-021-00343-2>
- Zhao, C., Wan, Y., Tang, G., Jin, Q., Zhang, H., & Xu, Z. (2021). Comparison of different fermentation processes for the vitamin K2 (Menaquinone-7) production by a novel *Bacillus velezensis* ND strain. *Process Biochemistry*, 102, 33-41. <https://doi.org/10.1016/j.procbio.2020.11.029>
- Zhao, X., and Kuipers, O. P. (2021). Synthesis of silver-nisin nanoparticles with low cytotoxicity as antimicrobials against biofilm-forming pathogens. *Colloids and Surfaces B: Biointerfaces*, 206, 111965. <https://doi.org/10.1016/j.colsurfb.2021.111965>
- Zheng, M., Wang, S., Liu, Z., Xie, L., & Deng, Y. (2018). Development of temozolomide coated nano zinc oxide for reversing the resistance of malignant glioma stem cells. *Materials Science and Engineering: C*, 83, 44-50. <https://doi.org/10.1016/j.msec.2017.07.015>
- Zhu, W., Bartos, P. J., & Porro, A. (2004). Application of nanotechnology in construction. *Materials and Structures*, 37(9), 649-658. <https://doi.org/10.1007/BF02483294>

APPENDICES

APPENDIX A. Effect salt concentrations on energy bandgap of ZnO NPs



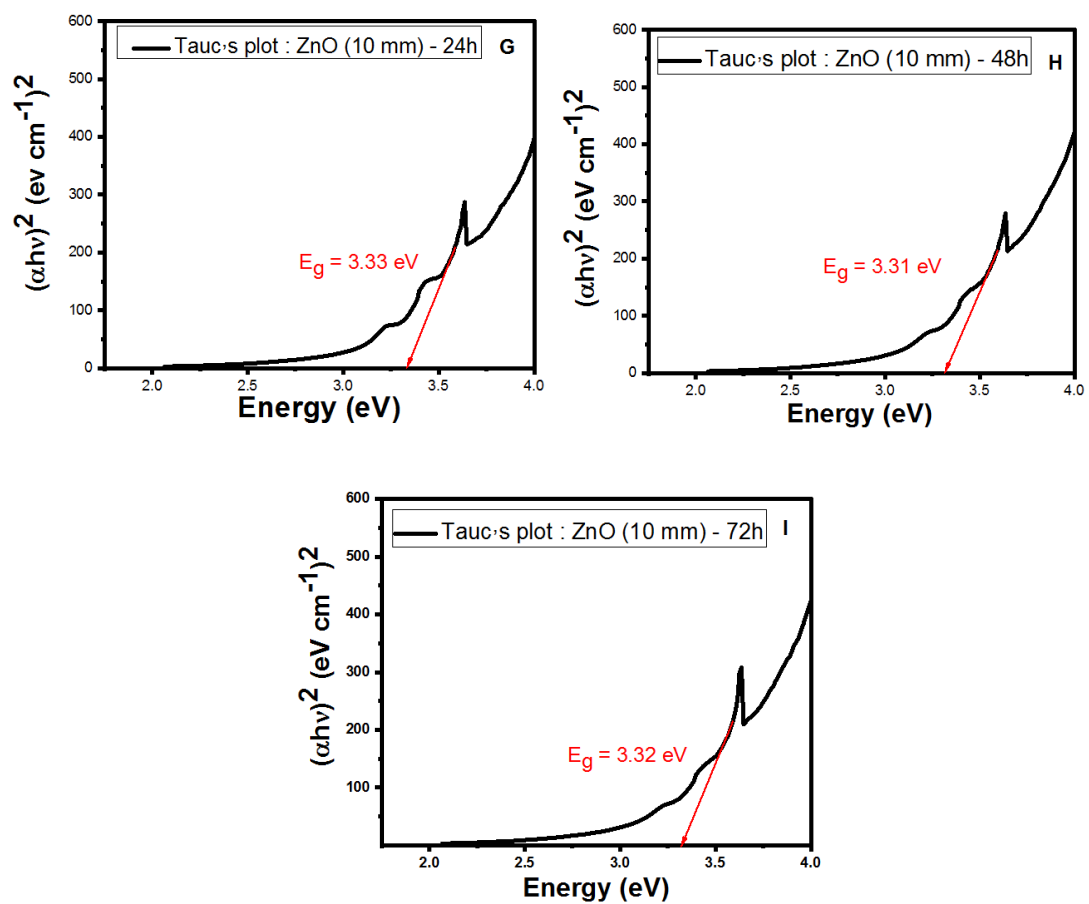
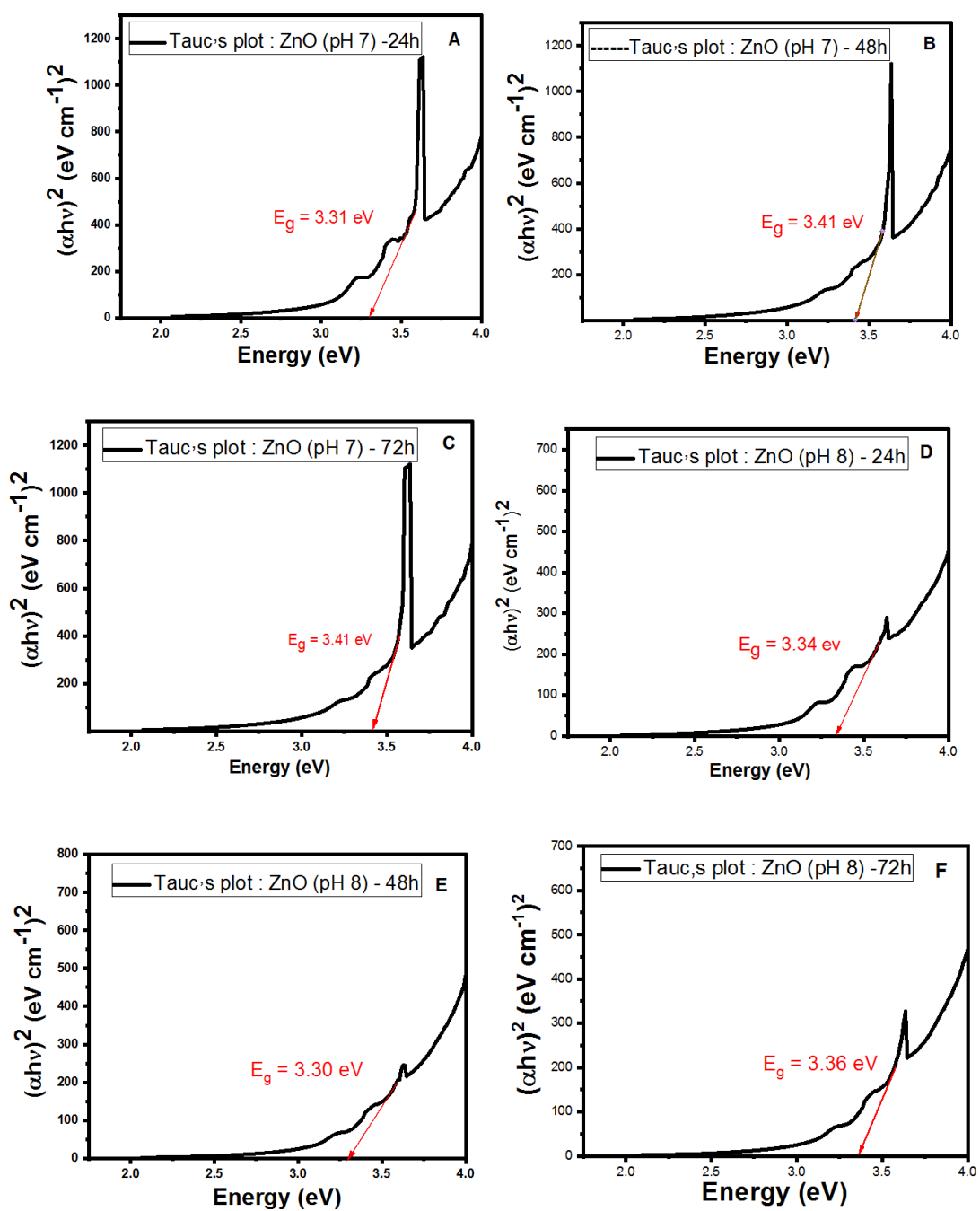


Figure A. Effect salt concentrations on energy bandgap of ZnO NPs at different times.

APPENDIX B. Effect pH on energy bandgap of ZnO NPs



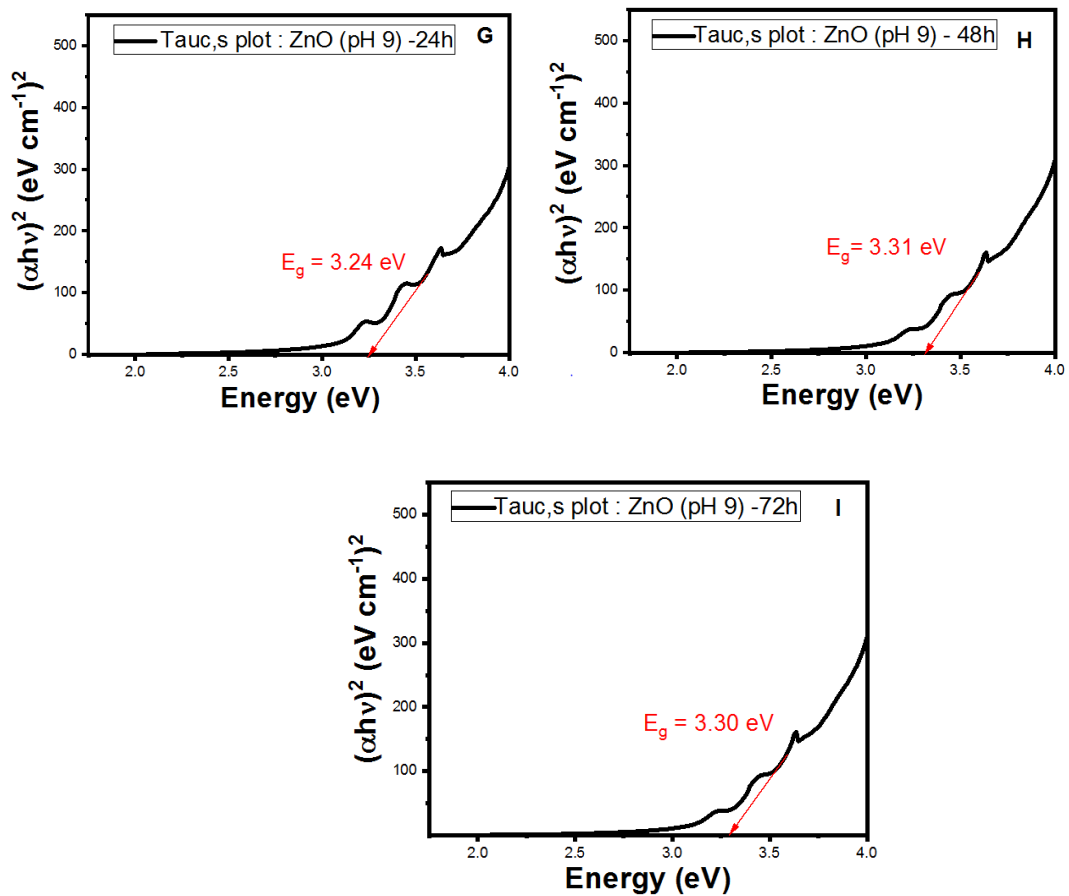


Figure B. Effect pH values on energy bandgap of ZnO NPs at different times.

CURRICULUM VITAE

Name Surname : Mohammed Hamk

EDUCATION

- **Undergraduate:** 2009, Tikrit University, College of agriculture, Department of Food science
- **Master:** 2012, Tikrit University, College of Agriculture, Department of Food Science, Identification and Determination of Microorganisms and Some Heavy Metals in Foods and Study the Biochemical and Hestopath effects in Rats.

PROFESSIONAL EXPERIENCE AND AWARDS:

- He worked as a Lecturer at the Slemani Polytechnic University – Halabja Technical College of Applied Sciences (From 2012 to present).
- Funding Author Mohammed Hamk has received research support from Presidency for Turks Abroad and Related Communities, Scholarship No: 18IQ001371 (From 2018 to present).

PUBLICATIONS, PRESENTATIONS AND PATENTS ON THE THESIS:

- Hamk, M., Akçay, FA., and Avcı, A. 2022. Green Synthesis of Zinc Oxide Nanoparticles Using *Bacillus Subtilis* ZBP4 and Their Antibacterial Potential Against Foodborne Pathogens. *Preparative Biochemistry & Biotechnology*, 1-10.
- Hamk, M., Avcı, A., and Akçay, FA. (2021, 24-26, November). Extracellular Synthesis of Zinc Oxide Nanoparticles Using *Bacillus* Sp. ZBP4 and its Antimicrobial Potential Against Foodborne Bacteria. 4th International Eurasian Conference on Biological and Chemical Sciences. p.131, Ankara/Turkey.
- Avcı A., Hamk M., and Akçay FA. (2021, 24-26 November). Zinc Oxide Nanoparticles as Potential Antibacterial Agents. 4th International Eurasian Conference on Biological and Chemical Sciences, p.1123, Ankara/Turkey.
- Hamk, M., and Avcı, A. (2022, 15-18, October). Nisin Conjugated Zinc Oxide Nanoparticle Biosynthesis by *Bacillus Subtilis* ZBP4. 2nd International Conference on Engineering and Applied Natural Sciences. p.129, Konya/Turkey.

OTHER PUBLICATIONS, PRESENTATIONS AND PATENTS:

- Hamk, M., and Thalij, K. M. 2012. Determination and Identification of Heavy Chemical Elements and Microorganisms That's Contaminated Food Canned Imported in Iraq. *J. of Tikrit Univ. for Agric. Sci.* Vol.12, No.2.
- Thalij, K. M., and Hamk, M. 2012. Ultra Structural Alterations Induced by Doses of Some Heavy Metal in the Kidney and Liver of Rat. *J. of Tikrit Univ. for Agric. Sci.* Vol.12, No., 2. (Article)
- Hamk, M., and Thalij, K. M. 2014. Assessment of Microbial and Heavy Metals Contamination in Some Foods and Drinking Water in Selected Iraqi Markets. *Journal of Zankoy Sulaimani- Part A, Special Issue*, Vol. 16.
- Hamk, M. 2015. Histological Changes of the Spleen Female Rats Treated Under Lethal Concentrations of Zinc and Tin. *Journal of Basrah Researches / sciences.* Part 1 B, No. 41 (Article)
- Hamk, M., and Thalij, K. M. 2015. Estimation of Cadmium and Copper in Some Foods and Drinking Water in Iraqi Markets and Illustrated the Ultra Structural Alterations of its Ranged in Rats Spleen. *International Journal of Current Microbiology and Applied Sciences*, Volume 4 Number 3, 174-181.
- Alabdulla, B. Y., Al-Saraj, A. F. and Hamk, M. 2015. Physiochemical and Phytochemical Properties of Pomegranate Concentrated in Kurdistan-Iraq. **2nd Scientific Conference**, University of Garmian, Vol 1.
- Jasim M. A., Salih G. M., and Hamk, M. 2018 . The Effect of Arabic Gum on Physicochemical and Sensory Properties of Camel Milk, Yogurt. *Journal of Zankoy Sulaimani, Part A, Special Issue.*
- Alfayadh, H. M. S., Hamk, M., Ibrahim, K. J., and Al-Saadi, J. M. S. 2018. Effect of Transglutaminase and Maillard Reaction on Textural and Sensory Properties of a Calcium-Induced Milk Gel. *Kurdistan Journal of Applied Research (KJAR)*, vo. 3, Iss.1.
- Hamk, M., Mohammed, M. J., Jamel, A. H., and Thalij, K. M. 2019. The Effectiveness of *Lactobacillus casei* and *Lactobacillus acidophilus* on Some Biological Parameters of Female Rats Exposed to the Bisphenol-A. *Biochem. Cell. Arch.* Vol. 19, No. 1, pp. 971-975.
- Avcı, A., Yıldırım, A., Cerit, I, Keskin, S. Y., Hamk, M., Keskin, C., S., and Demirko, O. 2022. Influence of Culture Age and Environmental Conditions on the Decolorization and Biodegradation of Reactive Orange 13 by *Bacillus* Sp. SBT8. *Biomass Conversion and Biorefnery.*
- Akçay, F. A., Avcı, A., and Hamk, M. (2021, 25-29, October). The Functionality of Bioactive Peptides Generated from Food Proteins via Enzymatic Hydrolysis. II. *International Congress of the Turkish Journal of Agriculture-Food Science and Technology*, p. 79, Gazimağusa, Cyprus/Turkey.
- Akçay, F. A., Çolak, M., İpekçioğlu, Y., Şahin, I, Karaca, M., Aras, B., Hamk, M., and Avcı, A. (2022, 15-18, October). Screening and Selection of Media Components for Amylase Production by *Bacillus* sp. Using Plackett-Burman Design. **2nd International Conference on Engineering and Applied Natural Sciences**, p. 263, Konya/Turkey.
- Keskin, S. Y., Avcı, A., Ali, L. A. A., and Hamk, M. (2022, 23-25, November). Investigation of Total Phenolics and Flavonoid Contents of *Polygala major* Using Different Solvents. **5th International Eurasian Conference on Biological and Chemical Sciences**. p. 319, Ankara/Turkey.